

## ABSTRACT

Title of Thesis: SPATIAL AND TEMPORAL VARIABILITY  
IN SUSPENDED SEDIMENT  
CHARACTERISTICS IN THE SURFACE  
LAYER OF THE UPPER CHESAPEAKE  
BAY

Stephanie Marie Barletta, Master of Science,  
2020

Thesis directed by: Professor Lawrence Sanford, University of  
Maryland Center for Environmental Science

Periodic high discharge events flush suspended sediments from the Susquehanna River and Conowingo Dam reservoir into the upper Chesapeake Bay, which extends from the mouth of the Susquehanna River to the Bay Bridge near Annapolis, MD. Sediment characteristics in the surface layer of the upper Bay and changes in these characteristics with varying river discharge and distance downstream are not well known. In order to develop an integrated understanding of surface layer sediment dynamics, several in-situ data sets were examined at the Bay head and downstream along the Bay's center channel, providing data on the spatial and temporal variability of suspended particle characteristics including concentration, settling speed, bulk density, and size. It was found that particles are entirely disaggregated at the Dam, later aggregating to a limited extent down Bay, and that downstream characteristics are more weakly linked to Susquehanna flow at lower flows and longer distances.

SPATIAL AND TEMPORAL VARIABILITY IN SUSPENDED SEDIMENT  
CHARACTERISTICS IN THE SURFACE LAYER OF THE UPPER  
CHESAPEAKE BAY

by

Stephanie Marie Barletta

Thesis submitted to the Faculty of the Graduate School of the  
University of Maryland, College Park, in partial fulfillment  
of the requirements for the degree of  
Master of Science  
2020

Advisory Committee:  
Dr. Lawrence Sanford, Chair  
Dr. Cindy Palinkas  
Dr. Grace Massey

© Copyright by  
Stephanie Marie Barletta  
2020

## Acknowledgements

Thank you to my friends, family, and professors for your untiring support, encouragement, and patience over the years. Thank you to my colleagues who helped collect and process the data presented in this thesis. Special thanks to my committee for being so involved and responsive during this process, and for their earnest dedication in helping me succeed. Financial support was received from Horn Point Laboratory Graduate Fellowship and a grant from Exelon and Maryland Department of Natural Resources.

# Table of Contents

Acknowledgements.....	ii
Table of Contents.....	iii
List of Tables.....	iv
List of Figures.....	v
Chapter 1: Introduction.....	1
Chapter 2: Upstream Particle Characteristics and Response to Susquehanna River Flow.....	9
2.1 Introduction.....	9
2.2 Methods.....	11
2.2.1 Owen Settling Tube Analysis.....	11
2.2.2 USGS Particle Size Analysis.....	15
2.3 Results and Discussion.....	18
Chapter 3: Particle Characteristics in the Surface Layer of the Upper Bay.....	41
3.1 Introduction.....	41
3.2 Methods.....	43
3.3 Results and Discussion.....	46
Chapter 4: Particle Mass Downstream and Response to Susquehanna River Flow ...	59
4.1 Introduction.....	59
4.2 Methods.....	61
4.3 Results and Discussion.....	64
Chapter 5: Summary, Synthesis, and Broader Implications.....	84
5.1 Summary.....	84
5.2 Synthesis.....	86
5.3 Broader Implications.....	90
Appendices.....	97
Bibliography.....	117

## List of Tables

Table 2.1 <i>Sampling at Conowingo Dam</i> .....	26
Table 2.2 <i>Weighted average and median settling speeds for 37-year USGS data</i> .....	27
Table 3.1 <i>Upper Chesapeake Bay surface layer average and median values</i> .....	52
Table 4.1 <i>Highest correlation antecedent days from antecedent calculations</i> .....	71
Table 5.1 <i>Median TSS values and (5.1) TSS estimates for the surface layer of the upper Bay</i> .....	95

## List of Figures

- Figure 2.1.* The settling tube apparatus used in this analysis equipped with two settling tubes insulated with reflective bubble wrap. Containers used for collecting interval samples line the base of the apparatus. .... 28
- Figure 2.2.* Screenshot of the Maplezzi (2013) analysis spreadsheet for the spill gate water sample on April 13th, 2015. A myriad of values are automatically calculated using settling tube experiment inputs (columns A through D), including settling speed (column P) and mass fraction (column Q). *Note.* Early on in this investigation, a minor spreadsheet error ultimately resulted in the  $w_s$  and conc distr values of the second to last April 13, 2015 spill gate and catwalk samples being approximately 10% larger than true experimental value. This error was not discovered until after the conclusion of this study, but the difference is insignificant and does not alter any findings. .... 29
- Figure 2.3.* Plots of sediment contribution during the 10 settling intervals from the Malpezzi (2013) spreadsheet for the spill gate water sample on April 13th, 2015. Cumulative contribution over time (left) and contribution per settling speed interval (right). .... 30
- Figure 2.4.* Fraction of total sediment (Frequency (%)) settling faster or slower than 0.015 cm/s (left) and initial concentration (TSS (mg/L)) of sediment settling faster or slower than 0.015 cm/s (right) for the spill gate water sample on April 13th, 2015. . 31
- Figure 2.5.* Malarkey et al. (2013) script's plot output for percent of total sediments ( $F(w_s)$ ) versus settling speed ( $w_s$ ). The six leftmost dots represent extrapolated details from the final Owen sample from the spill gate on April 13th, 2015. .... 32
- Figure 2.6.* Comparison of mass fraction and settling speed values from Excel and Matlab analyses for the spill gate water sample on April 13th, 2015. Vertical lines indicate thresholds of the four settling classes. .... 33
- Figure 2.7.* Mass contribution by settling speed class for the various sampling locations and analyses for Owen & USGS data sampled on May 13, 2015. .... 34
- Figure 2.8.* TSS values from Owen location spreadsheet outcomes. USGS particle size analysis outcomes sampled on or around the seven Owen sampling days (left). TSS for the three sampling regimes (Owen spill gate, Owen catwalk, USGS catwalk) on the four shared sampling dates (right). .... 35
- Figure 2.9.* Settling class mass fractions for the five analysis methods of Owen and USGS data on the four shared sampling dates. *Note.* Differences between methods within class are not statistically significant. .... 36

*Figure 2.10.* TSS and river discharge values and exponential fit of 37-year USGS data at Conowingo compared to similar established relationships (left). Exponential fit of 37-year USGS data compared to four-date Owen TSS values (right). *Note.* These figures are similar to those published in Palinkas et al. (2019) but use an updated dataset. .... 37

*Figure 2.11.* Per-class mass contributions by flow at Conowingo Dam for 37-year USGS data. *Note.* These figures are similar to those published in Palinkas et al. (2019) but use an updated dataset. .... 38

*Figure 2.12.* Weighted average settling speed ( $w_{s,ave}$ ) including (blue) and excluding (green) the fraction of sand-sized particles (settling class 4) plotted by river discharge on a semi-log scale. The red triangle marks the long-term average Susquehanna River discharge measured at Conowingo Dam (~38,000 cfs). .... 39

*Figure 2.13.* Cumulative mass fraction contributed by particles settling at certain speeds (logarithmically spaced and class characteristic settling speeds) under five flow conditions for the 37-year USGS disaggregated particle size data. The top plot shows sand-inclusive values, while the bottom plot shows sand-exclusive values. The intersections with the 0.5 fraction line (black, dashed) represent the median settling speed. The red box highlights the narrow range of median speeds across all flows, both including and excluding sand. .... 40

*Figure 3.1.* Cross-sectional contour plots of a BITMAX II axial survey taken on April 15, 2002. Panels shown are of TSS and LISST-derived particle parameters, with black salinity contours, which are the same in all panels. Head of Bay i.e. Havre de Grace, MD. .... 53

*Figure 3.2.* Cross-section of salinity (thin black lines) and TSS (coloration) from a BITMAX I axial survey taken on May 13, 2002. A depth grid overlay of blue (1m) and red (5m) horizontal lines is used for identification of surface layer depth. River km is river distance measured from Havre de Grace, M.D. .... 54

*Figure 3.3.* Surface layer data for key parameters (TSS,  $d_{50}$ ,  $bulkD$ ,  $w_s$ ) from upper Bay axial analysis, surveyed on April 15, 2007. Blue circles represent all sample data, while red lines indicate median values. .... 55

*Figure 3.4.* Surface layer average TSS at different surface layer median settling speeds from axial surveys data listed in Table 3.1. .... 56

*Figure 3.5.* Median settling speed ( $w_{s50}$ ) by median diameter ( $d_{50}$ ) (left), and median excess density ( $s-1$ ) by median diameter ( $d_{50}$ ) (right) of particles in the surface layer of the upper Bay for the 9 axial surveys from Table 3.1. .... 57

*Figure 3.6.* Image of suspended aggregated floc particles captured in situ at the northernmost axial station during April, 2017. .... 58



*Figure 4.1.* Map of the upper Chesapeake Bay with CBP station (red ‘x’) and BITMAX I & II station (black dot) locations. CBP stations are numbered in order from north to south..... 72

*Figure 4.2.* An example of CBP TSS by USGS BEAD TSS used to evaluate influence of sampling period. Circular markers are of size (BEAD Flow) / 1000 and color indicates samples taken prior (blue) or post (red) Conowingo Infill (1995). Location of sample marker above or below 1:1 line indicates an increase or decrease of sediment concentration between the dam and the downstream station. .... 73

*Figure 4.3.* Boxplot of TSS by salinity intervals under low flow conditions (<36,000 cfs). Conowingo data is represented by the leftmost box (C on the x-axis). The diagonal mixing line is determined by plotting a linear line that extends from median Conowingo TSS value to the point at which CBP TSS levels fall below the black background concentration line (7 mg/L). Red horizontal lines are median TSS values, red crosses are outliers, black dashed lines represent the upper and lower quartile of values. .... 74

*Figure 4.4.* Boxplot of TSS by salinity intervals under medium flow conditions (36,000-86,000 cfs). Conowingo data is represented by the leftmost box (C on the x-axis). The diagonal mixing line is determined by plotting a linear line that extends from median Conowingo TSS value to the point at which CBP TSS levels fall below the black background concentration line (7 mg/L). Red horizontal lines are median TSS values, red crosses are outliers, black dashed lines represent the upper and lower quartile of values. .... 75

*Figure 4.5.* Boxplot of TSS by salinity intervals under high flow conditions (>86,000 cfs). Conowingo data is represented by the leftmost box (C on the x-axis). The diagonal mixing line is determined by plotting a linear line that extends from median Conowingo TSS value to the point at which CBP TSS levels fall below the black background concentration line (7 mg/L). Red horizontal lines are median TSS values, red crosses are outliers, black dashed lines represent the upper and lower quartile of values. .... 76

*Figure 4.6.* Median values from salinity interval boxplots for low, medium, and high flow conditions. Conowingo data is represented by the leftmost box (C on the x-axis). Diagonal mixing lines are determined by plotting a linear line that extends from median Conowingo TSS value to the point at which CBP TSS levels fall below the black background concentration line (7 mg/L). .... 77

*Figure 4.7.* Boxplot of CBP salinity at each station. Red horizontal lines are median salinity values, red crosses are outliers, black dashed lines represent the upper and lower quartile of values..... 78

*Figure 4.8.* Boxplot of CBP TSS at each station. Red horizontal lines are median TSS values, red crosses are outliers, black dashed lines represent the upper and lower quartile of values..... 79

*Figure 4.9.* Statistical significance of differences in salinity concentration over distance down Bay by station number. Comparisons are read as “salinity at station (column number) is/is not significantly different than salinity at station (row number). Statistical significance is noted as either significant (‘Sig’, green) or insignificant (‘Not sig’, orange) in the intersecting boxes. *Note.* Visually, each column should be imagined as being a map of the upper Bay that starts as far north as station (column number) and ends at station 7 (CBP 3.3c), near the Bay Bridge to the south..... 80

*Figure 4.10.* Statistical significance of differences in TSS concentration over distance down Bay by station number. Comparisons are read as “TSS at station (column number) is/is not significantly different than TSS at station (row number). Statistical significance is noted as either significant (‘Sig’, green) or insignificant (‘Not sig’, orange) in the intersecting boxes. *Note.* Visually, each column should be imagined as being a map of the upper Bay that starts as far north as station (column number) and ends at station 7 (CBP 3.3c), near the Bay Bridge to the south..... 81

*Figure 4.11.* Comparisons of downstream CBP TSS at station 1.1 compared to upstream antecedent USGS TSS at Conowingo Dam under low (upper left), medium (upper right), high (lower left) and all (lower right) flow conditions. All plots are on a loglog scale with a diagonal black 1:1 reference line. .... 82

*Figure 4.12.* Comparisons of downstream CBP TSS at station 3.3c compared to upstream antecedent USGS TSS at Conowingo Dam under low (upper left), medium (upper right), high (lower left) and all (lower right) flow conditions. All plots are on a loglog scale with a diagonal black 1:1 reference line. .... 83

*Figure 5.1.* A conceptual diagram of the transport, transformation, and settling of Susquehanna River particles entering the upper Chesapeake Bay. The Conowingo Dam is at the top left of the figure. The blue contours represent the salinity gradient, with the saltwater intrusion in the darkest shade of blue. The ETM is located slightly right of the center of the figure. The upstream endmember sediments are primary particles ranging in size from sand to fine clays..... 96

## Chapter 1: Introduction

At the head of the Chesapeake Bay is the mouth of the Susquehanna River, which is responsible for 50% of the Chesapeake Bay's freshwater during a typical year (Langland et al., 1995) and consequently a substantial contributor of sediments and nutrients to the Bay (Langland, 2009). The Susquehanna is subject to periodic high discharge events that result in ecologically damaging sediment and nutrient fluxes into the Chesapeake Bay (Cronin et al., 2003; Langland & Cronin, 2003). The largest estuary in North America, the Chesapeake Bay is over 320 km in length, supports hundreds of species of fish, shellfish, and crabs, and has a 166,000 km<sup>2</sup> watershed (Figure 1.1) that extends through six states (Chesapeake Bay Program, 2020a, 2020b). As such, the Chesapeake Bay estuary and its watershed are of economic, ecological, and cultural importance, and are well studied and frequently the subject of political discourse and regulation.

North of the Bay, 16km upstream on the Susquehanna River, is the Conowingo hydroelectric dam (Figure 1.2). This valued asset to Maryland's power grid was established in 1928, but at the cost of disrupting sediment transport to the Chesapeake Bay (Langland, 2009); dam reservoirs act as a trap for sediments and particulate nutrients and pollutants, as they provide a comparatively low velocity environment that promotes deposition of suspended particles. However, because an inverse relationship exists between cross-sectional surface area and flow velocity, as these reservoirs fill with sediments, flow increases and sediment trapping efficiency is lowered (Hirsch, 2012; Lang, 1982). As a reservoir progressively infills, preferential

deposition of larger, faster settling sediments is typical, while smaller particles are able to remain in suspension and transport downstream (Langland, 2009; Langland & Cronin, 2003). Additionally, smaller particles can carry more nutrients (Gibbs et al., 1971; Lee & Wiberg, 2002), and so are responsible for greater contributions of particulate Phosphorus transport and ecological degradation downstream (Hainly et al., 1995; Horowitz et al., 2012). The Conowingo reservoir is estimated to be at virtually full sediment storage capacity, and exists in a state of “dynamic equilibrium” (Langland, 2015). In such a state, the reservoir is near capacity until scour events (river discharge of >300,000 cfs) evacuate sediment from the reservoir, thereby availing storage volume for sediment trapping until it again meets capacity (Hirsch, 2012; Langland & Cronin, 2003).

Scientific interest in these scour events and Bay ecosystem response has been consistent for nearly half a century, ever since high river discharge and high sediment concentrations resulting from Hurricane Agnes in 1972 decimated populations of Bay species. Ecological fallout from this storm and other environmental threats prompted the establishment of the United States Environmental Protection Agency’s Chesapeake Bay Program (CBP) which later enacted the 2010 Total Maximum Daily Load (TMDL) under the Clean Water Act. The TMDL outlined restrictions for industry and the public on sediment and nutrient inputs in order to improve the ecosystem in the Chesapeake Bay (United States Environmental Protection Agency, 2020). The following year saw Tropical Storm Lee, the largest storm to hit the bay since Agnes. In the aftermath of Tropical Storm Lee, which was responsible for 39% of total suspended sediment discharge for the entire preceding decade (Hirsch, 2012),

a popular National Aeronautics and Space Administration (NASA) satellite image depicting an opaque, brown sediment plume extending over 150km from the head of the Chesapeake Bay (Figure 1.3) illustrated the extent of these scour events for the broader public. Consequently, increased public and scientific attention has been drawn to the transport dynamics of suspended sediments in Chesapeake Bay.

Among these studies have been many involving the Chesapeake's Estuarine Turbidity Maximum (ETM), a region of convergent flow at the limit of the gravitational circulation of fresh surface water and saline bottom waters in the upper Bay (Sanford et al., 2001; Schubel, 1968). The Bay's ETM serves as the secondary defense against sediments that managed to escape the Conowingo Reservoir, as the complex physical dynamics present in this region also act as an effective sediment trap at low to moderate flows (Sanford et al., 2001). A combination of turbulent action and the introduction of ionically charged salts and organic material increase the number of collisions and the stickiness of particles, allowing suspended sediments to aggregate rapidly, by a process called flocculation, into larger particles called flocs that settle quickly out of the water column (Sanford et al., 2005; Van der Lee, 2000).

The Susquehanna River alone is responsible for 87% of freshwater discharge (Schubel & Pritchard, 1986) and 83% of organic and inorganic particulates entering into the upper third of the Bay (Biggs, 1970), and so the Susquehanna and upper Bay systems are closely coupled (Schubel & Pritchard, 1986). Despite decreasing trends in sediment and nutrient export from the Susquehanna watershed since the 1980s, sediment and phosphorus inputs to the Bay have shown increasing trends since the 1990s (Zhang et al., 2013), which is symptomatic of the Conowingo reservoir

reaching its capacity and being unable to continue to effectively trap sediments (Langland & Cronin, 2003; Zhang et al., 2013). Of the combined contribution by the nine largest Chesapeake tributaries, discharge from the Susquehanna is estimated to be responsible for ~92% of the rise in trend of suspended sediments and ~68% of the rise in trend of nutrients (Zhang, Hirsch, & Ball, 2016). An isolated, and more concerning, comparison of the Susquehanna's anticipated annual suspended sediment and nutrient (Total Phosphorus) loads after reaching Conowingo reservoir sediment storage capacity estimate increases of 150% and 50% respectively (Langland & Cronin, 2003).

While much of this knowledge is derived from robust long-term records of river discharge and suspended sediment and nutrient concentrations, sediment characteristic data that could indicate settling behavior and the fate of these sediments is scarce. Compounding this issue, the data from extreme events like Tropical Storm Lee and Hurricane Agnes are limited, so the magnitude of scour and fate of those sediments in the estuary are relatively unknown (Zhang, Hirsch, & Ball, 2016). Furthermore, the effect of moderate, more frequent scour events on the estuary and the characteristics and transformation of sediments from these events is uncertain.

To better understand the impact of storm events and Susquehanna discharge in general on the upper Bay, it is necessary to better understand Susquehanna sediments' fate and the processes that govern it. The following three chapters report the details and findings from three different but related investigations of the spatial and temporal transformation of suspended sediments that escape the Conowingo reservoir, and their relationship with Susquehanna discharge rates, as they travel downstream

through the upper Chesapeake Bay. The first investigation involves sediments at the Conowingo Dam, while the following two explore sediments in the surface layer of the upper Bay, an area extending from the bay head at Conowingo Dam to the Bay Bridge near Annapolis, MD. These latter two investigations focus solely on the surface layer over the shipping channel, as sediments here are likely to be from recent Susquehanna sediments rather than from shoreline erosion or resuspension (Langland & Cronin, 2003).

Of particular interest are measures of suspended sediment concentration, settling speed, grain size, and bulk density with distance downstream. While there is an established relationship between Susquehanna discharge and sediment concentration, it is unclear what relationships exist between these parameters and sediment settling speed and distance. This thesis investigates variation in these sediment characteristics in order to better predict the fate of Susquehanna sediments within Chesapeake Bay.

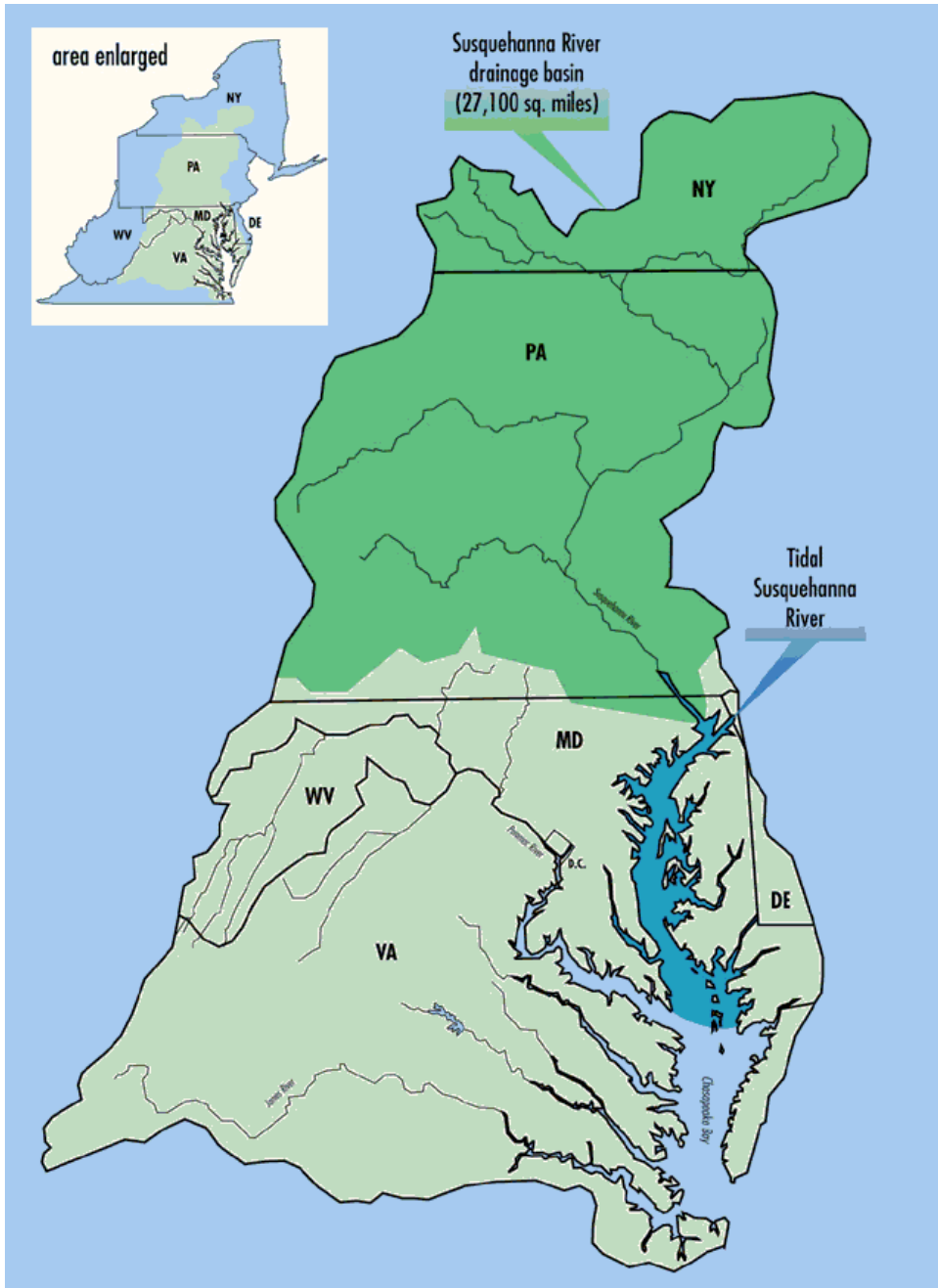


*Figure 1.1.* Map of the Chesapeake Bay watershed where thin black lines mark major inland rivers and thick black lines mark state borders. The Susquehanna River watershed is highlighted in dark green. Image credit: Chesapeake Bay Foundation.





*Figure 1.2.* Aerial photos of the Conowingo Hydroelectric Dam and reservoir during typical (top, Photo Credit: Will Parson, Chesapeake Bay Program) and high (bottom, Photo Credit: Cecil Whig) river discharge conditions.



*Figure 1.3.* NASA satellite image of a sediment plume over 150 km in length extending from the Susquehanna River in the North to far downstream in the Chesapeake Bay. Photo Credit: NASA Earth Observatory.

## Chapter 2: Upstream Particle Characteristics and Response to Susquehanna River Flow

### 2.1 Introduction

The impact of nutrient-laden sediments from the Susquehanna River on certain areas of the Chesapeake Bay vary under different river flow conditions due to the influence of flow rates on sediment transport. Under typical flow conditions, the Estuarine Turbidity Maximum (ETM) of the upper Bay traps 70-100% of Susquehanna sediments (Biggs, 1970; Donoghue et al., 1989; Schubel & Pritchard, 1986), but transport and settling fate is less certain during high river flow conditions. This uncertainty is due in part to lack of data but also to vastly different sediment fates observed during relatively similar high flow events (Sanford et al., 2001). The disparity in sediment fate of two similar events is suspected by Sanford et al. (2001) to be caused by seasonal changes in particle settling speeds. During an early fall event, Sanford et al. (2001) observed large, fast settling clusters of fine particles that would have settled much more slowly if they were disaggregated, like the fine disaggregated particles observed much further downstream in a late winter event.

Chesapeake Bay sediment transport models aim to forecast downstream sediment fates that best match historical observations. Settling speed is the most influential factor governing sediment transport, but there is considerable variability in settling speeds used for model inputs (e.g. Cerco et al., 2013; Cheng et al., 2013; Liu & Wang, 2014; Palinkas et al., 2014; Park et al., 2008). There is little data available

for particle settling speed of sediments entering the upper Bay, and therefore the United States Geological Survey (USGS) disaggregated particle grainsize data from their Conowingo Dam monitoring station may be particularly useful for the formulation of a characteristic settling speed; USGS water quality data and other particle size data is commonly used in formulation of particle settling speeds in upper Bay sediment transport models (e.g. Cerco et al., 2013, Cheng et al., 2013; Palinkas et al., 2014). However, it is reasonable to question if these disaggregated particle values are truly representative of the sediments passing through the dam, as particles have been known to aggregate in freshwater riverine conditions (Guo & He, 2011). It is also unclear whether potentially aggregated particles break apart when passing through Conowingo Dam's hydroelectric turbines. A simple solution used to produce more realistic model outcomes is to adjust sediment settling speed inputs until accurate results are produced (e.g. Cerco et al., 2013; Cheng et al., 2013, Palinkas et al., 2014). Despite the region's history of frequent flood events that scour faster settling reservoir bed materials, the models often do not account for changes in settling speed under different flow conditions, and at most consider only very limited changes in particle size distribution or in resuspension (e.g. Park et al., 2008). This chapter will investigate the settling behavior and physical characteristics of lower Susquehanna suspended sediments under various, but predominantly high, flow conditions. This will uncover how fast sediments actually settle at the Conowingo Dam, whether settling speeds are dissimilar to what can be estimated from USGS disaggregated particle size data, and if settling speeds change when passing through the dam or with changes in river flow.

## 2.2 Methods

### 2.2.1 Owen Settling Tube Analysis

In order to describe particle characteristics of suspended sediments entering the upper Bay, suspended particles from water sampled at the Conowingo Dam during river discharge events exceeding 100,000 (cfs) were analyzed for settling speed and mass contribution. Due to infrequency of high flow events during the field program, samples for settling speed analysis were collected on just seven days across a total of three high flow events. The settling speed procedures used were similar to those first described by Owen (1976) and later modified by Malpezzi et al. (2013) that use bottom withdrawal settling tubes (Figure 2.1) and accompanying analysis to measure particle settling speed. These experiments operate on the assumptions that the column of water within the tube is initially still and has a uniform distribution of sediment particles in suspension, and that these particles are non-uniform in characteristics and thus will settle at various rates. Samples are drawn from the bottom of the tube at geometrically spaced intervals, providing a snapshot of the particles that settled during that interval. Samples drawn from the bottom of the tube early on in the experiment would be mostly comprised of fast settling particles, while progressively later samples would be mostly comprised of progressively slower settling particles.

Sampling for Owen settling experiments occurred at similar times on each of the seven dates using 5 L carboys provided by the University of Maryland Center for Environmental Science (UMCES). Personnel from AECOM, an engineering company contracted for work at the dam, drew 5 L samples from a stilling well located between

two spill gates on the reservoir side of the dam. USGS personnel collected 5 L samples from the turbine outlets on the southwest side of the dam, working from the dam's catwalk where they have historically sampled. On four of the seven days, USGS also collected samples for their own disaggregated particle sizing procedures (Guy, 1969), as part of their multi-decadal water quality database (Table 2.1). The 5 L samples were promptly transferred to an on-site lab for settling speed experiments, usually within an hour. In the event of short delays, samples were refrigerated to inhibit flocculation.

Owen settling speed experiments employed a slightly modified version of the settling tube described in Malpezzi et al. (2013), the only modification being the use of a reflective bubble wrap jacket instead of a water jacket. The time period in which samples are taken was extended from 80 min to as much as 111 min, which allows for the settling of finer particles that are typical of the lower Susquehanna River and the reservoir (Cronin et al., 2003; Hobbs et al., 1992). The number of sampling intervals was increased to 10, which allows for finer resolution but also limits the amount of material available for analysis, which can be problematic when sediment concentrations are low. The settling tubes were flushed with deionized water, drained, and plugged before each experiment. Carboys were shaken to re-suspend any sediment that may have settled since sampling, and then the contents were poured into the settling tubes. Settling tubes were immediately capped to prevent contamination from dust, marking the start of timed sampling intervals (time 0). At the time of each interval, samples were drawn from the bottom of the settling tube, approximately filling one pre-washed and dried 500 ml bottle. During the final

interval of each experiment (111+ min), it was attempted to avoid sampling the last few milliliters of water; This water often contains an artificially high concentration of buoyant particles, and so it is preferable to exclude this from the final sample (Malarkey et al., 2013). Immediately after each sample withdrawal, the sample is measured for volume and then filtered under gentle vacuum using either 0.7  $\mu\text{m}$  2.5 cm glass fiber filters or 1.5  $\mu\text{m}$  14.2 cm membrane filters, depending on sample concentration. Filters had previously been labeled and weighed by UMCES Horn Point Lab Analytical Services, to whom we returned the sample filters for processing following their TSS standard operating procedures (United States Environmental Protection Agency, 1979).

Settling tube experiment data was analyzed using an Excel spreadsheet implementation of Owen (1976) techniques, published in supplemental materials accompanying Malpezzi et al. (2013), that calculates frequency distribution (a fraction of total sediment mass) and particle settling speed. Calculating sample settling speed, a measure of fall distance over time, is complicated by the decreases in water column height with each withdrawal. However, Owen's method uses the observed changes in particle mass and other properties to approximate their distributions as a function of settling speed. Spreadsheet inputs include sample volume, time, sediment mass, and a static measure of the settling tube's horizontal cross-sectional area (Figure 2.2).

The spreadsheet also produces a number of plots describing the distribution (Corrected Cumulative Fraction, Frequency (%)) of settling speeds ( $w_s$ ), including comparisons to the fraction of non-settling of particles (Figure 2.3, Figure 2.4). Very

fine and non-settling particles are typically a substantial fraction of sediment composition in this area (Cronin et al., 2003; Hobbs et al., 1992), and so it is important to assign it a reasonable  $w_s$  value for consideration in this analysis. A speed of  $<0.015$  mm/s is shown in Figure 2.2 for the final sample containing non-settling particles, as this is the slowest resolvable settling speed of particles that take less than 111 min to settle the 1 m maximum depth of the settling tube. Some of the 111+ min concentration values are artificially high due to human error in attempting to exclude the last few milliliters of highly concentrated non-settling particles. However, the data analysis procedures correct for this error.

Settling tube data was also analyzed using a curve-fitting Matlab implementation of Owen (1976) techniques (Malarkey et al., 2013) developed for use with Owen settling tube data. Like the Malpezzi (2013) spreadsheet, this Malarkey (2013) Matlab analysis calculates values of frequency distribution ( $F(w_s)$  (%)) of settling speed ( $w_s$ ), and produces associated plots, but with additional physical constraints that control the curve-fit to the cumulative fraction of suspended sediment over time. The Matlab analysis also expands upon the spreadsheet analysis by extrapolating the distribution of the substantial non-settling fraction of sediments found in the final sample, which is otherwise represented by one large spike in sediment contribution (0.75) of the slowest settling particles in the Malpezzi (2013) spreadsheet analysis (Figure 2.4). The Malarkey (2013) Matlab method yields a smoother fit to the settling speed distribution by fitting a polynomial curve to the data and basing the rest of the calculations on that function (Figure 2.5). The integral under the curve for the entire slow settling speed range is equal to the fraction of total



mass contributed by non-settling particles. Not much investment should be put in the high resolution extrapolations at the slower end of the settling range, as these estimations are well beyond the physical limits of the final sampling interval.

Preliminary comparisons of the two Owen analyses show similar distribution of sediment mass, but with the Matlab analysis appearing to have much greater range and resolution despite being based on the same set of data (Figure 2.6). This difference is due to the Matlab analysis extrapolating settling speeds at both the very high and very low ends of the range, and so the techniques agree very reasonably at the shared middle range of settling speeds. The comparison of these two curves also revealed that sediments could adequately be described as belonging to one of four settling speed classes:  $<0.01$  mm/s, 0.01-0.2 mm/s, 0.2-2 mm/s, and  $>2$  mm/s (Figure 2.6). The slowest settling class threshold,  $<0.01$  mm/s, was selected based on settling speeds of the typical next to last interval samples. Sediment contribution (MF) and settling speed ( $w_s$ ) values from each Owen procedure are binned by settling class, and a mean settling speed is calculated for each class, weighting each individual speed by its associated mass fraction and summing over all estimates in each category (Appendix 1). The settling classes provide a consistent format for comparison of results between particle characteristic data that may differ in sampling and analysis methods.

### 2.2.2 USGS Particle Size Analysis

The USGS has a number of long-term water quality monitoring sites across the United States, one of which is at the Conowingo Dam, site USGS 01578310. On four of the seven days that Owen sampling occurred, the USGS collected their own

suspended sediment samples at Conowingo Dam for standard particle size analysis (Guy, 1969). The resulting disaggregated particle size mass contribution data can be found within the USGS National Water Information System (NWIS) online database, a record of daily river discharge (cfs) and periodic lab water quality sampling for a variety of parameters, namely Total Suspended Solids (TSS, mg/L) and disaggregated particle diameter (mm,  $\mu\text{m}$ ), dating back to the 1970s. Between 1979-2016 there are a total of forty samples at Conowingo with a complete set of disaggregated particle size, TSS, and river discharge data; four of these samples coincide with Owen sampling dates during 2015-2016. Approximating settling speed for these samples can avail data similar to Owen outputs from a greater number and magnitude of flows, albeit a less certain and indirect measure of settling speed.

USGS NWIS sediment characteristic data from the four shared sampling dates was analyzed to fit the four settling classes. The standard methods for USGS grain size analysis are described in Guy (1969); the key detail being that sediment particles were disaggregated prior to sizing analysis. The resulting data are a measure of cumulative percent mass of sediments finer than a series of 10 particle sizes, with particle size thresholds measured by a combination of sieve diameter (1 mm, 0.5 mm, 0.25 mm, 0.125 mm, and 0.0625 mm or 62.5  $\mu\text{m}$ ) and fall diameter (31  $\mu\text{m}$ , 16  $\mu\text{m}$ , 8  $\mu\text{m}$ , 4  $\mu\text{m}$ , and 2  $\mu\text{m}$ ). The difference in cumulative percent mass yields mass contributions for each interval between size thresholds. Assigned to each interval is a single characteristic grain size value equivalent to the average of lower and upper threshold size values, the smallest endmember has no lower threshold and so an

approximate average size of 1  $\mu\text{m}$  is assigned. A characteristic settling speed for each size was then calculated using Stokes Law (2.1) for particles up to 62.5  $\mu\text{m}$ ,

$$w_s = \frac{1}{18} * \frac{(s-1)}{v} * g * d^2 \quad (2.1)$$

and using the approximate large particle expression of Soulsby (1997) (2.2) for particles larger than 62.5  $\mu\text{m}$ ,

$$w_s = \frac{10v}{d} \left[ \left( \frac{0.01(s-1)gd^3}{v^2} + 1 \right)^{0.5} - 1 \right] \quad (2.2)$$

where  $s = \rho_p / \rho$ ,  $\rho_p$  is particle density,  $\rho$  is fluid density,  $v$  is fluid kinematic viscosity, and  $d$  is particle diameter.

Estimating settling speed using particle size and Stokes Law is incidentally the inverse of the USGS procedures for finding mass contributions for the five smallest particle size thresholds ( $\leq 31 \mu\text{m}$ ). The resulting settling speed and mass fraction data was then sorted into settling class in the same manner as the Owen data (Appendix 1). Historical USGS disaggregated particle size data from all forty samples were also processed for later discussion involving corresponding USGS daily river discharge values from a long-term daily monitoring program at Conowingo Dam (Appendix 2). Per-class settling speed and mass fraction values for the four same-date USGS data were then statistically compared to Owen counterparts (Figure 2.7) to test for significant difference between datasets (Appendix 3).

Same-date, per-class, mass fraction values for the three settling analyses (Excel, Matlab, USGS particle size) and two sampling locations (Spill gate, Catwalk), henceforth referred to as five ‘methods’, are compared in Matlab using Kruskal-Wallis and Multiple Comparison tests to determine if differences between the

methods were statistically significant. Kruskal-Wallis is a valid way of applying analysis of variance (ANOVA) for a non-Gaussian population (The MathWorks, 1993). The test compares our method data sets, such that each set is individually compared to each other set, to determine if all possible combinations of method-comparisons agree with 95% certainty (p-value <0.05). Multiple Comparisons shows more detailed results from Kruskal-Wallis tests, revealing which specific method-pairings, if any, caused a disagreeing Kruskal-Wallis test result. In additional Kruskal-Wallis and Multiple Comparisons tests, method data sets were grouped by settling class, allowing more specific identification of the circumstances under which methods may disagree, if at all. This is especially important for isolating outlier classes or methods that might otherwise cause the methods to appear dissimilar. Comparing the methods overall on these four dates allows for a small, but statistically significant, sample size of 16 values per method type. However, testing between methods by settling class have only 4 samples per comparison, so it is reasonable to consider these per-class results with more scrutiny.

### 2.3 Results and Discussion

The range in sediment concentrations (11-118 mg/L) sampled on the four dates was considerably larger than the range of flows (107,000-171,000 cfs) observed during this time. And although TSS concentrations increased with increasing flow in general, the left hand plot of Figure 2.8 shows significant variability in concentrations between samples from similar flows. USGS TSS values were always higher than the TSS values from corresponding Owen tube samples collected at either the catwalk or

spill gate location (Figure 2.8), despite USGS also sampling at the catwalk. This reflects the slight losses in material from excluding the last few milliliters of water during the final Owen sampling interval, which is done to avoid buoyant particles and particles that stick to the tube walls during the experiment. However, these losses do not seem to affect the relative settling distributions of the overall sample (Malarkey et al., 2013; Malpezzi et al., 2013). Despite the higher USGS catwalk TSS values, Owen spill gate samples tended to have slightly higher TSS values than Owen catwalk samples (Figure 2.8). Palinkas et al. (2019) describes a positive power law relationship between TSS and flow at the Conowingo dam, and the observed TSS values cluster around this trend line, with particularly strong agreement at lower flows.

On the four shared sampling dates, mass fractions for different settling speed categories varied only slightly across the five methods. Compared to mass fraction values from the Owen tube Matlab analysis, mass fraction values from the Owen tube spreadsheet analysis appeared to be slightly higher for the slowest settling particle category ( $<0.01$  mm/s) and slightly lower for the second slowest category (0.01-0.2 mm/s). Mass fraction values for USGS disaggregated particle size data were consistent with results from both Owen tube analyses, tending to split any differences between them (Figure 2.9). For the range of flows sampled in this analysis, approximately 70% of particles settled slower than 0.01 mm/s, 25% settled between 0.01-0.2 mm/s, 4% settled between 0.2-2 mm/s, and 1% settled faster than 2 mm/s.

Despite these minor visual differences, statistical analysis showed no significant difference between any of the five methods as a whole across the four

dates (Appendix 3); when doing the same comparisons between data within a specific settling category, only the fastest settling category ( $>2$  mm/s) showed significant differences between some methods across all four dates (Appendix 3). The lack of significant difference indicates that settling speed estimates based on USGS particle sizing are representative of actual settling speed distributions. These findings also imply that particles passing through or over the dam face either become, or already are, effectively disaggregated by the energetic turbulent flow conditions found there.

Significant statistical agreement between empirical and estimated settling speed values justifies the further analysis of all available USGS disaggregated grain size data (Appendix 2). Over the 37-year period from 1976-2016, forty samples had complete sets of grain size, TSS, and river discharge data for which sampled flows ranged from 14,800-592,000 cfs, and TSS from 17-2,980 mg/l. The characteristic settling speeds for the four categories, defined as the average of all samples' weighted average settling speed in that category, were 0.005 mm/s, 0.068 mm/s, 1.175 mm/s, and 17.941 mm/s, respectively. The left hand plot of Figure 2.10 shows an exponential fit of the 37-year TSS and flow data that is similar to other established relationships between TSS and flow at Conowingo (e.g. Palinkas et al., 2019, Cheng et al., 2013). The slightly higher values in the 37-year trend could be due to the addition of new data that was not included in Palinkas et al. (2019). In accordance with four-date USGS data clustering around the Palinkas et al. (2019) curve, the right hand plot of Figure 2.10 shows reasonable agreement between four-date Owen data and this 37-year USGS data fit.

Classifying USGS disaggregated particle size data by estimated settling speed into the four categories and then pairing with USGS daily average river discharge data reveals the relative effect of flow on each category's contribution to total sediment mass (Figure 2.11). The linear fits for each class's contribution to the total mass shown in Figure 2.11 sum to 1, as they must to conserve mass. As Susquehanna River discharge increases, the fraction of total mass contributed by the slowest settling speed category decreases and the fraction of the middle two categories show a slight increase. The fastest settling category also experiences slight increases, but even at the highest flows it only contributes a small fraction (<2%) to total mass. The changes in mass contribution by settling categories is likely the result of faster river flow being capable of suspending larger particles.

Numbering the categories by increasing settling speed, with 1 being the slowest and 4 being the fastest, the linear fits for the 37-year data seen in Appendix 2 and in Figure 2.11 are (2.3),

$$f_1 = -5.41 * 10^{-7} * Flow + 0.863 \quad (2.3a)$$

$$f_2 = 2.47 * 10^{-7} * Flow + 0.131 \quad (2.3b)$$

$$f_3 = 2.39 * 10^{-7} * Flow + 0.006 \quad (2.3c)$$

$$f_4 = 5.53 * 10^{-8} * Flow \quad (2.3d)$$

Average settling speed per category for the 37-year data is shown in Appendix 2.

Using these average settling speeds, a mass-weighted average particle settling speed ( $w_{s,ave}$ ) across all categories is calculated as,

$$w_{s,ave} = \sum_{i=1}^4 f_i w_{s,i} \quad (2.4)$$

Sand-sized grains contribute only a small portion of total suspended particle mass, so  $w_{s,ave}$  is calculated again using only the first three settling categories; mass fractions for the fourth settling category in Appendix 2 and the values of  $f_4$  in (2.3d) are redistributed evenly across the three remaining categories, such that mass fractions and equations still sum to 1, in order to conserve mass. Mass-weighted average settling speed is susceptible to skew by the very small but very fast settling fraction of sand sized particles in the fourth settling class, which leads to major increases at higher flows, as seen in Figure 2.12; The  $w_{s,ave}$  that includes the sand fraction increases greatly at above average river flows (~38,000 cfs) in comparison to the sand-exclusive values.

Approximate cumulative settling speed distributions at incrementally greater flows are shown in Figure 2.13, beginning at a settling speed of 0.0001 mm/s which corresponds to particles small enough to meet the common operational definition of a dissolved substance (<0.45  $\mu\text{m}$ ). The cumulative plot assumes an even distribution of material settling at speeds slower than the characteristic settling speed of the first particle class (0.005 mm/s), after which values are calculated using the linear best-fit equations from Figure 2.11 (2.3a-d). The curves in Figure 2.13 intersect the dashed horizontal 0.5 contribution line at the median settling speed ( $w_{s50}$ ) of Conowingo sediments at respective levels of river flow. Median settling speed is sometimes reported in sedimentation studies because it is less susceptible to skew, and because of the assumption that material settling slower than 0.005 mm/s is evenly distributed, it can be linearly approximated for the various flow and sand conditions. The red box in Figure 2.13 highlights the very narrow range of median settling speeds across all



flows with and without sand; This shows that the median settling speed is virtually unchanged by the sand fraction and by flow, ranging from 0.003 to 0.004 mm/s.

Figure 2.12 shows a sand-inclusive weighted average settling speed of 0.069 mm/s at 38,000 cfs, and shows that exclusion of the sand fraction yields a much smaller  $w_{s,ave}$  value of 0.032 mm/s at the same rate of flow. This large difference is due to the small fraction of sand sized particles having settling speeds large enough to skew the average upwards. Palinkas et. al (2014) suggests that sand sized particles at Conowingo settle so quickly that they are unlikely to be transported beyond the Susquehanna Flats, a shallow area populated by aquatic vegetation located at the mouth of the Susquehanna River where it opens up to the head of the Bay, so it would be reasonable to ignore the sand fraction when identifying settling speeds that are characteristic of Conowingo sediments flowing into the upper Bay.

Table 2.2 lists the median ( $w_{s50}$ ) and weighted average ( $w_{s,ave}$ ) settling speeds both with (Sand) and without (No Sand) the sand fraction, and also lists the difference between the median and weighted average values ( $\Delta w_s$ ) as well as the difference between the sand inclusive and exclusive values ( $\Delta$  Sand). Median settling speeds with and without sand are much lower than their weighted average counterparts across the five flow conditions; sand exclusive median settling speeds ( $w_{s50}$  No Sand) range from 0.003-0.004 mm/s while sand exclusive weighted average settling speeds ( $w_{s,ave}$  No Sand) ranged from 0.026-0.179 mm/s. These median speeds are considerably lower than the slowest resolvable settling speed from the Owen tube experiments (0.015 mm/s). This is reasonable as all but two of the forty samples in Appendix 2 had over 50% of their sediment contribution from the very fine clay-sized

particles in the slowest (non-resolvable) settling category ( $<0.01$  mm/s), so the median settling speed from these particular data can only be less than that which can be measured. Median settling speed's resistance to skew by the sand fraction is reflected in Table 2.2, where sand inclusive and exclusive weighted average settling speeds across the five flows saw differences (row  $\Delta$  Sand, column  $w_{s,ave}$ ) of 0.019-0.485 mm/s, whereas the change in settling speed by sand for median settling speed (row  $\Delta$  Sand, column  $w_{s50}$ ) across the five flows only ranged from 0.000001-0.000006 mm/s.

The distinction between weighted average and median settling speeds with and without the sand fraction for these data has serious implications for the purposes of sediment transport modelling in the Chesapeake Bay. The settling speed values used in the models mentioned in Chapter 2.1 are the result of calibrating the models until the chosen settling speed yielded results that compare reasonably to observed transport (e.g. Cerco et al., 2013; Cheng et al., 2013; Liu & Wang, 2014; Palinkas et al., 2014; Park et al., 2008). Model settling speed values across various particle classes used ranged from 0.001-3.3 mm/s with both the median and mode value being 0.03 mm/s, and the settling speeds of the just the finest particle class of each model ranging from 0.001-0.012 mm/s and averaging 0.009 mm/s. The settling speeds of model particle classes overall are more similar to the  $w_{s,ave}$  values than the  $w_{s50}$  values from this investigation, and the speed of the finest particles were at least twice as fast as any  $w_{s50}$ ; this may indicate that  $w_{s,ave}$  is a more reasonable representation of the settling speed of a typical particle entering the upper Bay.

These models' settling speed values are generally very slow, which agrees with both this investigation and with Sanford et al. (2005), as these found that the majority of material coming from the Dam and of disaggregated material from downstream floes belongs to the clay fraction. There is a clear and significant influence by river flow on particle settling speed at the Dam, and Palinkas et al. (2019) recently found that using 4-class, flow-dependent values (like those derived here) significantly improved predictions relative to earlier modeling studies. Using more particle size classes, like those in Figure 2.11, and including the effect of river flow on settling speeds in Bay transport models, like in Palinkas et al. (2019) would be preferable but not always practical. However, it is still possible to select a settling speed for the typical Susquehanna particle that incorporates the influence of river flow, such as  $w_{s,ave}$  (without the sand fraction) from this investigation.

Table 2.1

*Sampling at Conowingo Dam*

Date	<u>4/13/2015</u>	<u>4/22/2015</u>	<u>4/23/2015</u>	<u>4/24/2015</u>	<u>2/26/2016</u>	<u>2/27/2016</u>	<u>2/28/2016</u>
Catwalk	y	y	y	y	y	y	y
Spill gate	y		y	y	y	y	y
USGS	y			y	y		y
River Flow (cfs)	155,000	108,000	109,000	107,000	149,000	171,000	145,000

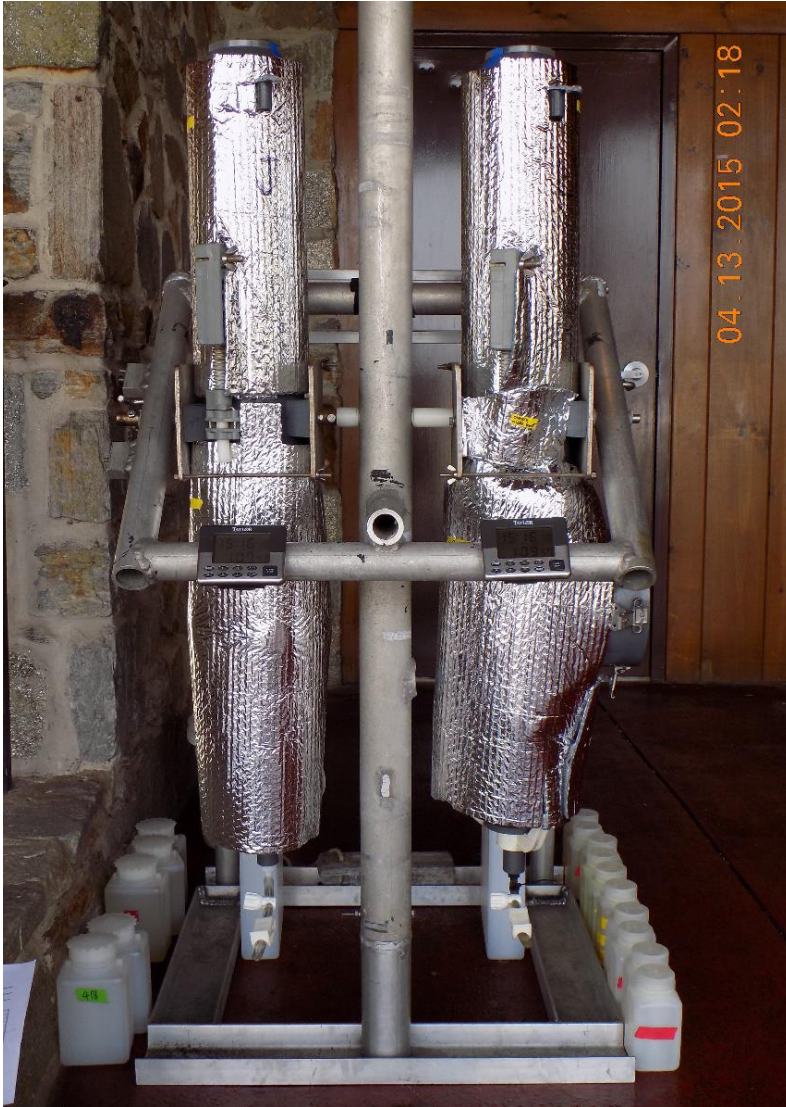
*Note.* Sampling dates (row 1) and locations (rows 2 and 3) for settling experiments and USGS particle sizing at Conowingo Dam (row 3). Sampling is represented by ‘y’; blanks indicate no sampling occurred.

Table 2.2

*Weighted average and median settling speeds for 37-year USGS data*

	20,000 cfs			40,000 cfs			100,000 cfs			250,000 cfs			500,000 cfs		
	$w_{s,ave}$	$w_{s50}$	$\Delta w_s$	$w_{s,ave}$	$w_{s50}$	$\Delta w_s$	$w_{s,ave}$	$w_{s50}$	$\Delta w_s$	$w_{s,ave}$	$w_{s50}$	$\Delta w_s$	$w_{s,ave}$	$w_{s50}$	$\Delta w_s$
Sand	0.046	0.003	0.043	0.072	0.003	0.069	0.149	0.003	0.146	0.342	0.003	0.339	0.664	0.004	0.660
No Sand	0.027	0.003	0.024	0.033	0.003	0.030	0.052	0.003	0.049	0.100	0.003	0.096	0.179	0.004	0.175
$\Delta$ Sand	0.019	0.000001		0.039	0.000003		0.097	0.00001		0.242	0.00002		0.485	0.00006	

*Note.* All values shown are in mm/s. Values in the last row display additional decimals to the first significant digit.



*Figure 2.1.* The settling tube apparatus used in this analysis equipped with two settling tubes insulated with reflective bubble wrap. Containers used for collecting interval samples line the base of the apparatus.

	A	B	C	D	E	F	G	H	I	J	K	L	M	N	O	P	Q	R	
1	Conowingo 1 Spillgate 4/13/15 start 14:06:21 EDT																		
2	Measured Inputs				Calculations based on measured inputs				Corrections to original calculations to compensate for water column shortening during bottom withdrawal				Calculations based on bottom withdrawal tube theory as summarized in the "Owen tube theory" worksheet.						
3	Sample#	Samp. Vol. (ml)	TSS (mg/l)	Sample Time (min)	TSS Mass (mg)	Height of sample (m)	Depth of fall (m)	Cumul. mass (mg)	Depth factor	Corr. Cumul. mass (mg)	Corr. Cumul. fraction	Corr time (min)	lg(corr. time)	lg(e) <sup>2</sup> dcumfrac / d(log)	cumulativ distr	ws (mm/s)	freq distr	conc distr	
4	0			0.0167				0.96	251.98	1.04	262.14	1.00	0.02	-1.76	-0.0062				
5	1	496.5	71.849	7	35.7	0.10	0.86	216.30	1.17	252.16	0.96	8.16	0.91	-0.0090	0.03	2.125	0.03	1.6	
6	2	425.0	63.949	13	27.2	0.09	0.77	189.13	1.30	245.85	0.94	16.90	1.23	-0.0366	0.03	1.026	0.00	-0.2	
7	3	505.0	58.071	18	29.3	0.11	0.66	159.80	1.51	240.64	0.92	27.11	1.43	-0.0471	0.03	0.640	0.01	0.5	
8	4	505.0	59.686	29	30.1	0.11	0.56	129.66	1.79	232.01	0.89	51.89	1.72	-0.0431	0.07	0.334	0.04	2.0	
9	5	465.0	52.785	40	24.5	0.10	0.46	105.11	2.16	227.53	0.87	86.58	1.94	-0.0606	0.07	0.200	0.00	0.0	
10	6	480.0	57.523	58	27.6	0.10	0.36	77.50	2.76	214.11	0.82	160.23	2.20	-0.0740	0.11	0.108	0.04	2.1	
11	7	495.0	49.706	74	24.6	0.10	0.26	52.90	3.86	204.35	0.78	285.88	2.46	-0.0539	0.17	0.061	0.06	3.1	
12	8	492.5	45.212	90	22.3	0.10	0.16	30.63	6.40	196.04	0.75	576.00	2.76	-0.0183	0.23	0.030	0.07	3.7	
13	9	450.0	40.841	101	18.4	0.09	0.06	12.25	16.00	196.04	0.75	1616.00	3.21	0.0000	0.25	0.0107	0.02	1.0	
14	10	300.0	40.841	101+	12.3	0.06	0.00	0.00							1.00	<0.015	0.75	40.8	
15																			
16	Area (cm <sup>2</sup> )	Tot. Vol.			average TSS (mg/l)					Fraction of Settling particles		0.25	13.8		ws50 settling		0.46		
17	48.00	4614			54.6					Fraction of Non-settling particles		0.75	40.8		ws50 total		0.01		

Figure 2.2. Screenshot of the Maplezzi (2013) analysis spreadsheet for the spill gate water sample on April 13th, 2015. A myriad of values are automatically calculated using settling tube experiment inputs (columns A through D), including settling speed (column P) and mass fraction (column Q). *Note.* Early on in this investigation, a minor spreadsheet error ultimately resulted in the  $w_s$  and conc distr values of the second to last April 13, 2015 spill gate and catwalk samples being approximately 10% larger than true experimental value. This error was not discovered until after the conclusion of this study, but the difference is insignificant and does not alter any findings.

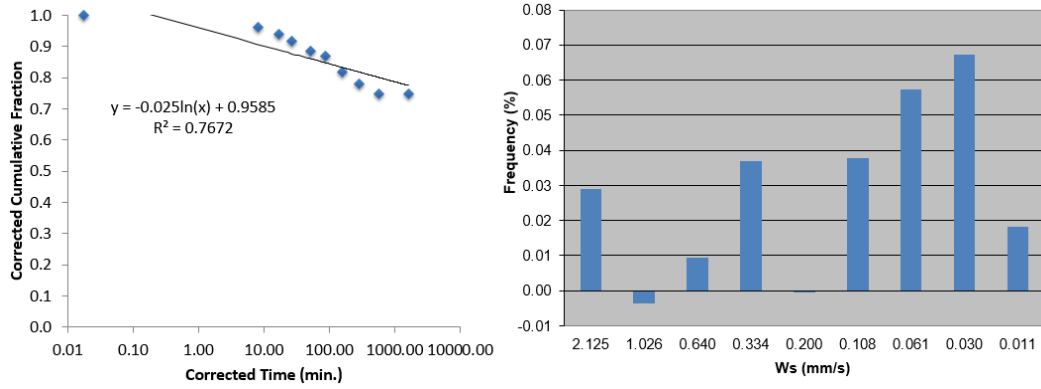
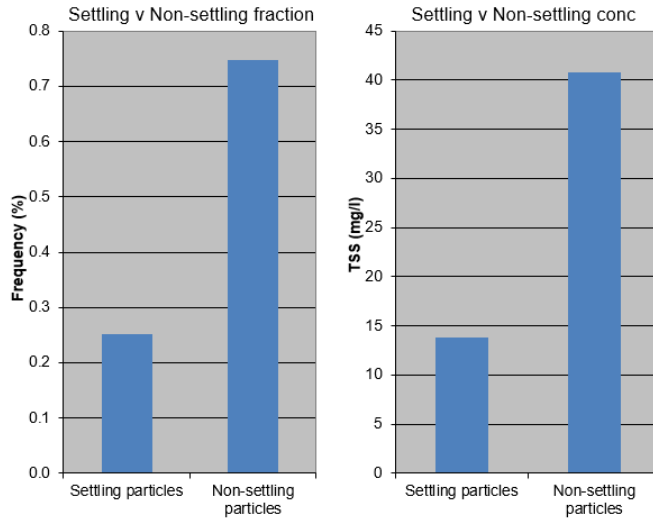


Figure 2.3. Plots of sediment contribution during the 10 settling intervals from the Malpezzi (2013) spreadsheet for the spill gate water sample on April 13th, 2015. Cumulative contribution over time (left) and contribution per settling speed interval (right).





*Figure 2.4.* Fraction of total sediment (Frequency (%)) settling faster or slower than 0.015 cm/s (left) and concentration (TSS (mg/L)) of sediment settling faster or slower than 0.015 cm/s (right) for the spill gate water sample on April 13th, 2015.

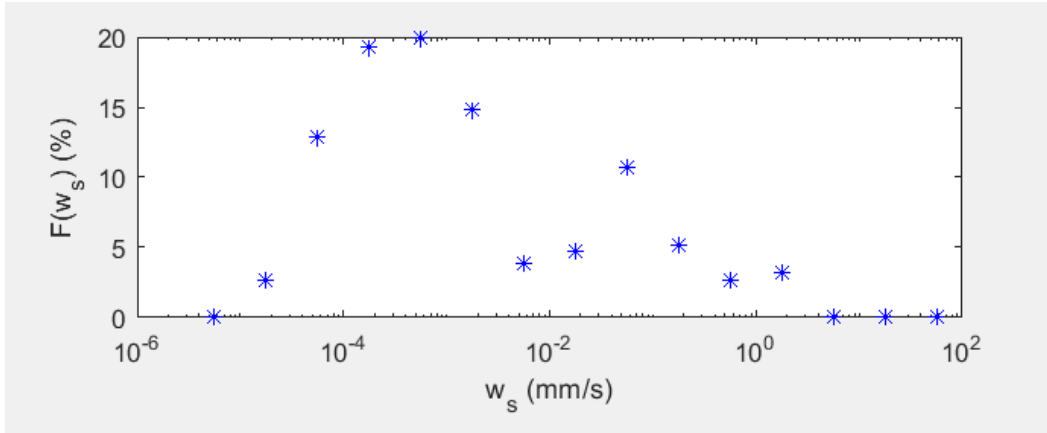
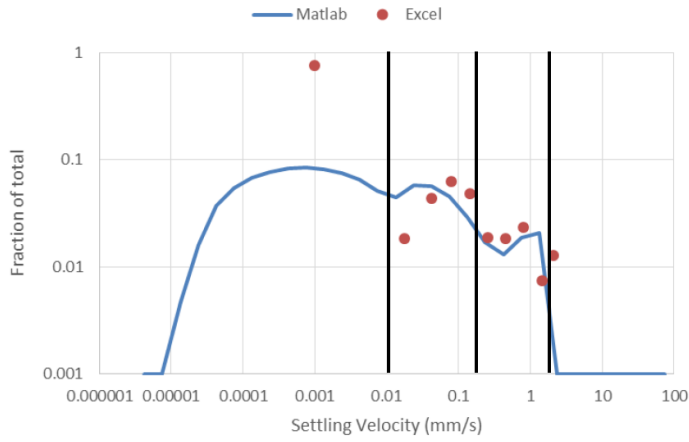


Figure 2.5. Malarkey et al. (2013) script's plot output for percent of total sediments ( $F(w_s)$ ) versus settling speed ( $w_s$ ). The six leftmost dots represent extrapolated details from the final Owen sample from the spill gate on April 13th, 2015.



*Figure 2.6.* Comparison of mass fraction and settling speed values from Excel and Matlab analyses for the spill gate water sample on April 13th, 2015. Vertical lines indicate thresholds of the four settling classes.

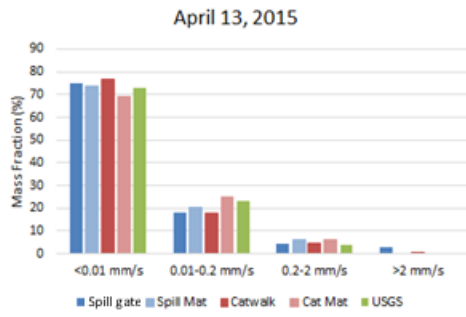


Figure 2.7. Mass contribution by settling speed class for the various sampling locations and analyses for Owen & USGS data sampled on May 13, 2015.

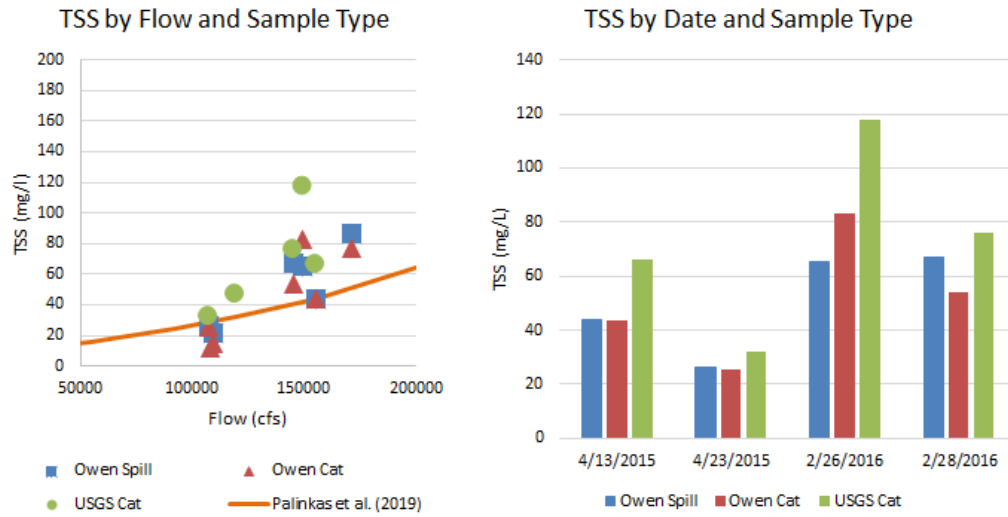


Figure 2.8. TSS values from Owen location spreadsheet outcomes. USGS particle size analysis outcomes sampled on or around the seven Owen sampling days (left). TSS for the three sampling regimes (Owen spill gate, Owen catwalk, USGS catwalk) on the four shared sampling dates (right).

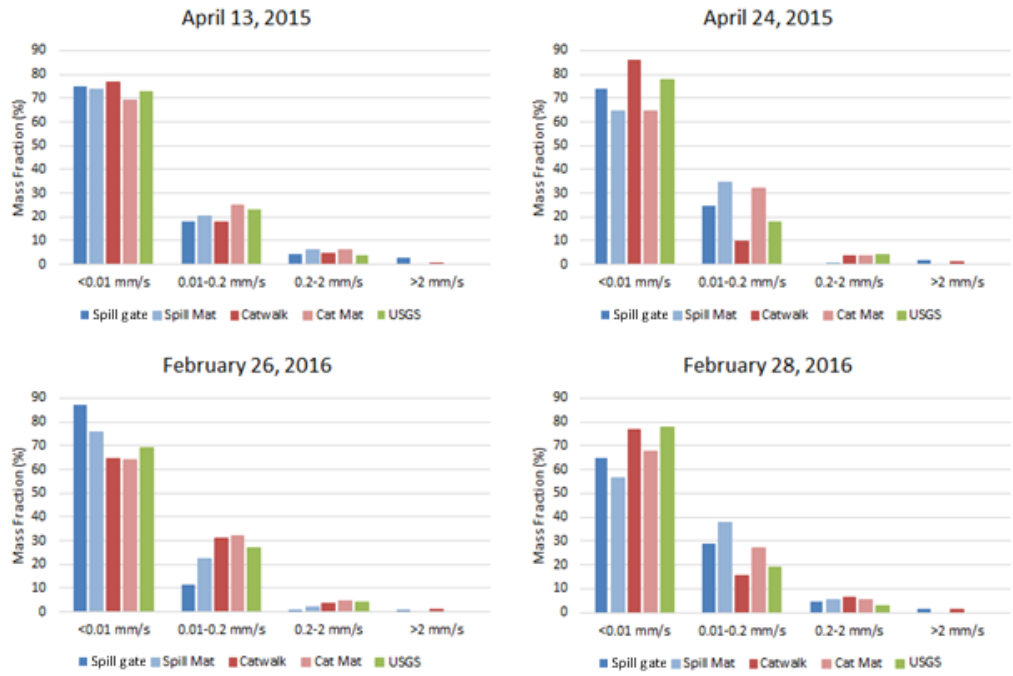


Figure 2.9. Settling class mass fractions for the five analysis methods of Owen and USGS data on the four shared sampling dates. *Note.* Differences between methods within class are not statistically significant.

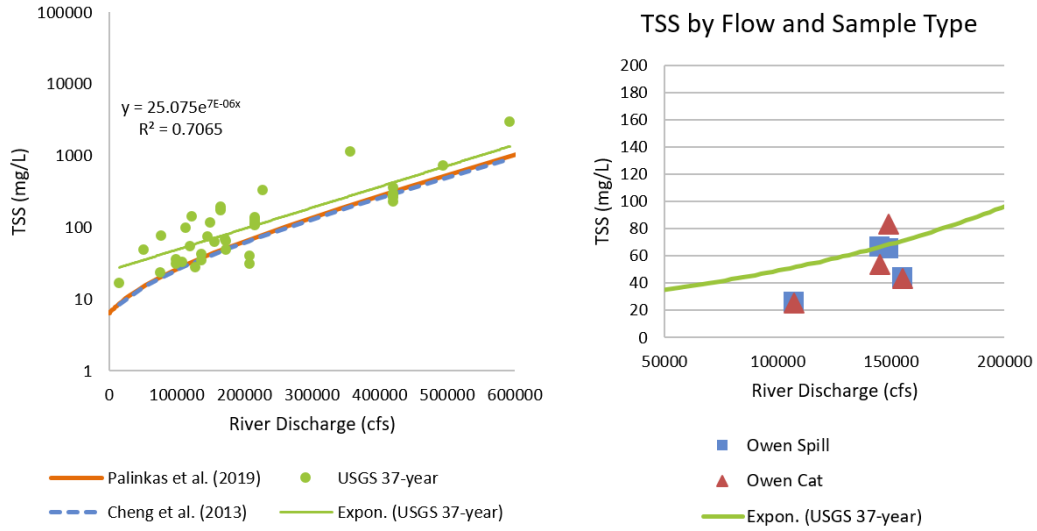
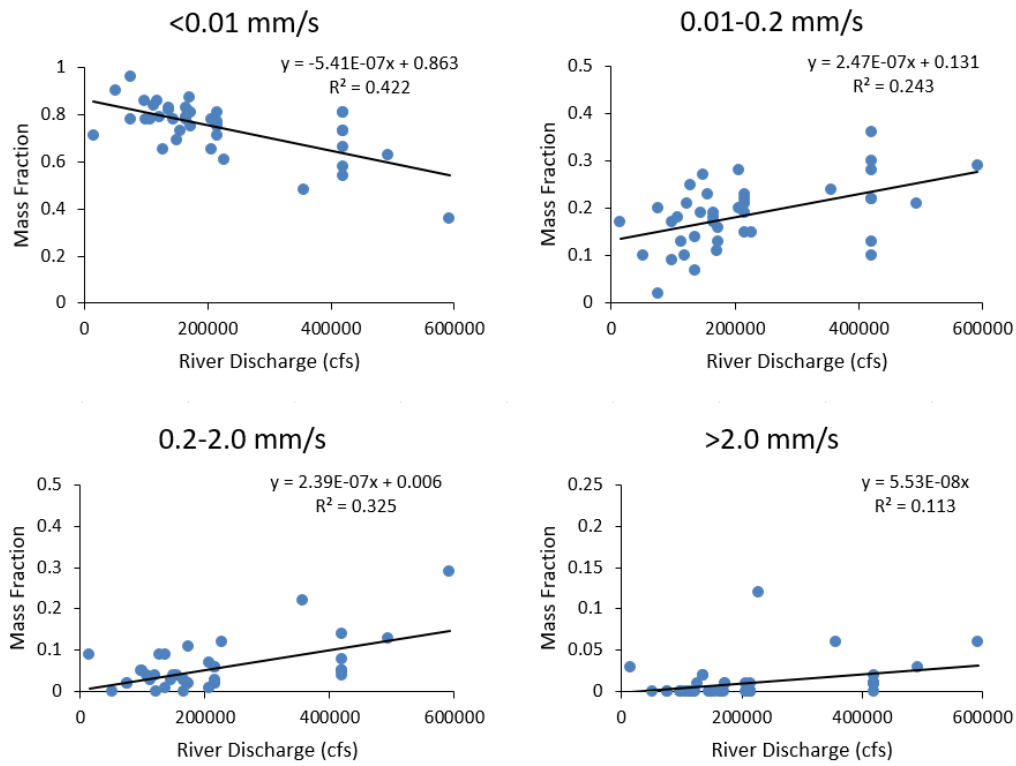


Figure 2.10. TSS and river discharge values and exponential fit of 37-year USGS data at Conowingo compared to similar established relationships (left). Exponential fit of 37-year USGS data compared to four-date Owen TSS values (right). *Note.* These figures are similar to those published in Palinkas et al. (2019) but use an updated dataset.



*Figure 2.11.* Per-class mass contributions by flow at Conowingo Dam for 37-year USGS data. *Note.* These figures are similar to those published in Palinkas et al. (2019) but use an updated dataset.



## With and Without Sand Fraction

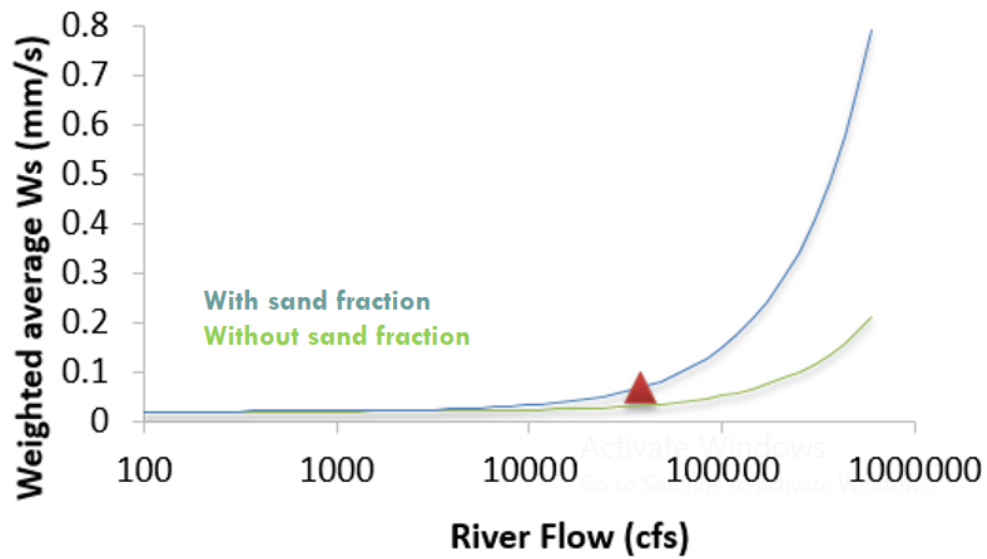


Figure 2.12. Weighted average settling speed ( $w_{s,ave}$ ) including (blue) and excluding (green) the fraction of sand-sized particles (settling class 4) plotted by river discharge on a semi-log scale. The red triangle marks the long-term average Susquehanna River discharge measured at Conowingo Dam (~38,000 cfs).

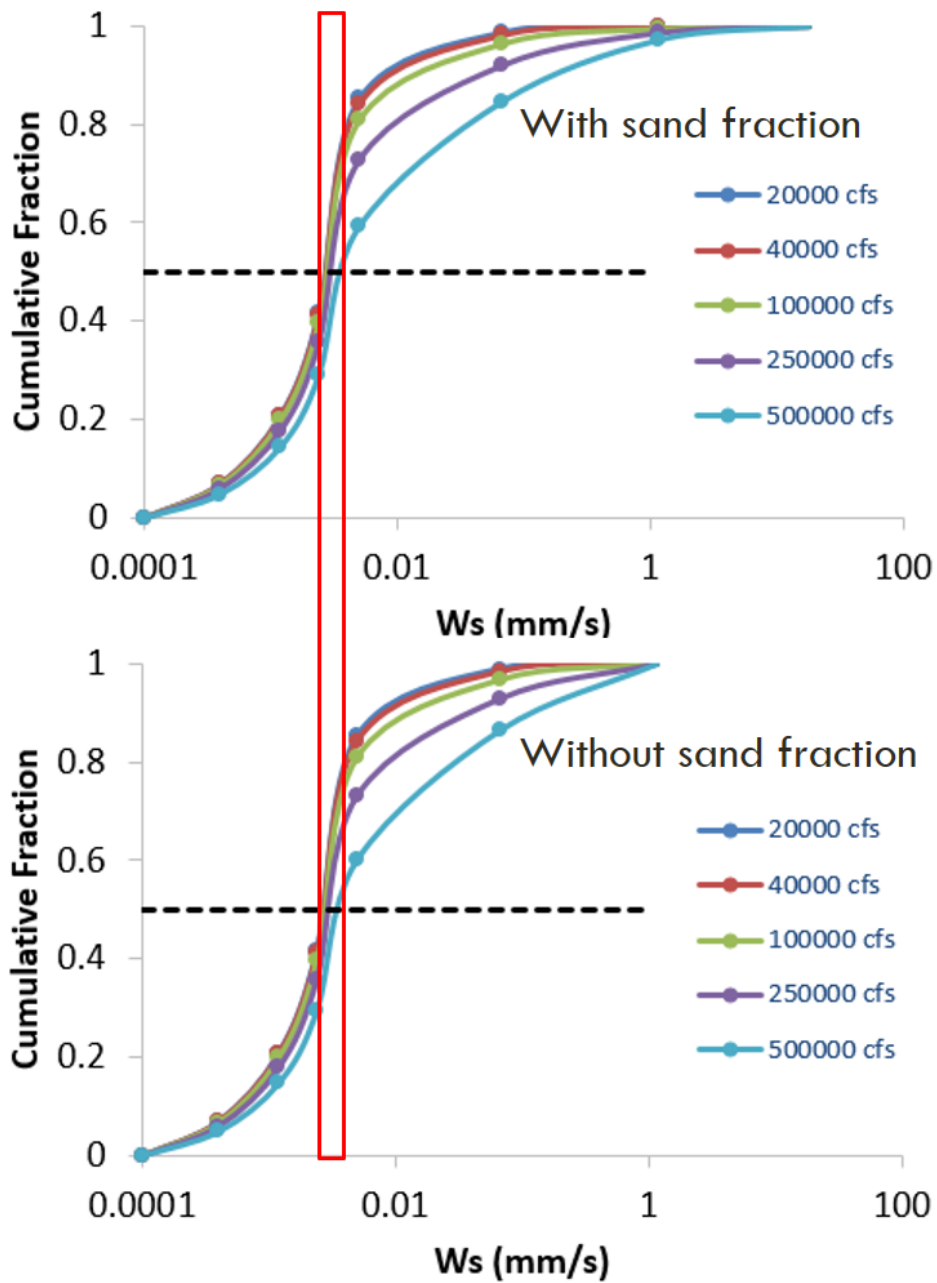


Figure 2.13. Cumulative mass fraction contributed by particles settling at certain speeds (logarithmically spaced and class characteristic settling speeds) under five flow conditions for the 37-year USGS disaggregated particle size data. The top plot shows sand-inclusive values, while the bottom plot shows sand-exclusive values. The intersections with the 0.5 fraction line (black, dashed) represent the median settling speed. The red box highlights the narrow range of median speeds across all flows, both including and excluding sand.

# Chapter 3: Particle Characteristics in the Surface Layer of the Upper Bay

## 3.1 Introduction

Under typical flow conditions, Susquehanna freshwater extends about 40 km down Chesapeake Bay from the river mouth at Havre de Grace, MD, further in the surface layer than in the bottom layer, though there is not a fixed distance due to fluctuations in freshwater flow and wind (Sanford et al., 2001). Until this point downstream the water column is well mixed and fresh, but this is where two-layered circulation develops as freshwater from the Susquehanna first meets with the saltwater intrusion at the limit of the estuarine circulation (Sanford et al., 2001; Schubel & Pritchard, 1986). The area of fresh to salt transition usually coincides with Chesapeake Bay's estuarine turbidity maximum (ETM), an area characterized by high turbidity and sediment trapping, the surface layer downstream of which is about 5 m thick with a sharp pycnocline separating it from the lower layer (Sanford et al., 2001). The surface layer becomes gradually saltier with distance downstream of the ETM due to upward transport from the saline lower layer (Schubel, 1968). In the days following major storm events in the Susquehanna watershed, large sediment plumes can develop due to the massive loads of sediment being flushed downstream as noted in Hirsch (2012) and studied and modeled in Palinkas (2014) and Cheng (2013). The large volume of freshwater being discharged into this relatively narrow part of the bay can steepen the pycnocline and thus inhibit mixing with the lower layer, pushing

the ETM tens of kilometers downstream or bypassing it entirely (Langland & Cronin, 2003; North et al., 2002; Sanford et al., 2001).

Surface layer Total Suspended Solids (TSS) concentrations typically decrease with distance downstream in the Bay due to settling, but levels are elevated near the ETM (Sanford et al., 2005; Schubel, 1968). Under typical conditions, the ETM serves as an effective sediment trap, leading to markedly increased concentrations of settling particles in the region of near-bottom flow convergence where freshwater and saltwater meet (Sanford et al., 2001; Schubel, 1968). Suspended particles tend to aggregate into clusters called flocs in the ETM, which settle faster and promote trapping (Sanford et al., 2005). Flocculation can occur in freshwater (Guo & He, 2011), but the formation of flocs is facilitated by the presence of sticky organic material and ionic charge in saltwater; when particles are in close proximity or collide under such conditions, molecular attraction and polymeric binding allow multiple small primary particles to package themselves into one larger floc with a low density open structure (Cartwright, 2011). Thus, the high TSS saline waters of the ETM make for an ideal location for flocculation, as these are the factors most important for particle aggregation (Mehta et al., 1989). Flocculation further increases the loss of suspended sediment from the surface layer downstream of the ETM, as it allows the small buoyant particles to aggregate into larger, faster settling particles and sink (Sanford et al., 2005). However, the fractal structure of flocs inherently causes larger particles to contain a larger fraction of water, and so these particles sink much more slowly than similarly sized solid mineral particles (Sanford et al., 2005).

Building on Chapter 2, this chapter seeks to describe the changes in particle characteristics, especially size, density, and settling speed, of suspended sediments in the upper Chesapeake Bay. A retrospective analysis of research cruise data from studies in 2001-2002 and 2007-2008 is done in order to characterize sediment settling behavior at various points within the upper Chesapeake Bay. A series of measurements of suspended particle parameters describes spatial distributions of sediment characteristics throughout the upper Bay. Suspended sediment concentration (TSS, mg/L), settling speed ( $w_s$ , mm/s), median grain size ( $d_{50}$ ,  $\mu\text{m}$ ), and effective particle density ( $\text{bulkD}$ ,  $\text{g/cm}^3$ ) reveal the state of flocculation at different points downstream. This reanalysis focuses on the surface layer of the upper Bay, assessing the characteristics of suspended particles under a variety of river flow conditions, and comparing observed behaviors to expected behaviors.

### 3.2 Methods

This investigation aims to identify changes in suspended particle characteristics and settling behavior in the surface layer of the upper Bay through reanalyzing historical water quality and sediment characteristic data from upper Bay field studies carried out during the 2000's. These studies, named *Bio-physical Interactions in the Turbidity Maximum (BITMAX)* (2001-2002) & *BITMAX II* (2007-2008) focused on the role(s) of the ETM in promoting trophic transfers starting with detrital and nutrient loads from the watershed through bacterioplankton, phytoplankton, and zooplankton to anadromous fish larvae. The key component of these studies for purposes of this investigation are research cruises that consisted of

replicate axial transects of the upper Chesapeake Bay, following the deep center channel, that collected depth profiles of particle characteristics and water quality parameters at a series of fixed stations between the Bay Bridge at Annapolis, MD and the head of the Bay near Havre de Grace, MD. Data were collected, analyzed, and archived from throughout the water column, but the primary physical feature of these studies was the near bottom convergence in suspended particle transport that defines ETMs (Malpezzi et al., 2013; Sanford et al., 2005; Sanford et al., 2001). In contrast, the present analysis examines the archived surface layer data from the axial cruises to examine changes in downstream transport.

All cruises included two axial transects of the upper Bay, during which the ship's primary Conductivity, Temperature, and Depth (CTD) frame, equipped with a Laser In-Situ Scattering and Transmissometry (LISST-100C) particle sizing instrument, and standard optical turbidity instrumentation, as well as a hose for obtaining pumped suspended sediment samples, were deployed at each of the thirteen stations along the deep channel in the upper Bay. While the vessel was stopped at each axial station, deploying the instrumentation to collect the vertical profiles of multiple water quality parameters, suspended sediment samples were collected for calibration of the turbidity sensors.

The particle sizing instrumentation, a Sequoia Scientific LISST 100-C, samples at a rate of 5 Hz (data is logged at a rate of 1 Hz) can detect particles ranging in size from 2.5-500  $\mu\text{m}$  (equivalent to scattering at 0.04-7.5° in water) at resolutions based on 32 logarithmically spaced intervals, and ranging in concentration from 1-800 mg/L at a resolution of <1 mg/L (Sequoia Scientific, 2007). LISST size detection

is biased towards the lower middle range of the detection spectrum, and the range and resolution of concentration detection limits is dependent on median particle diameter. At too low of sediment concentrations, size distributions can appear noisy, while in too high of concentrations the lower end of the distribution can appear degraded. Critically, during these cruises, concentrations did not reach either extreme and so size distributions are unlikely to be degraded or distorted by much noise.

Sensor calibrations and LISST data processing followed standard procedures as described in Sanford et al. (2005), from which useful outputs include volume concentration ( $\mu\text{L/L}$ ) of particles in thirty-two size bins spaced geometrically between 2.5-500  $\mu\text{m}$  and percent transmission converted into TSS ( $\text{mg/L}$ ). These data were further processed to yield estimates of median particle size ( $d_{50}$ ) and particle bulk density ( $\text{bulkD}$ ,  $\rho_b$ ), which is a derived measure that includes the density of the water in the pore space of aggregated particles as part of total particle density, such that

$$\text{bulkD} (g/cm^3) = \frac{\text{TSS} (mg/L)}{\text{Vol.Conc.} (\mu\text{L/L})} .$$

Figure 3.1 is a product of the original BITMAX analyses, which visualizes the final form of the parameters from BITMAX processing: TSS,  $d_{50}$ ,  $\text{bulkD}$ , total volume concentration, volume concentration  $> 66.5 \mu\text{m}$ , and volume concentration  $< 66.5 \mu\text{m}$ . Of the axial survey parameters presented in Figure 3.1, this investigation will involve TSS, salinity,  $d_{50}$ , and  $\text{bulkD}$ . The derived  $\text{bulkD}$  and  $d_{50}$  were used to estimate a median settling speed ( $w_{s50}$ ), just as in Chapter 2, but instead using  $\rho_b$  in place of  $\rho_p$  in the expression of specific gravity ( $s$ ), such that  $s = \rho_b / \rho$ .

Predicated on Owen sampling events from Chapter 2, only data from axial surveys taken following moderate to high flow events (40,000-100,000 cfs) were

selected for reanalysis. Of these data, nine axial surveys remained, all of which were from cruises that took place during the spring freshet, a consistently occurring high river discharge event responsible for 50% of the Susquehanna's annual sediment input into the upper Bay (Schubel & Pritchard, 1986). Pycnocline depth at each station was visually identified using a depth grid overlay on the salinity contours of cross-sectional axial plots in order to isolate surface layer data from the overall axial cruise data (Figure 3.2).

Average salinity, average temperature, and median particle property values were then calculated for the surface layer at each station and later used to calculate upper Bay surface layer averages and medians for the nine axial surveys (Table 3.1). Figure 3.3 shows an example of the axial distributions of particle properties and their median values for all surface layer samples on April 15, 2007, also shown in Figure 3.1. Plots of all axial survey distributions used for this analysis are presented in Appendix 4.

### 3.3 Results and Discussion

The salinity structures and TSS seen in Figures 3.1 and 3.2 are similar, with notably higher TSS concentrations in the vicinity of the ETM. Median particle size near the ETM is approximately 50  $\mu\text{m}$ , and bulk densities in the surface layer appear to range from about 1.05-1.2  $\text{g}/\text{cm}^3$ , which is much lower than the density of a solid mineral particles of  $\sim 2.65 \text{ g}/\text{cm}^3$ . The steep increase in grain size near the middle of the pycnocline combined with particularly low particle densities might at first appear to reflect very large flocs in the area, but this sudden change is most likely just an



artifact produced by the LISST as it passes through a very sharp density interface (Styles, 2006). However, since the threshold for isolating surface layer data is at the top of the pycnocline, these anomalies are excluded from the analyses.

In most cases, particle size distributions from throughout the water column were bimodal with peaks around 2.5-50  $\mu\text{m}$  and 250  $\mu\text{m}$ ; often these peaks were skewed towards the smaller sizes with tails at the coarser ends. However, in the surface layer there is only one substantial peak in particle size distributions (at or below 50  $\mu\text{m}$ ) that is generally skewed far left, with distributions again tailing towards the coarser ends; in some cases, there are hints of the former second peak that appear as a slight bump in distribution at  $\sim 250 \mu\text{m}$ .

Across all nine surveys reanalyzed in this investigation (Table 3.1, Figure 3.3, and Appendix 4), there were no apparent universal patterns for changes in particle characteristics with distance downstream among the distributions. Conversely, the most notable feature of these surface layer isolations is the amount of variability between surveys, despite some being sampled just days apart during the same research cruise. The variability seen is greater than what can be explained solely by source variability in the suspended solids at Conowingo Dam, despite the fact that the Susquehanna River is responsible for the vast majority of sediment delivery to the upper Bay (Schubel & Pritchard, 1986).

It could be reasoned that patterns can be still be found in these upper Bay profiles, but in short segments; in Figure 3.3 at 42-49 km river distance, there is a minor decrease in  $d_{50}$  in concert with a large increase in  $\text{bulkD}$  (so an increase in the fraction of primary particles), a substantial decrease in  $w_s$ , and a massive decrease in

TSS. This is a pattern entirely consistent with flocs settling out of the surface layer, although this pattern is also only apparent over the short distance between just two axial stations.

The lack of more persistent patterns in particle characteristic changes with distance could be the result of the conditions that influence flocculation, such as salinity, temperature, time elapsed, and availability of sticky organic material (Mehta et al., 1989), varying irregularly with distance downstream or in response to Susquehanna river flow (Sanford et al., 1994). Trends could also be obscured by different settling processes occurring simultaneously e.g. Cartwright (2011), who observed large low density flocs forming more quickly than denser primary particles were able to settle out.

Figure 3.4 compares the relationship between median TSS and  $w_s$  values across all surveys, showing that lower TSS is well-correlated to higher settling speeds, which is reasonable, as faster settling particles are more likely to settle out of the surface layer resulting in lower concentrations.

The relationships between the particle characteristic properties of settling speed, diameter, and density are particularly important for investigating the prominence of flocculation at various points downstream. Excess density is floc bulk density minus the density of water, or  $\text{excessD} = \text{bulkD} - \rho$ , which controls whether a particle will float or sink. Normalizing by the density of water, such that  $s_b = \text{bulkD} / \rho$ , yields a modified floc Stokes equation,

$$w_{sf} = \frac{1}{18} * \frac{(s_b - 1)}{\nu} * g * d_f^2 \quad (3.1)$$

where  $w_{sf}$  and  $d_f$  are the settling speed and diameter of a floc, respectively.

Winterwerp (2002) showed that,

$$s_b - 1 = 1.65 * \left(\frac{d_f}{d_r}\right)^{D3-3} \quad (3.2)$$

where  $D3$  is the floc fractal dimension. From these relationships, it can be shown (Hill & McCave, 2001) that,

$$w_{sf} = w_{sr} * \left(\frac{d_f}{d_r}\right)^{D3-1} \quad (3.3)$$

where  $w_{sr}$  and  $d_r$  are the settling speed and diameter of a reference disaggregated particle. These relationships reveal that in regions where flocculation is dominant, the floc fractal dimension controls the relationships between  $d_{50}$  ( $=d_f$ ),  $w_{s50}$  ( $=w_{sf}$ ). Sanford et al. (2005) found that in the lower layer of the upper Chesapeake Bay, the fractal dimension of flocs is about 2, which predicts that settling speed will increase linearly with diameter because floc density decreases as diameter<sup>-1</sup>. These relationships revert back to standard Stokes settling for solid particles, for which  $D3=3$ .

Figure 3.5 further shows comparisons between the particle characteristic properties. Median particle sizes detected downstream by the LISST ranged from 20-120  $\mu\text{m}$ , sizes comparable to silts and fine sands but much larger than the clay sized particles observed at the dam in Chapter 2. Additionally, excess densities seen range from 0.05-0.25 g/L, which is far less than the expected density of a solid mineral particle of about 1.65 g/L. The left plot of Figure 3.5 implies  $D3=2.24$ , and the right plot of Figure 3.5 implies  $D3=2.36$ , so there is a consistent indication that the fractal dimension in the surface layer of the upper Chesapeake Bay is approximately 2.3.

The fractal non-solid particle behavior illustrated in Figure 3.5 strongly suggests that the increases in size and settling speed that are allowing sediments to settle out of the surface layer are the result of flocculation. Sanford et al. (2005) found particle fractal dimensions were about 2 throughout the lower layer in the upper Bay, which indicates that the surface layer has more non-flocculated particles than the lower layer. This is reasonable, as flocculation can still continue in the lower layer, and because the lower layer typically has higher concentrations of aggregate particles due primarily to resuspension of pelleted bottom sediment (Schubel, 1968). This is also in agreement with surface layer particle size distributions, which were heavily dominated by the finer range of detectable particle sizes.

Further evidence of the flocculation of smaller particles coming over the dam as they move downstream in the upper estuary is provided in Figure 3.6, which shows an image from a particle imaging camera that was deployed in freshwater at the northernmost station during an axial survey in April 2007. A number of large flocs as well as many smaller flocs are clearly apparent in Figure 3.6, however, due to the minimum resolution of the imaging camera being 30  $\mu\text{m}$ , it is possible that there are other much smaller particles present but not visible.

From this investigation, it is abundantly clear that flocculation of the disaggregated particles is responsible for the settling of fine sediment particles as they move down Bay. However, as sediments flocculate and settle out of the surface layer, it reduces the sediment concentration and thus the rate of flocculation in the surface layer with distance downstream. As the rate of flocculation slows, the clay particles that are left behind likely make up the “background concentration” of essentially non-

settling particles (Sanford et al., 1994; Schubel, 1971; Scientific Technical Advisory Committee, 2007).

Table 3.1

*Upper Chesapeake Bay surface layer average and median values*

	<u>5/7/2001</u>	<u>5/8/2001</u>	<u>5/14/2001</u>	<u>5/11/2002</u>	<u>5/13/2002</u>	<u>4/9/2007</u>	<u>4/15/2007</u>	<u>5/8/2007</u>	<u>5/14/2007</u>
Median TSS (mg/L)	22.4	23.1	18.3	7.3	12.9	29.1	32.9	9.9	18.4
Median d50 ( $\mu\text{m}$ )	44.1	24.0	31.0	119.6	64.5	49.9	40.5	128.5	64.8
Median BulkD ( $\text{g}/\text{cm}^3$ )	1.209	1.206	1.231	1.126	1.092	1.133	1.117	1.057	1.085
Median ExcessD ( $\text{g}/\text{cm}^3$ )	0.209	0.206	0.231	0.126	0.092	0.133	0.117	0.057	0.085
Median $w_s$ (mm/s)	0.220	0.070	0.150	0.970	0.240	0.190	0.100	0.410	0.180
Avg. Pycnocline Depth (m)	5.7	6.2	4.2	4.6	6.1	7.1	6.6	3.8	5.0
Avg. Salinity (psu)	4.1	3.2	4.2	3.7	4.8	1.9	2.1	1.9	1.4
Avg. Temperature ( $^{\circ}\text{C}$ )	17.3	17.5	17.6	16.8	17.9	7.3	8.6	15.7	19.3

*Note.* Values presented are for BITMAX I & II survey data sampled above the pycnocline.

BM0702- LISST 2<sup>nd</sup> Axial Survey: April 15, 2007

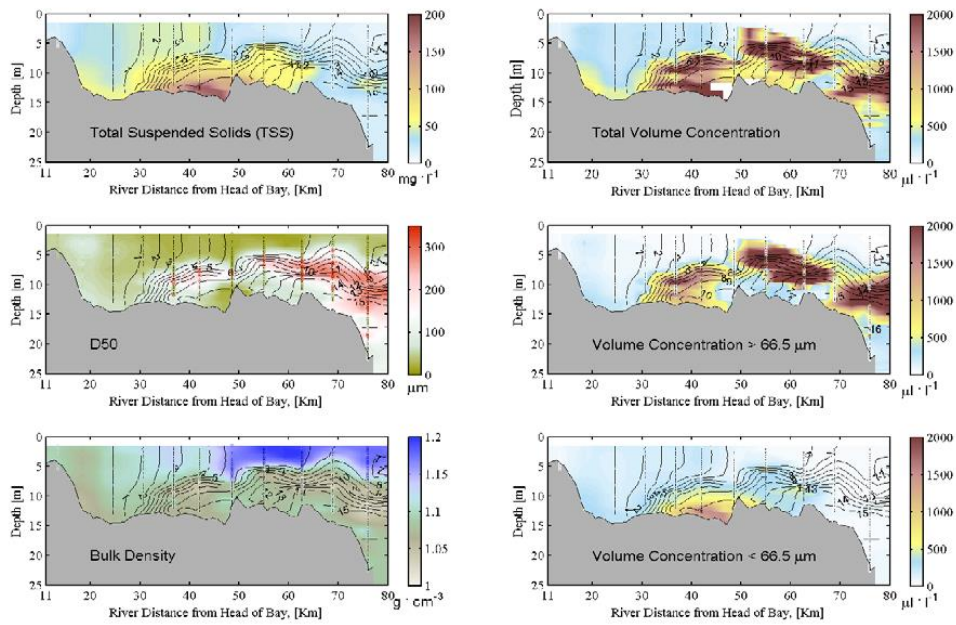


Figure 3.1. Cross-sectional contour plots of a BITMAX II axial survey taken on April 15, 2002. Panels shown are of TSS and LISST-derived particle parameters, with black salinity contours, which are the same in all panels. Head of Bay i.e. Havre de Grace, MD.

ETM02\_01, Third Hydrographic Survey, May 13, 2002

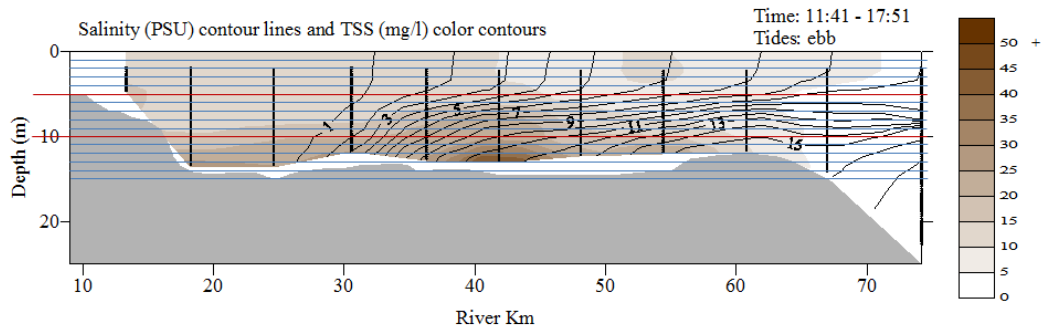


Figure 3.2. Cross-section of salinity (thin black lines) and TSS (coloration) from a BITMAX I axial survey taken on May 13, 2002. A depth grid overlay of blue (1m) and red (5m) horizontal lines is used for identification of surface layer depth. River km is river distance measured from Havre de Grace, M.D.



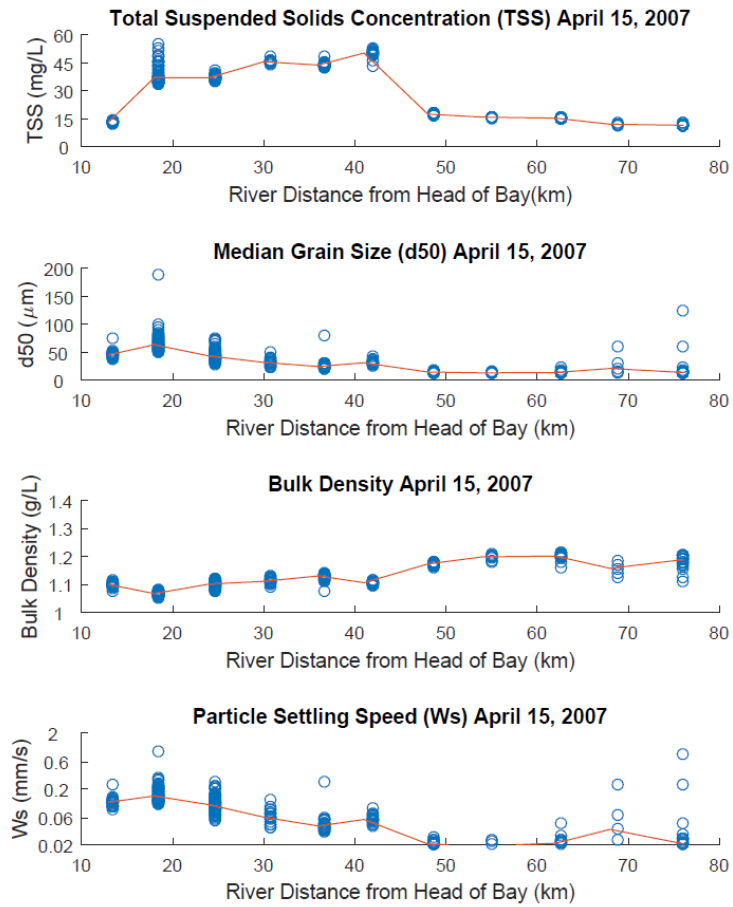
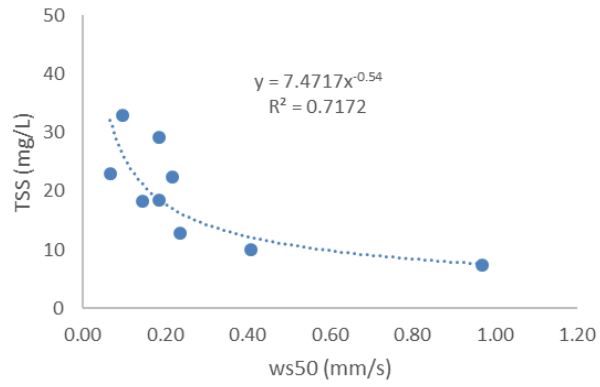


Figure 3.3. Surface layer data for key parameters (TSS, d50, bulkD,  $w_s$ ) from upper Bay axial analysis, surveyed on April 15, 2007. Blue circles represent all sample data, while red lines indicate median values.



*Figure 3.4.* Surface layer average TSS at different surface layer median settling speeds from axial surveys data listed in Table 3.1.

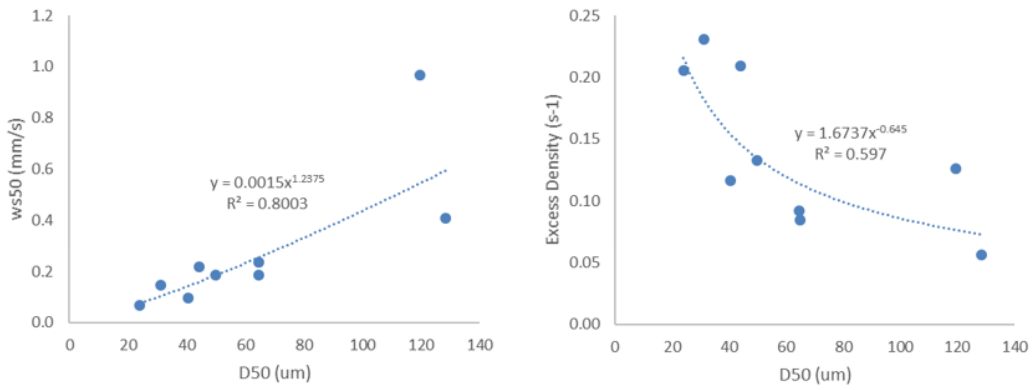
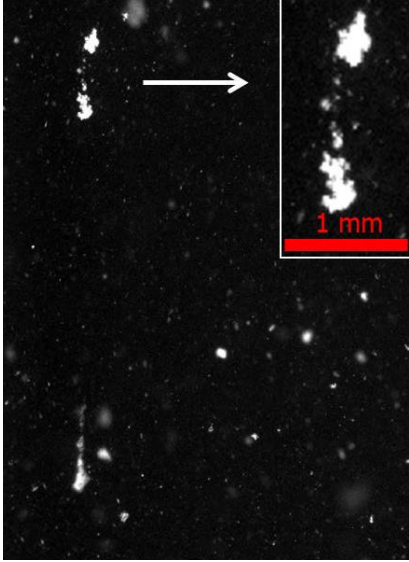


Figure 3.5. Median settling speed ( $w_{s50}$ ) by median diameter ( $d_{50}$ ) (left), and median excess density ( $\text{s}^{-1}$ ) by median diameter ( $d_{50}$ ) (right) of particles in the surface layer of the upper Bay for the 9 axial surveys from Table 3.1.



*Figure 3.6.* Image of suspended aggregated floc particles captured in situ at the northernmost axial station during April, 2017.

## Chapter 4: Particle Mass Downstream and Response to Susquehanna River Flow

### 4.1 Introduction

Dams interrupt downstream sediment transport in rivers, leading to trapping of sediment in the reservoirs immediately upstream (Langland & Cronin, 2003). Over time the accumulation of sediments alters the reservoir's bathymetry, gradually reducing the cross-sectional area for water flow (Langland & Cronin, 2003) and causing a proportional increase in flow velocity in order to conserve water mass. Eventually reservoirs reach a state of sediment infill such that heightened flow velocities prohibit further settling, allowing virtually all suspended sediments to pass downstream (Langland & Cronin, 2003). It has generally been accepted that the Conowingo Dam's reservoir is nearing its sediment storage capacity since the 1990's (Langland, 2009; Zhang et al., 2013), but it is difficult to pinpoint an exact date because the Conowingo reservoir exists in a state of dynamic equilibrium; frequent, high discharge events scour the Conowingo reservoir's bed sediments, which temporarily increases the reservoir's cross-sectional area and allows for further trapping of sediments (Langland & Cronin, 2003).

Due to the effect of river flow on the ability of particles to remain in suspension long enough to escape the reservoir, and also due to the change in particle characteristics with flow shown in Chapter 2, it is important to analyze settling of sediment downstream with consideration to Susquehanna River discharge. This chapter will rely greatly on the sediment concentrations in the upper Chesapeake Bay

to draw conclusions about sediment settling, and because of this it is important to note that the Chesapeake Bay has a low background Total Suspended Solids (TSS) concentration which is comprised of very fine and less aggregated particles that settle too slowly to settle out of suspension (Sanford et al., 1994; Schubel, 1971; Scientific Technical Advisory Committee, 2007) that is uniformly distributed throughout the water column (Schubel & Biggs, 1969). Sanford et al. (1994) found that sediment concentrations fell rapidly to 7 mg/L following elevated Susquehanna flows, then varying from 4-8 mg/L in response to changes in salinity due to both Susquehanna flow and proximity to the Estuarine Turbidity Maximum (ETM). For purposes of this investigation, we will assume a constant background concentration of 7 mg/L under all flow conditions. Higher concentrations of sediments promote flocculation of the particles in suspension due in part to an increase in the frequency of particle collisions (Hill et al., 2013), so the low background concentration comparatively inhibits flocculation and thus limits the settling out of small background particles.

The previous chapter establishes that sediments from the Conowingo Dam transform in the upper Bay at least in part due to flocculation, however it does not delve into the mass of sediments in the surface layer throughout the upper Bay. The previous chapter also does not cover downstream response to upstream conditions under either low or very high flows. Because the Susquehanna discharge is the dominant factor determining variation in TSS concentrations in the upper Bay (Liu & Wang, 2014), this chapter will expand upon the previous two through careful analysis of the distribution of suspended sediment in the surface layer of the upper Bay with distance downstream and under differing river flow conditions.

## 4.2 Methods

The primary focus of this investigation was Chesapeake Bay Program (CBP) water quality data from their routine long-term monitoring program, for which water is regularly sampled at various water column depths from many monitoring stations located throughout the Chesapeake Bay. The six monitoring stations of interest to this study (named CB1.1, CB2.1, CB2.2, CB3.1, CB3.2, and CB3.3c, henceforth only referred to by their number) are located in the upper Bay along a similar path to the axial survey transects seen in Chapter 3 (Figure 4.1). Data used in this investigation consist of surface layer salinity (psu) and TSS (mg/L) values under various river flow conditions since July 1984. United States Geological Survey (USGS) river discharge and TSS data from the Conowingo Dam sampling site are used for upstream comparisons in this investigation.

In order to investigate changes in TSS with distance down Bay, to look for relationships between spatial distribution and flow, and to see whether TSS behaves conservatively or non-conservatively as it enters the surface layer of the upper Bay, the period of time that it a parcel of water to traverse the distance from the Dam to the six CBP stations downstream is needed. For purposes of this study, this period of time is referred to as antecedent days, and is measured as a whole number of days prior to CBP station sampling dates. It is also assumed that the number of antecedent days for each station cannot decrease with distance downstream, as the surface layer of the upper Bay has a dominant downstream flow (Guo & Valle-Levinson, 2007). A Matlab script that evaluates the fit of antecedent USGS Conowingo river discharge to corresponding downstream CBP TSS was developed and used to test for the date of

Susquehanna discharge that most likely preceded each downstream water quality sample.

For each CBP sampling date, the script assigned antecedent USGS Conowingo river discharge (cfs) and TSS (mg/L) in two ways: by taking instantaneous values from X number of days before the sampling date, and by averaging all of the values between the sampling date and X number of days prior. Applying calculations developed previously for finding the residence time of water in the upper Bay (throughout the water column, as a function of river flow) to antecedent river flows for the nine cruises in Chapter 3 yielded residence times ranging from 13-25 days (S. Suttles, unpublished data). However, advection of the thin, fast, seaward moving surface layer takes far less time to turn over than that of the entire body of freshwater in the upper Bay. Furthermore, Sanford et al. (1994) found that suspended particles in the upper Bay have a rapid advective response to variations in Susquehanna River discharge, so a maximum X of 10 days was selected for use in the Matlab script. Traversing the 78 km distance between the Dam and the furthest downstream station, 3.3, in a period of 10 days corresponds to a seaward velocity of 9 cm/s, which is a very reasonable mean surface layer velocity in the upper Bay (Fugate et al., 2007; Pritchard & Vieira, 1984) Antecedent lag times greater than 10 days were explored at first, but initial experimentation did not show improvements in correlation. The dataset was split and again ran through the script in order to observe possible influence by the infilling of the Conowingo reservoir on the relationship between downstream TSS and upstream antecedent flow; the midpoint of the study period (1995) coincides with the approximate time of the Conowingo



reservoir approaching its sediment capacity (the 1990's), so data were categorized into pre-infill (1984 through 1995) and post-infill (1996 through 2018) datasets. The script would plot CBP TSS by antecedent USGS river discharge and calculate the r-squared value of a linear best fit. The X number of antecedent days with the highest r-squared values can be found in Table 4.1.

Despite employing a variety of approaches for evaluating upstream antecedents of downstream values (i.e. instantaneous, averaged, pre-infill, post-infill), it was not immediately apparent that any one approach was better correlated than the others (Figure A5). Because of this, a single Best Estimate Antecedent Day (BEAD) is identified per station as the integer mean of the highest correlated X number of antecedent days from all of the various approaches, with consideration for the assumption that the number of antecedent days needed to travel to that station cannot decrease with distance downstream (Table 4.1).

Initial comparisons of upstream BEAD USGS TSS to each downstream CBP station TSS revealed variation in distribution among stations, in addition to considerable skew in the distribution of samples above or below the 1:1 line at low flows. There was no apparent pattern indicating an influence of pre or post infill (Figure 4.2), which could be due, in part, to there being comparatively much less post-infill data available; this is especially the case for USGS data, which seems to have been sampled much more frequently in earlier years. Guided by these considerations, in further analyses data is categorized by flow and distance downstream, but not by sampling date.

Three different flow classifications were used in all subsequent analyses: low (<38,000 cfs), medium (38,000-86,000 cfs) and high (>86,000 cfs). Flow category thresholds were selected based on below-average (low) and above-average (medium) river discharge at Conowingo, and the rate at which the first spill gate is opened at Conowingo Dam that also corresponds to the 90<sup>th</sup> percentile of flow (high) used in Palinkas et al. (2019).

Other simplifications were also made to the flow-categorized data set to be used in all subsequent analyses. Replicate CBP values sampled on the same date were averaged per station. Replicate USGS TSS values sampled on the same date were also averaged. Any USGS sampling date that did not have a USGS TSS value was removed, reducing the sample size of Conowingo river discharge and TSS values by two thirds. Another Matlab script used BEAD values to assign CBP sampling date TSS and salinity values to corresponding antecedent USGS TSS and river discharge values. The unique sampling date Conowingo data was then added to the data set as station 'Cono Dam' or 'C' to represent samples from the upstream endmember, the Conowingo Dam. For Conowingo data, the downstream TSS and upstream antecedent TSS are simply the same value, and the antecedent river discharge would simply be that same day's value. Conowingo ('C') was uniformly assigned a symbolic salinity value of -0.5 psu to differentiate USGS data from CBP data in plots.

#### 4.3 Results and Discussion

When investigating the relationship between flow, TSS, and downstream distributions, there are two valid options for evaluating position downstream: salinity

and CBP station number. There is a consistent and gradual increase of salinity from the head to the mouth of the Bay (Wells et al., 1928), with salinity being the best indicator of water mass mixing and transport (Fisher et al., 1988). Station number can also be used as a measure of river distance for certain comparisons due to the evenly spaced nature of the station locations along the upper Bay, as seen in Figure 4.1. Using either of these approximations, patterns in settling behavior downstream can be observed.

To reveal the relationship between TSS and salinity under different flow regimes, TSS and salinity values were binned by 0.5 psu salinity intervals (Figures 4.3-4.6). Figures 4.3-4.6 feature straight diagonal mixing lines to help identify the conservative or non-conservative nature of suspended sediment under each flow regime. Concentrations falling along the straight mixing line would be indicative of conservative sediment behavior, such that changes in concentration can be explained through simple dilution of the high concentration, fresh Susquehanna water mixing with the low concentration, saline upper Bay water. If concentrations seem to fall above or below a straight mixing line, however, then there must be a source of material, such as the ETM, or a sink of material, such as flocculation driven settling, influencing the concentrations beyond the effects of dilution alone.

The mixing lines in Figures 4.3-4.6 extend from median TSS concentration at Conowingo Dam until the salinity at which CBP TSS concentrations fall below the approximate background concentration (7 mg/L). For purposes of this investigation, the background concentration of sediments in the upper Chesapeake Bay is assumed to be the same throughout the surface layer and under all flow conditions.

Under low flow conditions, concentrations are much lower at the freshest values (0-0.5 psu) and then steeply increase until peaking at 1.5-2 psu (Figure 4.3). This rapid increase and peak in TSS at the onset of saline waters is likely indicative of fresh Susquehanna discharge prevailing downstream until the ETM, where salinity and sediment concentrations are increased through mixing with the saline and turbid waters of the ETM. Further increases in salinity see a gradual decrease in concentration until TSS levels off at the background concentration (7 mg/L).

Under medium flow conditions the lack of a bump in TSS makes the influence of the ETM on sediment concentrations less clear than what was seen under low flow. However, the ETM's trapping effect is still clear, as concentrations drop sharply after ~2 psu, followed by a steady decrease in TSS with salinity until again meeting the approximate background concentration.

Figure 4.5 establishes a steep non-conservative (rapid, nonlinear) loss of material from surface layer under high flow conditions; A significant fraction of the inflowing suspended sediments of sediments settle from the surface layer at or before ~2 psu, and then concentration continues to decrease with increases in salinity until it nears the background concentration. Behavior during medium flows appears more conservative, with a likely balance between sediments gradually settling out with increases in salinity and input from the ETM until concentrations fall to the background level.

For easier comparison between flow regimes, the median TSS value was extracted from each salinity interval for all three flows and plotted together (Figure 4.6). This figure emphasizes the differences between flow behavior; addition of

material from ETM dominates concentrations under low flows, under medium flows mixing appears conservative, and under high flows there are significant losses of material in the first few salinity intervals.

Individual analyses of salinity by station number and of TSS by station number help to further inform the relationship between distance downstream and water quality in the upper Bay. Figure 4.7 shows CBP salinity data, and Figure 4.8 shows USGS and CBP TSS data, binned by station number (Cono Dam, 1.1, 2.1, 2.2, 3.1, 3.2, 3.3).

As mentioned earlier, the surface layer of the upper Bay remains largely fresh with distance downstream until mixing with the saltier turbid waters of the ETM, which allows for identification of the ETM under different flow conditions through water quality observations. Figure 4.7 shows very clearly that under increasingly higher flows the onset of salinity is pushed further downstream with increasing flow, and gradual increases in salinity in the surface layer occur from this point onwards under all flow conditions.

The effects of the ETM on water quality are also evident in station TSS observations (Figure 4.8); injection of material into the surface layer by the ETM can be seen as peaks in TSS around station 2.1 under low flow and station 2.2 under medium flow conditions, after which there is a gradual loss of material through the remainder of the upper Bay until TSS reaches background levels. Despite the absence of a definitive peak under high flows, the sediment trapping effect of the ETM can still be seen in the low variance gradual decline in TSS that occurs around station 3.1. The apparent locations of the ETM from Figure 4.8 agree with the salinity changes in

Figure 4.7. What remains uncertain is whether the changes seen in these figures are statistically significant.

To determine if differences and similarities in parameter values between stations seen in Figures 4.7 and 4.8 were statistically significant, salinity and TSS datasets for each of the now seven stations under three flow conditions were evaluated in Matlab using the Kruskal-Wallis and Multiple Comparison tests, as used in Chapter 2. Kruskal-Wallis was again selected due to the nature of the data sets, as it is a valid way of applying ANOVA for a non-Gaussian population (The Mathworks, 1993). The test compares parameter values at each station to that same parameter's value at all other stations to determine if and where significant differences in salinity and TSS values occur. Multiple Comparisons shows more detailed results from Kruskal-Wallis tests, revealing the results of each individual pairing and allowing the creation of a visualization of the statistical differences in salinity (Figure 4.9) and TSS (Figure 4.10) with distance downstream.

Testing results show no significant difference between salinity values at the stations until a certain point downstream (that varies for the different flow regimes), after which there are significant differences in salinity values between almost every station continuing down Bay (Figure 4.9). This is indicative of the fresh Susquehanna headwaters dominating the surface layer of the upper Bay until the ETM, after which the surface layer begins mixing and entrains saltwater from the pycnocline, becoming significantly saltier.

Under low and medium flow conditions, testing showed that most stations' TSS concentrations are significantly different from one another, meaning that

significant changes in sediment concentrations occur throughout much of the surface layer of the upper Bay. This also means that peaks at stations 2.1 and 2.2 that are presumed to be effect of the ETM are significant. Under medium flow conditions, most stations' concentrations were also significantly different. For high flows concentrations are not significantly different until station 3.1, after which sediment concentrations gradually, but significantly, decrease with distance downstream. This also substantiates the idea that higher flows push the ETM further down bay, after which there is a loss of material in the surface layer.

When plotting by station it may seem like there are contradictions in the data set because very rapid yet opposite changes occur in the vicinity of the ETM: sudden increases in TSS under mostly low and medium conditions, and sudden decreases under high flow conditions. This is because there are two competing influences on TSS: settling out of the surface layer and injection into the surface layer at the ETM. At low flows the influence of the ETM dominates, and as flow increases settling begins to dominate and the signature of the ETM appears to become muted, eventually reversing and leaving a decrease in TSS at the ETM at high flows.

To see the influence of upstream conditions on individual stations' conditions, each downstream station's CBP TSS is compared to its upstream antecedent BEAD TSS (Figures 4.11 and 4.12, Appendix 7). Proximity of 'All' flow data to the 1:1 line at the various stations shows that at upstream stations TSS generally seems fairly dependent on bay head TSS measured at the Conowingo Dam (e.g. bottom right panel of Figure 4.11), whereas at lower stations that relationship is weaker or nonexistent and that TSS instead seems largely determined by the background concentration (e.g.

bottom right panel of Figure 4.12). This agrees with preliminary findings found while formulating BEAD calculations, where for upstream stations it was typical to see  $r^2$  values upwards of 0.784, with values mostly over 0.4 and well defined peaks in correlation amongst antecedent day lags (Appendix 13). Correlations across all lags and approaches decreased with distance downstream until near the end of the ETM at station 3.1, after which the relationship between upstream flow and local TSS seemingly falls apart, judging by the weaker correlations and ill-defined peaks

Comparisons of BEAD and CBP TSS also show that under low and medium flows, station TSS is more strongly influenced by the background concentration and not dependent on upstream values (e.g. top panels of Figures 4.11 and 4.12), while at higher flows the relationship seems more influenced by upstream TSS (fits 1:1 line) (e.g. bottom left panel of Figures 4.11 and 4.12). This is in partial agreement with a second iteration of BEAD calculations that was performed using by-flow-class separated data, which revealed that some correlations for shorter lags (flows from a number of antecedent days fewer than the BEAD value at any given station) were stronger at high flows (Appendix 6). However, this is unsurprising, as most of the data used to calculate BEAD comes from medium and low flows, and so the BEAD result is a very good representative for medium and low flows, and less so for high flows. However, BEAD values were still the best correlated overall, only ever being slightly weaker at higher lags, and for this reason further analysis was not pursued in response to these second iterations. It should also be noted that although these BEAD versus CBP plots do not present any averaged values, they do depend on BEAD selections, which were in part influenced by averaged lags.

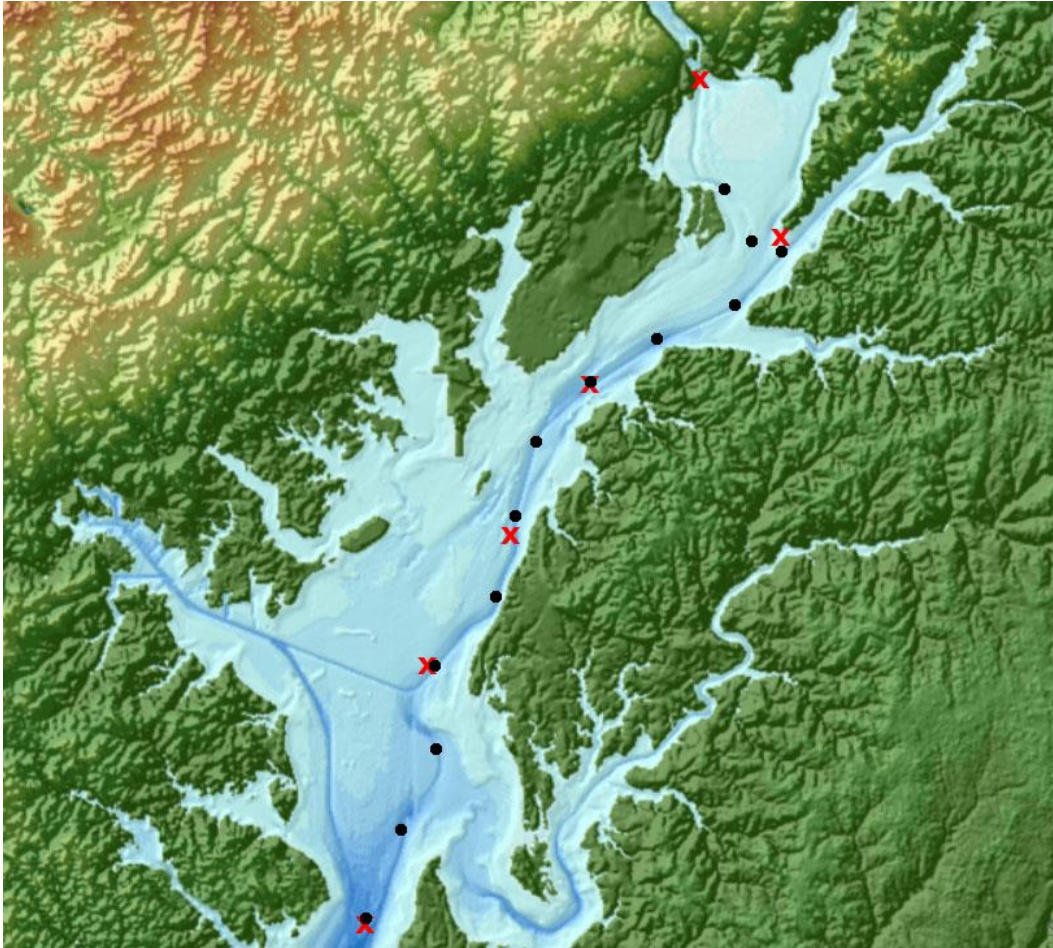


Table 4.1

*Highest correlation antecedent days from antecedent calculations*

<u>Antecedent Approach</u>	<u>CBP Station Number</u>					
	<u>1.1</u>	<u>2.1</u>	<u>2.2</u>	<u>3.1</u>	<u>3.2</u>	<u>3.3</u>
Instantaneous	1	2	2	4	3	2
Instantaneous Pre-Infill	0	2	2	4	4	8
Instantaneous Post-Infill	2	2	3	4	3	2
Averaged	2	3	3	7	7	10
Averaged Pre-Infill	1	2	3	5	5	10
Averaged Post-Infill	2	3	3	8	8	10
Mean (BEAD)	1	2	3	5	5	7

*Note.* Mean (BEAD) values operate under the assumption that the number of antecedent days is a whole number that cannot decrease with distance downstream (increasing station number).



*Figure 4.1.* Map of the upper Chesapeake Bay with CBP station (red 'x') and BITMAX I & II station (black dot) locations. CBP stations are numbered in order from north to south.

CBP2.1s TSS by USGS TSS according to Antecedent River Discharge and Year

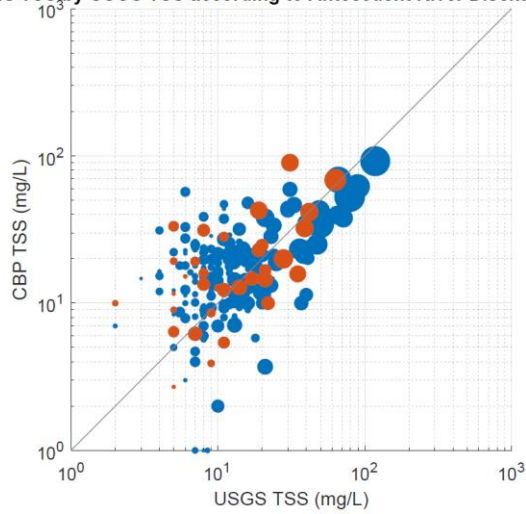


*Figure 4.2.* An example of CBP TSS by USGS BEAD TSS used to evaluate influence of sampling period. Circular markers are of size (BEAD Flow) / 1000 and color indicates samples taken prior (blue) or post (red) Conowingo Infill (1995). Location of sample marker above or below 1:1 line indicates an increase or decrease of sediment concentration between the dam and the downstream station.

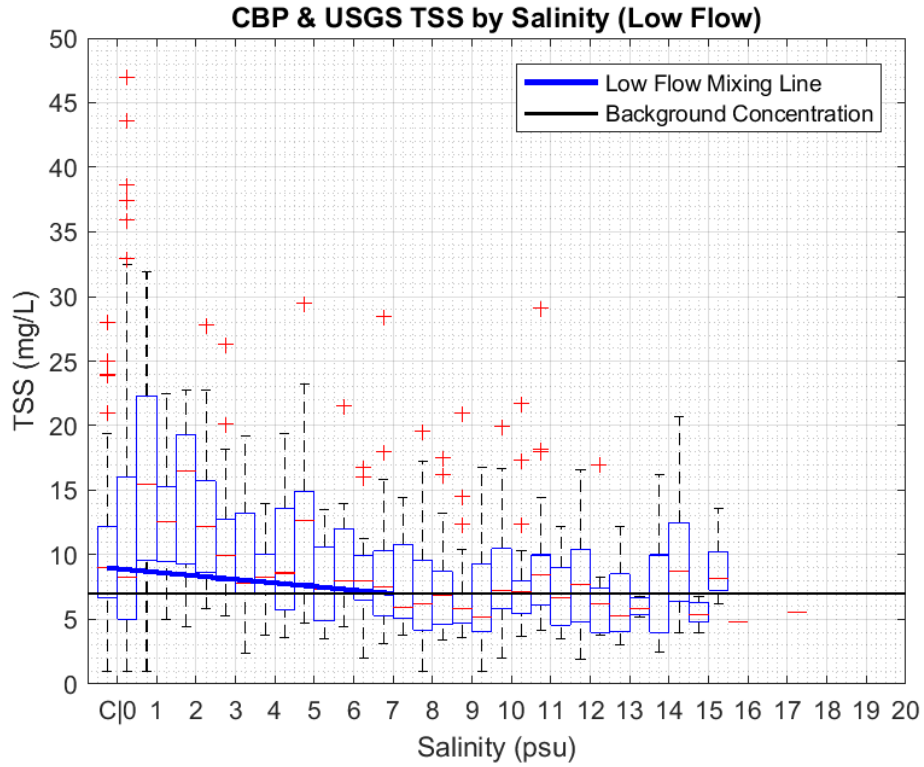


*Figure 4.3.* Boxplot of TSS by salinity intervals under low flow conditions (<36,000 cfs). Conowingo data is represented by the leftmost box (C on the x-axis). The diagonal mixing line is determined by plotting a linear line that extends from median Conowingo TSS value to the point at which CBP TSS levels fall below the black background concentration line (7 mg/L). Red horizontal lines are median TSS values, red crosses are outliers, black dashed lines represent the upper and lower quartile of values.

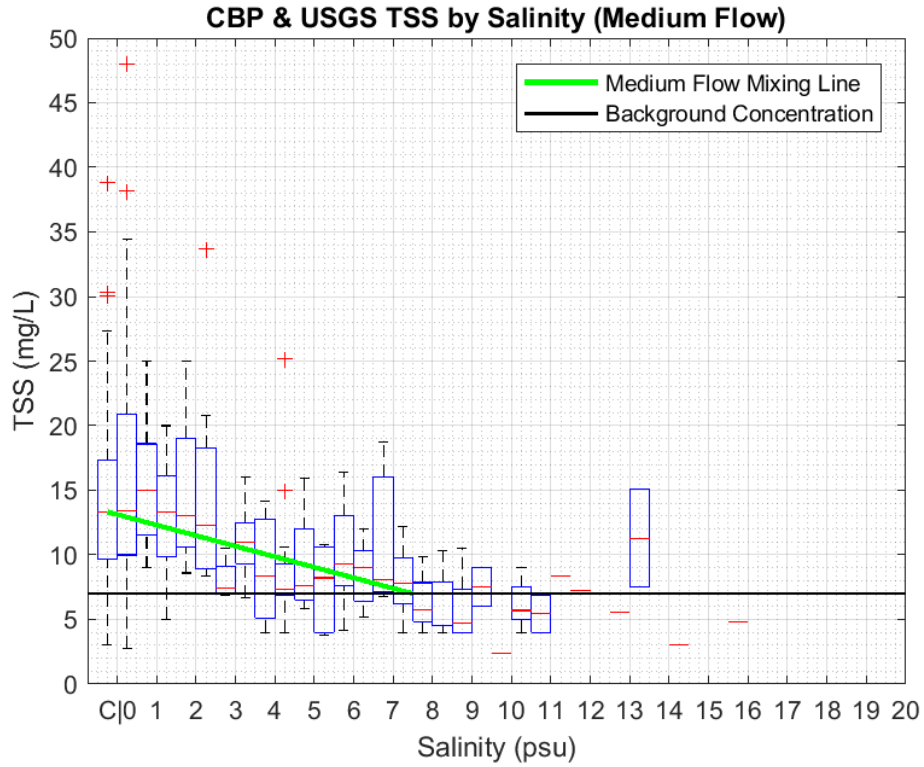
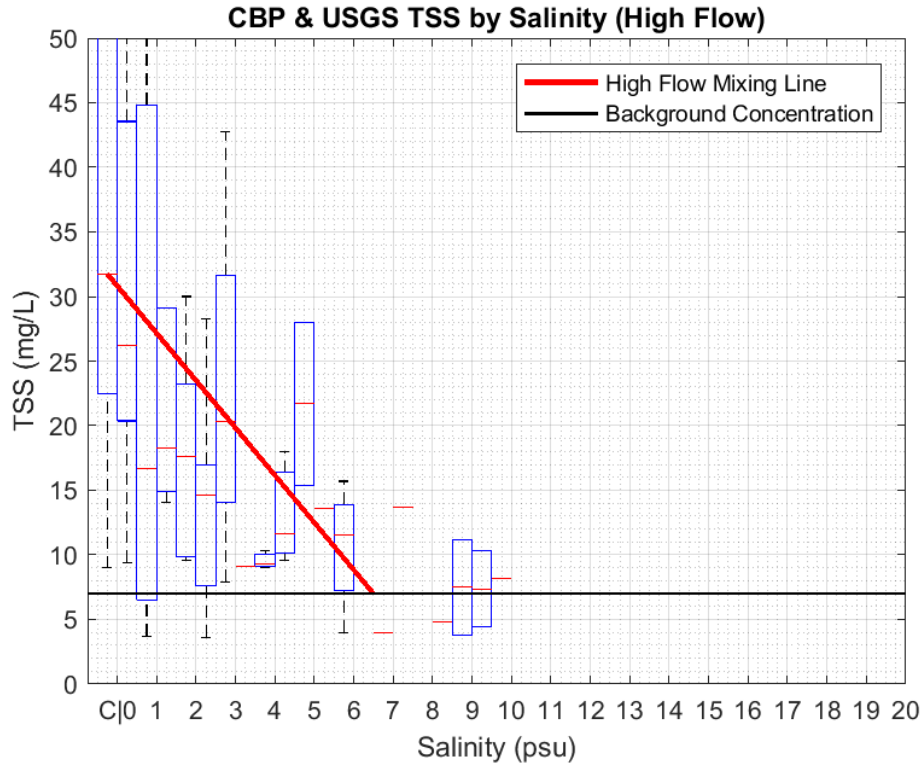


Figure 4.4. Boxplot of TSS by salinity intervals under medium flow conditions (36,000-86,000 cfs). Conowingo data is represented by the leftmost box (C on the x-axis). The diagonal mixing line is determined by plotting a linear line that extends from median Conowingo TSS value to the point at which CBP TSS levels fall below the black background concentration line (7 mg/L). Red horizontal lines are median TSS values, red crosses are outliers, black dashed lines represent the upper and lower quartile of values.



*Figure 4.5.* Boxplot of TSS by salinity intervals under high flow conditions (>86,000 cfs). Conowingo data is represented by the leftmost box (C on the x-axis). The diagonal mixing line is determined by plotting a linear line that extends from median Conowingo TSS value to the point at which CBP TSS levels fall below the black background concentration line (7 mg/L). Red horizontal lines are median TSS values, red crosses are outliers, black dashed lines represent the upper and lower quartile of values.

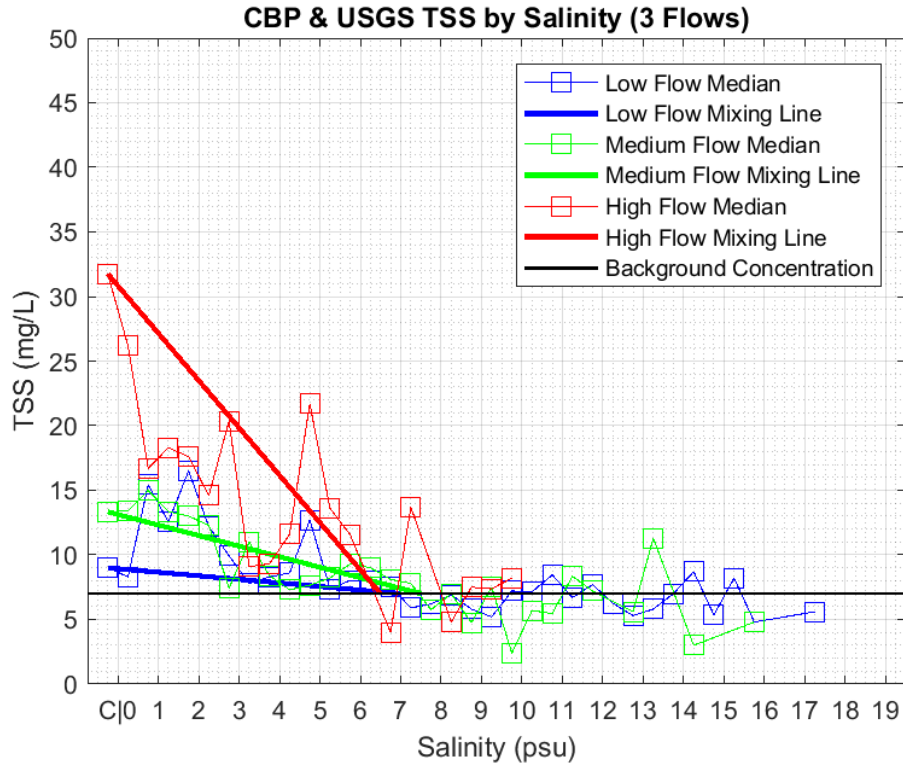


Figure 4.6. Median values from salinity interval boxplots for low, medium, and high flow conditions. Conowingo data is represented by the leftmost box (C on the x-axis). Diagonal mixing lines are determined by plotting a linear line that extends from median Conowingo TSS value to the point at which CBP TSS levels fall below the black background concentration line (7 mg/L).

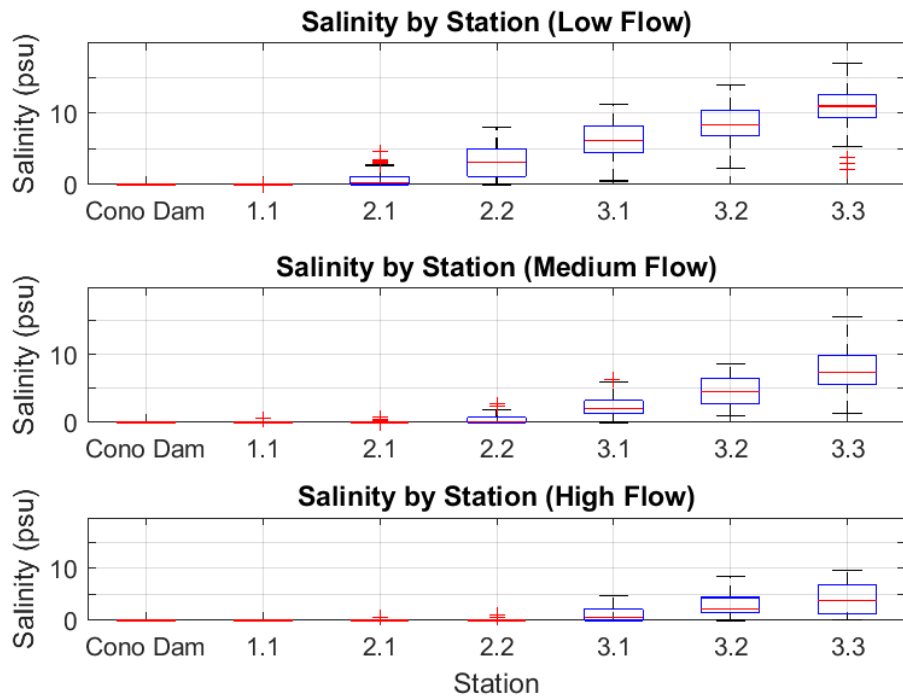


Figure 4.7. Boxplot of CBP salinity at each station. Red horizontal lines are median salinity values, red crosses are outliers, black dashed lines represent the upper and lower quartile of values.



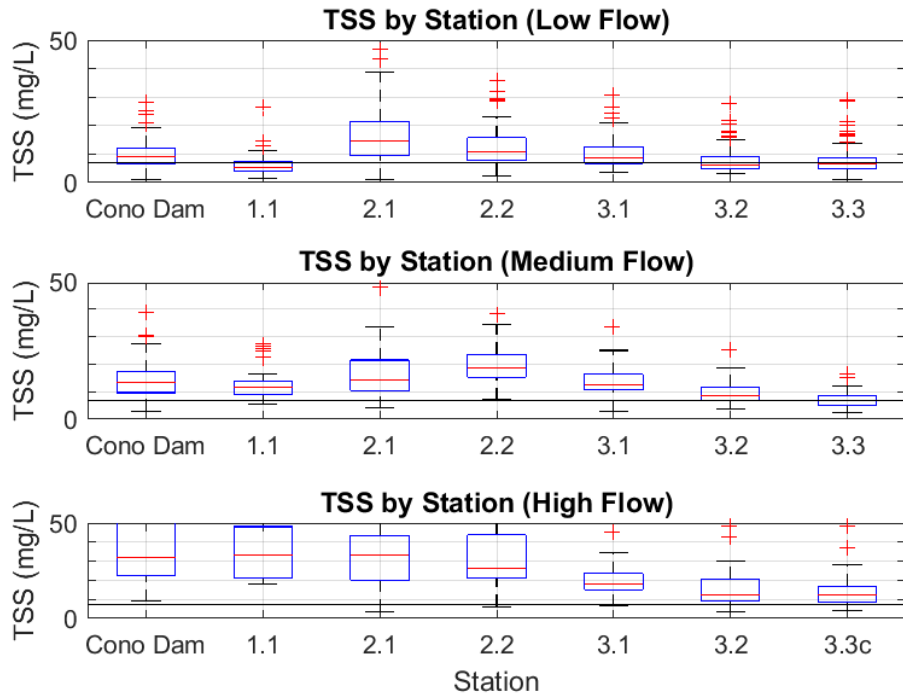


Figure 4.8. Boxplot of CBP TSS at each station. Red horizontal lines are median TSS values, red crosses are outliers, black dashed lines represent the upper and lower quartile of values.

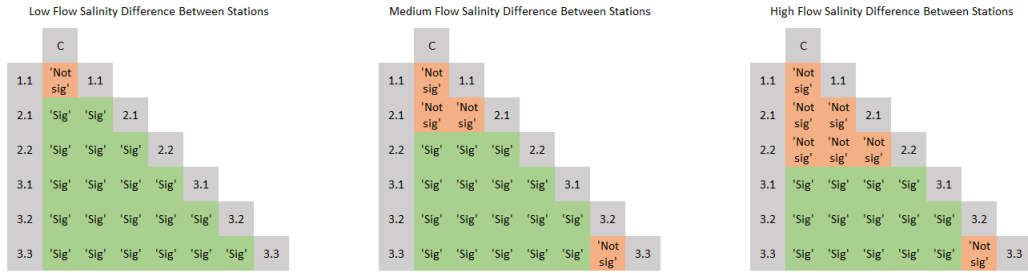


Figure 4.9. Statistical significance of differences in salinity concentration over distance down Bay by station number. Comparisons are read as “salinity at station (column number) is/is not significantly different than salinity at station (row number). Statistical significance is noted as either significant (‘Sig’, green) or insignificant (‘Not sig’, orange) in the intersecting boxes. Note. Visually, each column should be imagined as being a map of the upper Bay that starts as far north as station (column number) and ends at station 7 (CBP 3.3c), near the Bay Bridge to the south.

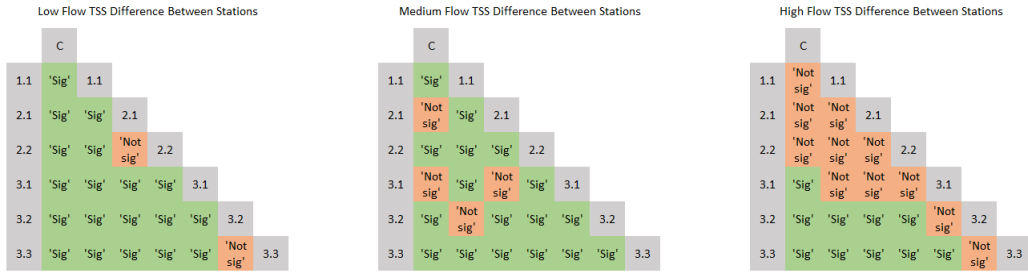
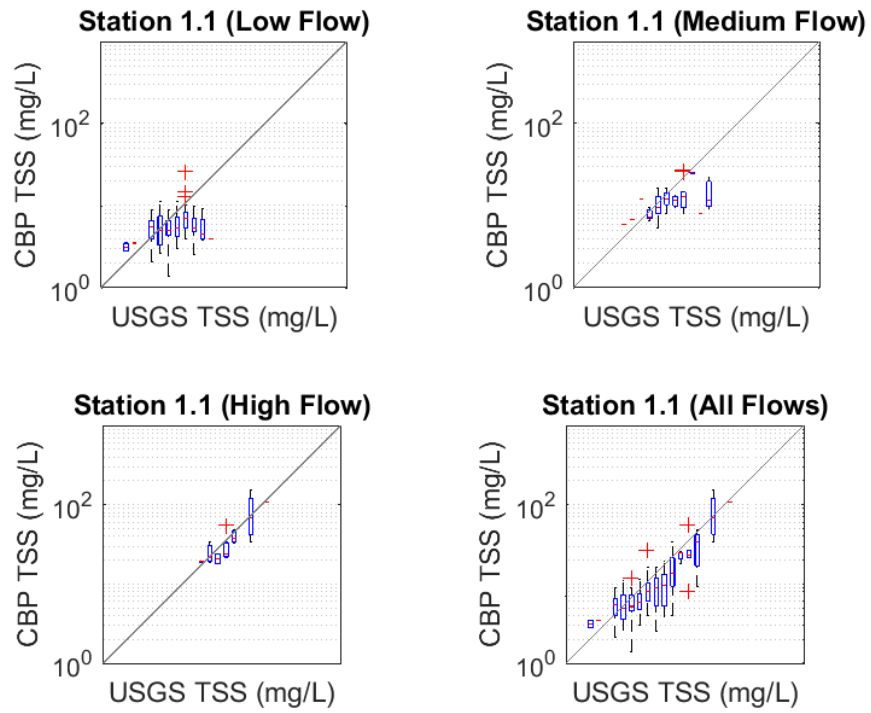
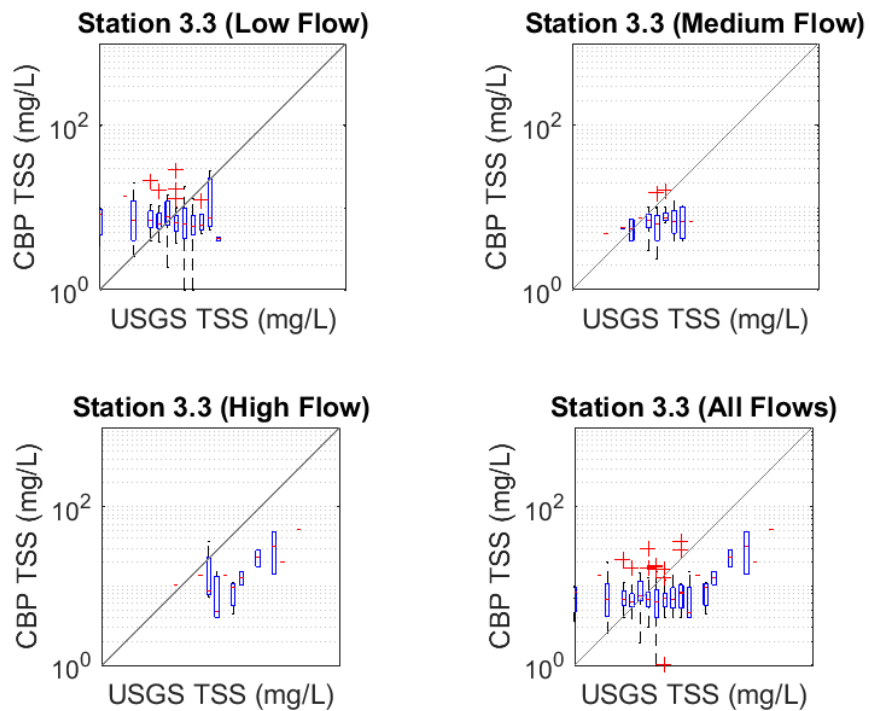


Figure 4.10. Statistical significance of differences in TSS concentration over distance down Bay by station number. Comparisons are read as “TSS at station (column number) is/is not significantly different than TSS at station (row number). Statistical significance is noted as either significant (‘Sig’, green) or insignificant (‘Not sig’, orange) in the intersecting boxes. Note. Visually, each column should be imagined as being a map of the upper Bay that starts as far north as station (column number) and ends at station 7 (CBP 3.3c), near the Bay Bridge to the south.



*Figure 4.11.* Comparisons of downstream CBP TSS at station 1.1 compared to upstream antecedent USGS TSS at Conowingo Dam under low (upper left), medium (upper right), high (lower left) and all (lower right) flow conditions. All plots are on a loglog scale with a diagonal black 1:1 reference line.



*Figure 4.12.* Comparisons of downstream CBP TSS at station 3.3c compared to upstream antecedent USGS TSS at Conowingo Dam under low (upper left), medium (upper right), high (lower left) and all (lower right) flow conditions. All plots are on a loglog scale with a diagonal black 1:1 reference line.

## Chapter 5: Summary, Synthesis, and Broader Implications

### 5.1 Summary

Perhaps the most important finding from Chapter 2 is that the wealth of historical disaggregated particle size data found at the Conowingo Dam is sufficient for estimating true sediment settling speeds ( $w_s$ ) of particles found there; statistical similarity between Owen and United States Geological Survey (USGS) data from waters sampled above and below the Dam indicates that no notable flocculation occurs upstream and that sediment remains disaggregated after passing through or over the Dam. During moderately high river flows, 98% of sediment mass passing through the Conowingo Dam is comprised of very fine and slowly settling disaggregated mineral particles, however, the fraction of mass contributed by faster settling silts and sands were shown to change as a function of flow; the slowest settling speed category's fraction of total mass decreased with increase in river discharge, while the mass fractions of the remaining three categories all increased with increases in flow. The small fraction of sand-sized particles is likely to fall out of the surface layer nearly immediately, leaving only the fine particles remaining suspended downstream in the surface layer of the upper Chesapeake Bay. Because of the impact of flow on sediment distribution and settling speeds, a settling speed that represents the typical Susquehanna River particle with consideration to Susquehanna flow that could be considered for use in models is  $w_{s,ave}$  excluding the sand fraction, which at the average river flow (38,000 cfs) is 0.032 mm/s.

Reanalysis of historical axial cruise data in Chapter 3 showed that particle characteristics, especially size, density, and settling speed, in the surface layer are already vastly different in the vicinity of the Estuarine Turbidity Maximum (ETM) than they were at the Dam; the median particle size of  $\sim 50 \mu\text{m}$  is typical of very fine sand or coarse silt sized grains, but particle densities seen ranged from 1.05-1.25  $\text{g/cm}^3$ , which is less than half of the expected density of a solid mineral particle ( $\sim 2.65 \text{g/cm}^3$ ). This is entirely consistent with results from Sanford et al. (2005), where median disaggregated particle sizes in the highly flocculated lower layer were almost entirely in the clay range. Chapter 3's analysis of sediment settling characteristics throughout the surface layer of the upper Bay found fractal dimensions of 2.24 and 2.36, far less than the solid particle dimension of 3 but greater than the fractal dimension of 2 seen throughout the lower layer in past studies (Sanford et al., 2005). These observations make it abundantly clear that considerable flocculation of the fine disaggregated Dam particles is responsible, at least in part, for the increases in settling speed that are allowing sediments to fall out of the surface layer as they move down river and into the upper estuary. Chapter 3 also revealed high degree of variability in sediment characteristics in surveys taken during similar flow conditions only days apart. The variability seen is greater than what can be explained solely by source variability in the suspended solids at Conowingo Dam that are ultimately transported down bay.

Chapter 4 further informs the narrative of sediment settling in the upper Bay through the additions of mass balance and consideration for river flow. A long and rich data set of surface layer sediment concentrations revealed that the loss and gain

of sediment mass in the upper Bay depends on both antecedent river flow and distance downstream; sediment concentrations throughout the surface layer of the upper Bay were less closely tied to antecedent conditions at Conowingo Dam during lower flows and at further distances downstream, seemingly due in part to influences by the ETM and background concentration on sediment concentrations down Bay. The differences in water quality that are the signature of the ETM (onset of salinity and local increases in Total Suspended Solids (TSS) concentration) were statistically significant, and were seen one station further downstream under each progressively higher flow regime. The ETM's sediment injection signature is obscured during the highest flows, however it is also during the highest flows that the loss of surface layer sediment due to settling past the ETM appeared strongest.

## 5.2 Synthesis

Figures 4.11 and 4.12 and Appendix 7 shows the relationships between USGS TSS and Best Estimate Antecedent Day (BEAD) TSS at Conowingo and downstream Chesapeake Bay Program (CBP) TSS per station from Chapter 4. Downstream TSS values were on average approximately 3-29% lower than at Conowingo depending on river flow (Appendix 8). Figure 3.4 is a comparison between median TSS and median settling speed values across all axial surveys from Chapter 3, which offers a likely explanation for the decreases seen in Chapter 4 and Appendix 8. Notably, lower TSS is well-correlated to higher settling speeds, indicating that the loss of material could simply be due to the settling out of particles from the surface layer, which was found by Schubel (1968) to be primarily responsible for Bay sediment concentrations.



Weighted average settling speeds ( $w_{s,ave}$ ) from the Chapter 2 USGS disaggregated particle size analysis (Appendix 2) and BEAD time intervals (the time required for sediments to reach a downstream station) from Chapter 4 (Table 4.1) can be used to test the assumption that downstream concentrations are solely due to the settling out of Susquehanna material from the surface layer. If all of the sediment coming from the Conowingo Dam were to settle without resuspending, then downstream sediment concentrations should change according to,

$$C_0 * e^{\frac{-w_s}{h} * t} \tag{5.1}$$

where  $C_0$  is the initial TSS measured at Conowingo Dam,  $h$  is surface layer depth in mm, and  $t$  is the time in seconds that it takes for water to reach a downstream station according to BEAD findings. The value of the second term in (5.1) is the percentage of material that is expected to remain in suspension in the surface layer at the distance of a downstream station. Suppose that under Chapter 4's low flow conditions (<38,000 cfs) an appropriate settling speed for estimating loss of material at the downstream stations is 0.027 mm/s, the weighted average settling speed (without sand) for 20,000 cfs used in Figure 2.13 in Chapter 2. For this calculation a single characteristic upper Bay surface layer depth of 5000 mm is reasonable. Resulting estimates for the fraction of material expected to remain at each of the downstream CBP stations from median Conowingo TSS under the three flow conditions can be found in Table 5.1.

Approximate TSS from (5.1) (5.6 mg/L) was very similar to empirical median TSS measured at the first station (5.4 mg/L) under low flow conditions. However, (5.1) strongly under estimates TSS at all other stations, although the discrepancies

between approximate and empirical values are generally smaller with distance downstream (Table 5.1). These similarities and discrepancies can almost entirely be explained by conclusions from Figure 4.8; the sudden increase in TSS beginning at station 2.1 in Figure 4.8 is presumed sediment input from the ETM, after which concentrations gradually decrease until they level out near the presumed background concentration (7 mg/L). (5.1) not only assumes no resuspension occurs, but also that there are no other sources of sediment like the ETM or the background concentration. Loss of sediment between the Dam and the first station is almost exactly as estimated by (5.1), which is reasonable as station 1.1 is north of the limit of tidal influence (Mitchell et al., 2017) and along the deep center channel, making it less susceptible to resuspension from tidal, wave, and wind forcing (Sanford et al., 1994).

Median settling speeds from Chapter 2's investigation of Susquehanna source material and Chapter 3's investigation of the surface layer can be used to further evaluate the loss of material over the length of the upper Bay. Data shown in Figure 3.4 and in Table 3.1 have median surface layer settling speeds that are orders of magnitude greater than median settling speeds estimated from USGS disaggregated particle size sampling at Conowingo, investigated in Chapter 2. The upper Bay median settling speeds in Table 3.1 range from 0.07-0.97 mm/s, whereas median settling speed ( $w_{s50}$ ) estimates from the disaggregated particle analysis (Table 2.2) ranged from 0.003-0.004 mm/s. The upper Bay median settling speeds in Table 3.1 are much more similar to the weighted average settling speeds ( $w_{s,ave}$ ) found in Table 2.2.

The discrepancy in settling speeds between the Dam and upper Bay may be explained in part by Laser In-Situ Scattering and Transmissometry (LISST-100C) sampling bias; The LISST can only detect particles larger than 2.5  $\mu\text{m}$ , so the LISST could be significantly overestimating the median size of particles in the surface layer. Most of the particles in the USGS disaggregated particle analysis came from the slowest settling fraction, which was calculated using an average particle size threshold of 2  $\mu\text{m}$ , so it may be that the LISST is overlooking a substantial portion of particles suspended in the surface layer. Corroborating this possibility, the fractal dimensions found in Chapter 3 (2.24 and 2.36) are higher than the fractal dimension of 2 found by Sanford et al. (2005) in the lower layer, which is typically dominated by a population of flocculated particles (Sanford et al., 2005). This indicates that, while notable flocculation is occurring to some extent in the surface layer, a substantial portion of sediments in the surface layer is non-flocculated primary particles. Additionally, if material in the surface layer had settling speeds like those from the Chapter 3 analysis, then the water column would clear very rapidly. Instead, there is a persistent background concentration of material, which implies that the flocculation and settling out of material only occurs for a limited portion of the total mass.

If material were to fall out at speeds seen in Chapter 3, which are characteristic of a very flocculated particle population, then changes in sediment concentrations with increasing salinity examined in Chapter 4 (Figures 4.3-4.6) would appear as a rapid, non-conservative loss of material. However, concentrations appear conservative under all but high flow conditions, which must mean that either: 1) the

contribution to total sediment mass by fast settling flocs is relatively small or 2) that material from below the pycnocline is upwelling into the surface layer, countering the effect that the settling out of flocs has on concentration. It is more likely that both of these processes are occurring. There is significant upwelling at the tip of the salt intrusion in ETMs (Geyer, 1993), which may account for the sudden increase in TSS at the ETM under low flow conditions. But it is also reasonable to assume that there is an unknown portion of surface layer material that is smaller and slower settling than the LISST detected in the Chapter 3 investigation.

Only at very high flows was a large fraction of mass visibly lost between the Dam and higher salinities. This non-conservative loss of material, as observed in Chapter 4, is entirely consistent with Chapter 2's finding that higher flows carry a higher concentration of larger, faster settling particles. Interestingly, there is great concern over the potential for downstream damage caused by higher flows with larger inputs of material to the upper Bay and Bay-proper, but Chapters 2 and 4 especially show that high flows experience the greatest loss of material through the length of the upper Bay.

### 5.3 Broader Implications

There is abundant evidence from this investigation and other studies (e.g. Sanford, 1994; Sanford et al., 2001; Schubel, 1971) of a substantial population of very fine, non-settling background material in the surface layer that persists downstream in the upper Bay. Suspended particles impact the optical qualities of the water column by scattering incoming light (Wozniak, 2018). Very fine particles, like

those comprising the background concentration, scatter light much more effectively than similar concentrations of larger particles, contributing to persistent high measures of turbidity downstream in the upper Bay and into the main stem, resulting in greater light attenuation and lowered rates of primary production (Acker & Liu, 2011; Sanford et al., 2005).

Although it is a color enhanced image, the National Aeronautics and Space Administration (NASA) satellite image of the Tropical Storm Lee sediment plume (Figure 1.3) illustrates the optical effect of a large population of fine particles suspended near the water's surface; The totally opaque, brown sediment plume persists far downstream until the water column gradually clears, possibly due to either a sufficient decrease in particle concentration or sufficient increase in particle size of the suspended sediment population in the surface layer. Both of these could be the result of flocculation enhanced by the high concentration plume, which Hill et al. (2000) found to significantly contribute to the rapid settling out of particles and deposition under the plume. Jiang & Xia (2016) describe and model Chesapeake Bay sediment plumes at depths typically less than 5 m, so a significant portion of the scattering and clearing seen in the very turbid waters of Figure 1.3 can be attributed to having occurred in the shallow surface layer.

The transformation, transport, and settling of Susquehanna particles, from plumes or otherwise, is described in a conceptual diagram (Figure 5.1). Clay, silt, and sand-sized suspended particles from the Conowingo reservoir pass through the Dam, with the largest sand-sized particles falling out nearly immediately, well upstream of the northernmost stations in the Chapter 3 and Chapter 4 investigations. Larger

primary particles continue to settle out of the surface layer with time and distance downstream for the entire length of the upper Bay. When they begin to encounter brackish water, smaller primary particles begin to aggregate until they form a floc large enough to settle. A low concentration of primary non-settling background particles is left remaining in the surface layer, but flocs that had previously settled out are sometimes reinjected into the surface layer, most commonly at the ETM.

The role of flocculation in sediment settling behavior has been studied in regions similar to the Susquehanna and upper Bay, in that they experience seasonal and storm extreme river discharge events on the order of ~100,000 cfs; The Po River flows into the northern Adriatic Sea at an average rate of 53,000 cfs, with periodic extreme flood events from spring snowmelt and fall storms (Milligan et al., 2007). Like the Susquehanna, the Po delivers large loads of very fine sediments downstream, but unlike the Susquehanna, the sediments in the Po River rapidly flocculate (floc settling velocities observed on the order of ~1 mm/s), resulting in the majority of suspended material falling out of suspension within 1-2 km of the river mouth (Fox et al., 2004). Compared to low and moderate flow conditions, Milligan et al. (2007) found that during floods flocculation is slower, but still significant. Conflicting processes may be contributing to this result, as high flows carry high sediment concentrations that may enhance flocculation rates in otherwise floc-inhibitive fresh flood waters. Contrary to the Po studies, these upper Bay investigations saw less significant flocculation overall, presumably due to much lower sediment concentrations in the Susquehanna River and upper Bay; Suspended sediment concentrations observed during flood events in the Po were on the order of ~1000

mg/L (Milligan et al., 2007), while the Susquehanna and upper Bay typically experienced concentrations on the order of 100 mg/L under high flows. These investigations also found that the strongest stratification and the most rapid settling of particles out of the surface layer both occur during the highest flows, whereas stratification and flocculation were both strongest in the Po during low to moderate summer flows (Milligan et al., 2007).

The direct influence by both river flow and salt stratification on simple settling and flocculation in the upper Bay could lead to significant alterations in sediment settling behavior due to the effects of climate change. The intensity and variability of storms and river flow is expected to increase in the coming years and decades due to anticipated changes in climate (Najjar et al., 2010). These changes are likely to cause higher flows carrying greater concentrations of suspended material (Langland & Cronin, 2003), the impact of which is uncertain. Sufficiently high flows have also been known to steepen the pycnocline and cause the fresh surface layer to bypass the ETM and its sediment trapping potential which may lead to larger sediment loads escaping the upper Bay (Langland & Cronin, 2003; North et al., 2002; Sanford et al., 2001). However, these investigations observed the largest contributions from coarser grains, and accordingly the greatest loss of material over the length of the upper Bay, during the highest flow conditions, and so the downstream effects of increased flow and sediment loads may ultimately be minimal. Sea level rise in the Bay is anticipated to lead to increased variability in tidal height, coastal flooding and wetland subsidence, and allow the salt wedge to intrude upstream for longer durations due to extended droughts, which in combination with increased variability in river

discharge is expected to lead to increased variability in bay salinity (Najjar, 2010). It is uncertain, but reasonable, to expect variability in the position of the ETM, and associated enhanced sediment trapping and flocculation, in accordance with the upstream position of the salt intrusion.

Continued study of suspended particle transformation and transport in the upper Bay is imperative in order to gain a better understanding of the nature and magnitude of changes in settling behavior resulting from changes in climate and sea level. Future studies can improve upon these investigations and other past works through 1) use of innovative equipment that allows for a greater range and resolution of particle sizing and 2) increased sampling frequency throughout the water column along the center channel, especially during a greater range of flow conditions. The future of sediment transport in the upper Chesapeake Bay is uncertain in the face of climate change, but the potential for climate to alter the conditions governing sediment transport is large.

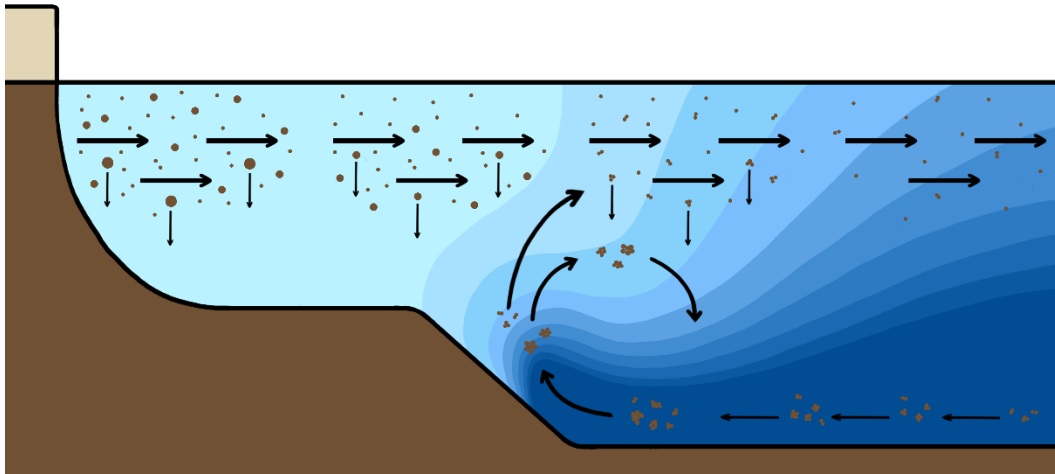


Table 5.1

*Median TSS values and (5.1) TSS estimates for the surface layer of the upper Bay*

	CBP station					
	<u>1.1</u>	<u>2.1</u>	<u>2.2</u>	<u>3.1</u>	<u>3.2</u>	<u>3.3</u>
Median TSS (mg/L)	5.4	14.6	11.0	8.8	6.2	6.6
Eq. 5.1 TSS (mg/L)	5.6	3.5	2.2	0.9	0.9	0.3
$\Delta$ TSS (mg/L)	-0.2	11.0	8.8	7.9	5.3	6.3

*Note.* Median TSS at Conowingo ( $C_0$ ) under low flows is 9.0 mg/L,  $w_s$  is 0.027 mm/s, and surface layer depth is 5000 mm. Results from (5.1) (middle row) assume no particle resuspension and no background concentration.  $\Delta$  TSS is Median TSS minus (5.1) TSS.



*Figure 5.1.* A conceptual diagram of the transport, transformation, and settling of Susquehanna River particles entering the upper Chesapeake Bay. The Conowingo Dam is at the top left of the figure. The blue contours represent the salinity gradient, with the saltwater intrusion in the darkest shade of blue. The ETM is located slightly right of the center of the figure. The upstream endmember sediments are primary particles ranging in size from sand to fine clays.

## Appendices

Appendix 1 <i>Owen data and USGS data sampled on or near the same dates in 2015-2016</i> .....	98
Appendix 2 <i>Fraction of total mass for each settling category for 37-year USGS data</i> .....	99
Appendix 3 Results from Chapter 2 Statistical Tests .....	100
Appendix 4 Median particle characteristics for Chapter 3 surface layer data .....	102
Appendix 5 Initial BEAD calculations' r2 values for linear correlations.....	110
Appendix 6 <i>Second iteration of BEAD calculations classified by flow class from first iteration</i> .....	111
Appendix 7 Station TSS versus BEAD TSS for 4 flows for stations 2.1-3.2.....	112
Appendix 8 <i>Median BEAD TSS, median station TSS, and downstream averages ...</i>	116

## Appendix 1

### *Owen data and USGS data sampled on or near the same dates in 2015-2016*

<u>Date</u>	<u>Location</u>	<u>W<sub>s</sub></u> <u>(mm/s)</u>	<u>Mass</u> <u>Frac.</u>	<u>W<sub>s</sub></u> <u>(mm/s)</u>	<u>Mass</u> <u>Frac.</u>	<u>W<sub>s</sub></u> <u>(mm/s)</u>	<u>Mass</u> <u>Frac.</u>	<u>W<sub>s</sub></u> <u>(mm/s)</u>	<u>Mass</u> <u>Frac.</u>	<u>TSS</u> <u>(mg/L)</u>	<u>Flow</u> <u>(cfs)</u>
4/13/2015	Spillway	<0.01	0.748	0.054	0.181	0.346	0.042	2.125	0.029	43.9	155,000
4/13/2015	Spill Mat	<0.01	0.736	0.078	0.205	1.235	0.059				155,000
4/13/2015	Catwalk	<0.01	0.768	0.093	0.179	0.275	0.046	2.144	0.007	43.6	155,000
4/13/2015	Cat Mat	<0.01	0.689	0.077	0.248	0.562	0.063				155,000
4/13/2015	USGS	0.003	0.730	0.079	0.230	0.731	0.040			66.0	155,000
4/14/2015	USGS	<0.01	0.641	0.048	0.243	0.207	0.095			47.0	119,000
4/22/2015	Catwalk	<0.01	0.753	0.073	0.178	0.214	0.049	2.132	0.020	11.5	108,000
4/22/2015	Cat Mat	<0.01	0.552	0.051	0.379	0.562	0.069				108,000
4/23/2015	Spillway	<0.01	0.641	0.048	0.243	0.207	0.095	2.121	0.021	21.0	109,000
4/23/2015	Spill Mat	<0.01	0.595	0.074	0.340	0.601	0.065				109,000
4/23/2015	Catwalk	<0.01	0.754	0.063	0.213	0.398	0.011	2.126	0.022	14.7	109,000
4/23/2015	Cat Mat	<0.01	0.706	0.065	0.256	1.333	0.037				109,000
4/24/2015	Spillway	<0.01	0.741	0.085	0.245	6.441	-0.003	2.155	0.017	26.3	107,000
4/24/2015	Spill Mat	<0.01	0.647	0.079	0.347	0.562	0.006				107,000
4/24/2015	Catwalk	<0.01	0.861	0.022	0.096	0.246	0.034	2.130	0.009	25.4	107,000
4/24/2015	Cat Mat	<0.01	0.644	0.027	0.321	0.562	0.035				107,000
4/24/2015	USGS	0.003	0.780	0.059	0.180	0.613	0.040			32.0	107,000
2/26/2015	Spillway	<0.01	0.869	0.069	0.115	0.187	0.009	2.144	0.006	65.6	149,000
2/26/2015	Spill Mat	<0.01	0.759	0.046	0.222	0.562	0.019				149,000
2/26/2015	Catwalk	<0.01	0.645	0.082	0.313	0.136	0.034	2.142	0.008	83.1	149,000
2/26/2015	Cat Mat	<0.01	0.638	0.100	0.318	0.564	0.044				149,000
2/26/2015	USGS	0.003	0.690	0.075	0.270	0.731	0.040			118.0	149,000
2/27/2016	Spillway	<0.01	0.700	0.064	0.259	0.144	0.028	2.139	0.013	86.7	171,000
2/27/2016	Spill Mat	<0.01	0.560	0.057	0.397	0.566	0.043				171,000
2/27/2016	Catwalk	<0.01	0.702	0.061	0.257	0.126	0.028	2.126	0.012	77.1	171,000
2/27/2016	Cat Mat	<0.01	0.653	0.067	0.310	0.562	0.037				171,000
2/28/2016	Spillway	<0.01	0.648	0.072	0.290	0.207	0.046	2.129	0.016	66.9	145,000
2/28/2016	Spill Mat	<0.01	0.566	0.075	0.379	0.562	0.055				145,000
2/28/2016	Catwalk	<0.01	0.769	0.070	0.154	0.169	0.064	2.145	0.014	53.9	145,000
2/28/2016	Cat Mat	<0.01	0.676	0.078	0.271	0.562	0.053				145,000
2/28/2016	USGS	0.002	0.780	0.088	0.190	0.652	0.030			76.0	145,000
Average	Spillway	<0.01	0.725	0.065	0.222	1.255	0.036	2.136	0.017	51.7	139,333
Average	Spill Mat	<0.01	0.644	0.068	0.315	0.682	0.041				139,333
Average	Catwalk	<0.01	0.750	0.066	0.199	0.223	0.038	2.135	0.013	44.2	134,857
Average	Cat Mat	<0.01	0.651	0.066	0.300	0.673	0.048				134,857
Average	USGS	0.003	0.724	0.070	0.223	0.587	0.049			67.8	135,000

*Note.* Settling speed ( $w_s$ ), mass fraction (Mass Frac.), and sediment concentration (TSS) values are from the Malpezzi spreadsheet (Spill gate, Catwalk), Malarkey Matlab (Spill Mat, Cat Mat), and USGS grain size (USGS) analyses.

Appendix 2

*Fraction of total mass for each settling category for 37-year USGS data*

<u>Date</u>	<u>Flow (cfs)</u>	<u>TSS (mg/L)</u>	<u>&lt;.01 mm/s</u>	<u>.01-.2 mm/s</u>	<u>.2-2 mm/s</u>	<u>&gt;2 mm/s</u>
8/8/1979	14,800	17	0.71	0.17	0.09	0.03
10/16/1979	51,200	50	0.90	0.10	0.00	0.00
3/22/1980	173,000	49	0.81	0.16	0.02	0.01
3/23/1980	215,000	113	0.76	0.22	0.02	0.00
3/23/1980	215,000	123	0.71	0.23	0.06	0.00
3/23/1980	215,000	132	0.81	0.15	0.03	0.01
3/23/1980	215,000	107	0.77	0.21	0.02	0.00
3/23/1980	215,000	138	0.75	0.19	0.06	0.00
3/31/1980	136,000	43	0.82	0.07	0.09	0.02
3/31/1980	136,000	35	0.83	0.14	0.01	0.02
4/2/1980	207,000	40	0.65	0.28	0.07	0.00
4/2/1980	207,000	31	0.78	0.20	0.01	0.01
2/13/1981	165,000	173	0.83	0.17	0.00	0.00
2/13/1981	165,000	183	0.79	0.18	0.03	0.00
2/13/1981	165,000	194	0.78	0.19	0.03	0.00
2/14/1981	122,000	144	0.79	0.21	0.00	0.00
2/17/1984	420,000	359	0.81	0.10	0.08	0.01
2/17/1984	420,000	295	0.54	0.30	0.14	0.02
2/17/1984	420,000	293	0.58	0.36	0.05	0.01
2/17/1984	420,000	276	0.66	0.28	0.05	0.01
2/17/1984	420,000	235	0.73	0.22	0.05	0.00
2/17/1984	420,000	282	0.81	0.13	0.05	0.01
2/17/1984	420,000	265	0.73	0.22	0.04	0.01
9/8/2011	592,000	2980	0.36	0.29	0.29	0.06
9/10/2011	493,000	741	0.63	0.21	0.13	0.03
9/11/2011	356,000	1150	0.48	0.24	0.22	0.06
9/12/2011	227,000	332	0.61	0.15	0.12	0.12
5/18/2014	171,000	70	0.87	0.11	0.02	0.00
5/19/2014	173,000	65	0.75	0.13	0.11	0.01
3/16/2015	75,800	24	0.96	0.02	0.02	0.00
4/7/2015	127,000	28	0.65	0.25	0.09	0.01
4/8/2015	98,500	31	0.78	0.17	0.05	0.00
4/9/2015	97,900	36	0.86	0.09	0.05	0.00
4/13/2015	155,000	63	0.73	0.23	0.04	0.00
4/14/2015	119,000	55	0.86	0.10	0.04	0.00
4/24/2015	107,000	33	0.78	0.18	0.04	0.00
2/26/2016	149,000	118	0.69	0.27	0.04	0.00
2/28/2016	145,000	76	0.78	0.19	0.03	0.00
2/29/2016	113,000	99	0.84	0.13	0.03	0.00
3/2/2016	76,000	78	0.78	0.20	0.02	0.00
Characteristic Settling Speed (mm/s):			0.005	0.068	1.175	17.941

*Note.* The characteristic settling speed for each category is the average of all samples' weighted average settling speed in that category.

### Appendix 3. Results from Chapter 2 Statistical Tests

#### *Difference between analysis method results for four 2015-2016 samples*

---

<u>Method A</u>	<u>Method B</u>	<u>Significance</u>
Spill gate	Spill Mat	Not Sig'
Spill gate	Catwalk	'Not Sig'
Spill gate	Cat Mat	'Not Sig'
Spill gate	USGS	'Not Sig'
Spill Mat	Catwalk	'Not Sig'
Spill Mat	Cat Mat	'Not Sig'
Spill Mat	USGS	'Not Sig'
Catwalk	Cat Mat	'Not Sig'
Catwalk	USGS	'Not Sig'
Cat Mat	USGS	'Not Sig'

---

*Note.* Column 3 indicates whether the difference between results from two analysis methods (columns 1 and 2) is statistically significant ('Sig') or not ('Not Sig') with 95% certainty.

*Difference between analysis method results by settling speed category*

<u>&lt;0.01 mm/s</u>			<u>0.01-0.2 mm/s</u>		
<u>Method A</u>	<u>Method B</u>	<u>Significance</u>	<u>Method A</u>	<u>Method B</u>	<u>Significance</u>
Spill gate	Spill Mat	'Not Sig'	Spill gate	Spill Mat	'Not Sig'
Spill gate	Catwalk	'Not Sig'	Spill gate	Catwalk	'Not Sig'
Spill gate	Cat Mat	'Not Sig'	Spill gate	Cat Mat	'Not Sig'
Spill gate	USGS	'Not Sig'	Spill gate	USGS	'Not Sig'
Spill Mat	Catwalk	'Not Sig'	Spill Mat	Catwalk	'Not Sig'
Spill Mat	Cat Mat	'Not Sig'	Spill Mat	Cat Mat	'Not Sig'
Spill Mat	USGS	'Not Sig'	Spill Mat	USGS	'Not Sig'
Catwalk	Cat Mat	'Not Sig'	Catwalk	Cat Mat	'Not Sig'
Catwalk	USGS	'Not Sig'	Catwalk	USGS	'Not Sig'
Cat Mat	USGS	'Not Sig'	Cat Mat	USGS	'Not Sig'

<u>0.2-2 mm/s</u>			<u>≥2 mm/s</u>		
<u>Method A</u>	<u>Method B</u>	<u>Significance</u>	<u>Method A</u>	<u>Method B</u>	<u>Significance</u>
Spill gate	Spill Mat	'Not Sig'	Spill gate	Spill Mat	'Sig'
Spill gate	Catwalk	'Not Sig'	Spill gate	Catwalk	'Not Sig'
Spill gate	Cat Mat	'Not Sig'	Spill gate	Cat Mat	'Sig'
Spill gate	USGS	'Not Sig'	Spill gate	USGS	'Sig'
Spill Mat	Catwalk	'Not Sig'	Spill Mat	Catwalk	'Sig'
Spill Mat	Cat Mat	'Not Sig'	Spill Mat	Cat Mat	'Not Sig'
Spill Mat	USGS	'Not Sig'	Spill Mat	USGS	'Not Sig'
Catwalk	Cat Mat	'Not Sig'	Catwalk	Cat Mat	'Sig'
Catwalk	USGS	'Not Sig'	Catwalk	USGS	'Not Sig'
Cat Mat	USGS	'Not Sig'	Cat Mat	USGS	'Not Sig'

*Note.* Columns 3 and 6 indicate whether the difference between results from two analysis methods (columns 1 & 2 and 4 & 5 respectively) is statistically significant ('Sig') or not ('Not Sig') with 95% certainty.

Appendix 4. Median particle characteristics for Chapter 3 surface layer data

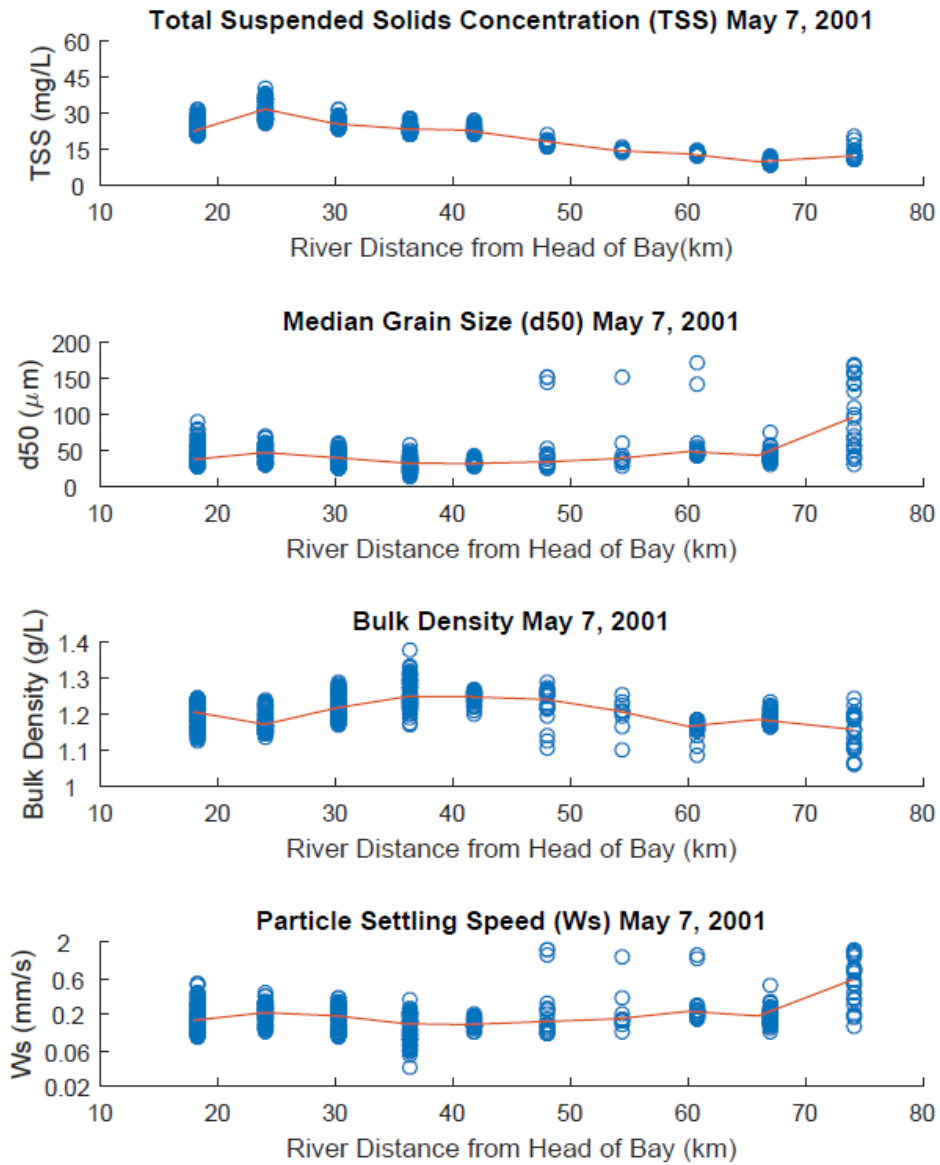


Figure A4.1. Surface layer data for key parameters (TSS, d50, bulkD,  $w_s$ ) from upper Bay axial analysis, surveyed on May 7, 2001. Blue circles represent all sample data, while red lines indicate median values.



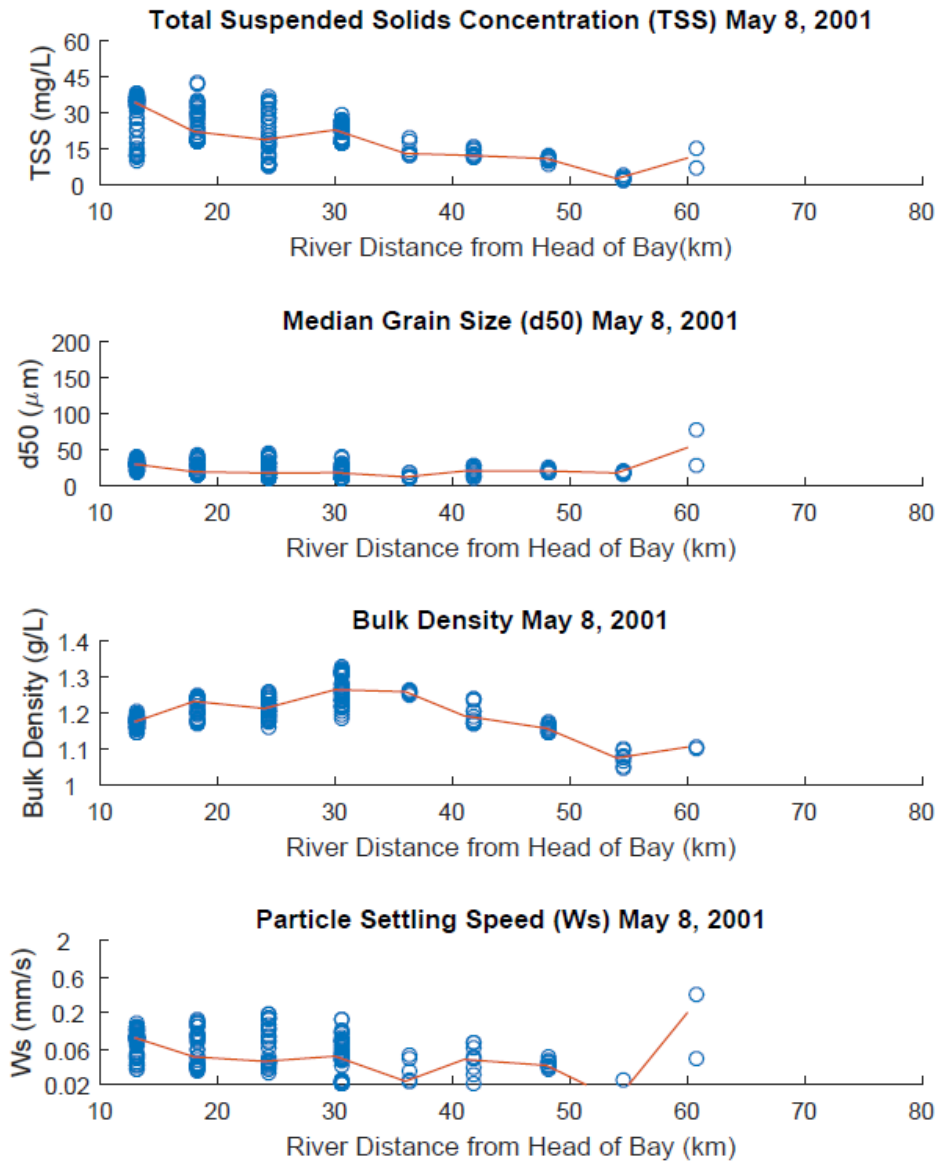


Figure A4.2. Surface layer data for key parameters (TSS, d50, bulkD,  $w_s$ ) from upper Bay axial analysis, surveyed on May 8, 2001. Blue circles represent all sample data, while red lines indicate median values.

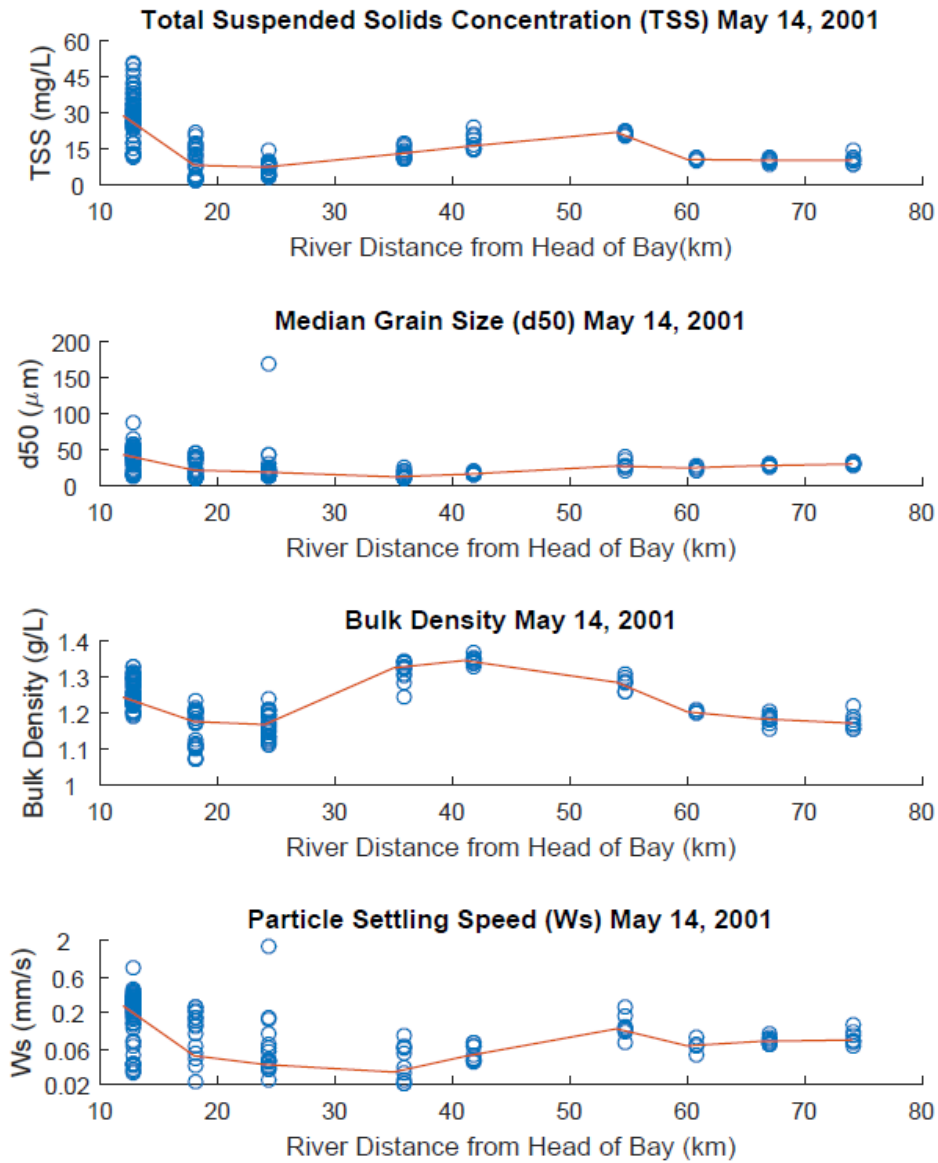


Figure A4.3. Surface layer data for key parameters (TSS, d50, bulkD,  $w_s$ ) from upper Bay axial analysis, surveyed on May 14, 2001. Blue circles represent all sample data, while red lines indicate median values.

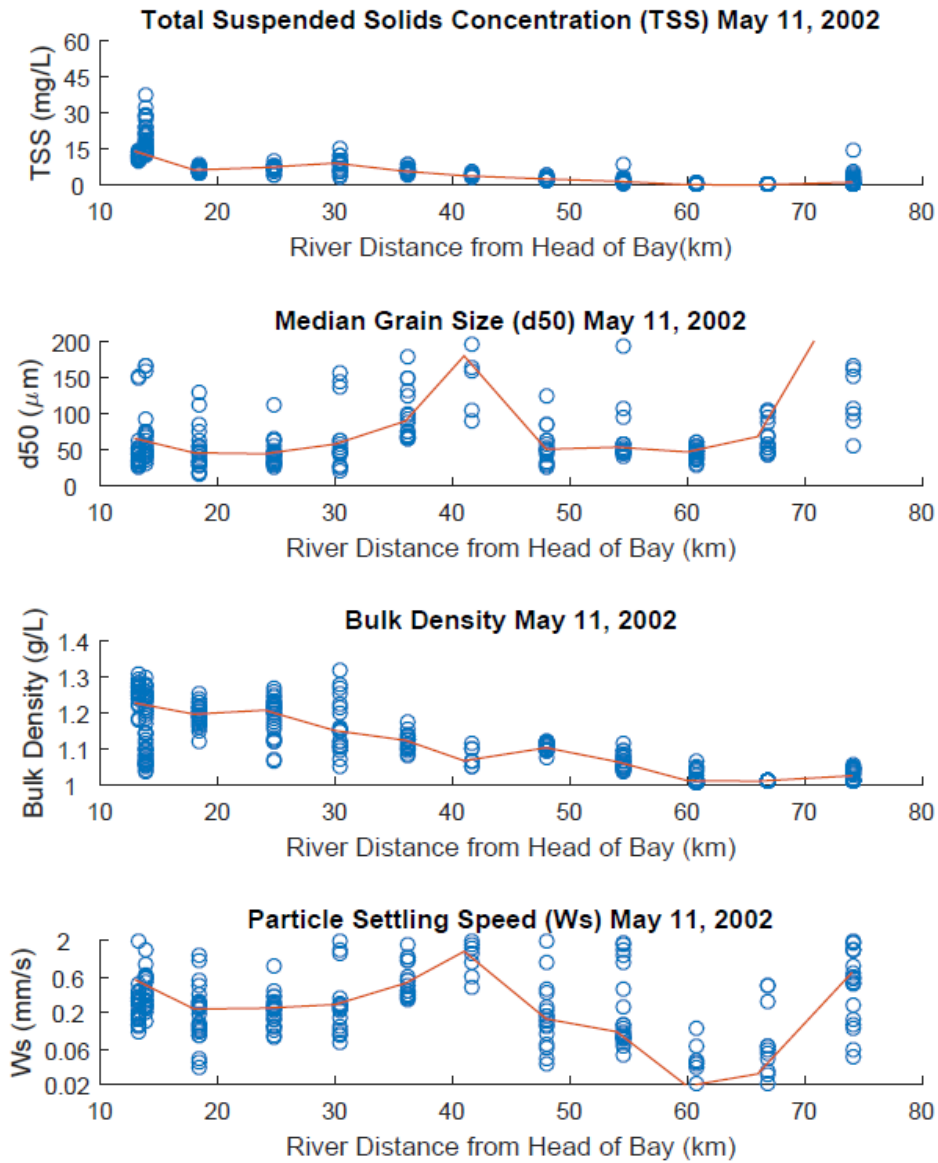


Figure A4.4. Surface layer data for key parameters (TSS, d50, bulkD,  $w_s$ ) from upper Bay axial analysis, surveyed on May 11, 2002. Blue circles represent all sample data, while red lines indicate median values.

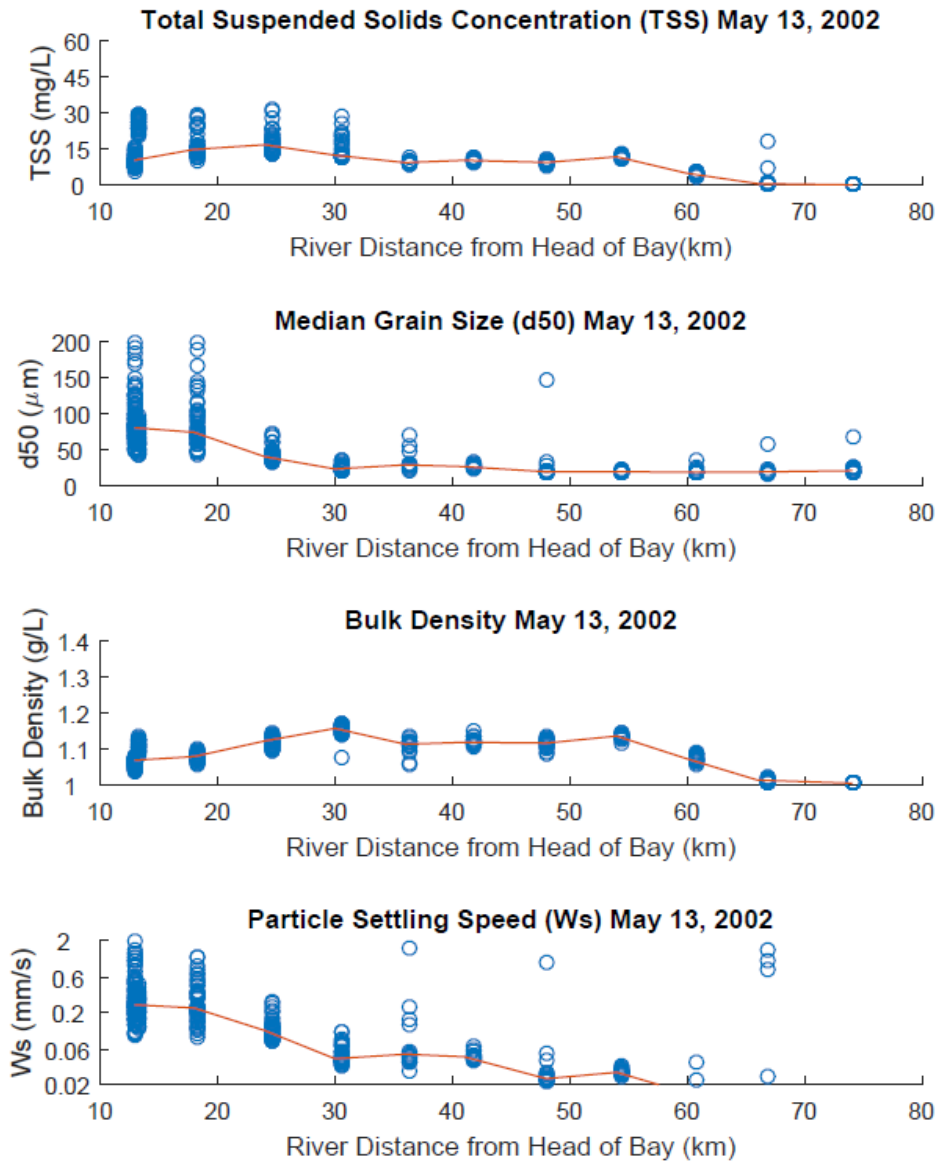


Figure A4.5. Surface layer data for key parameters (TSS, d50, bulkD,  $w_s$ ) from upper Bay axial analysis, surveyed on May 13, 2002. Blue circles represent all sample data, while red lines indicate median values.

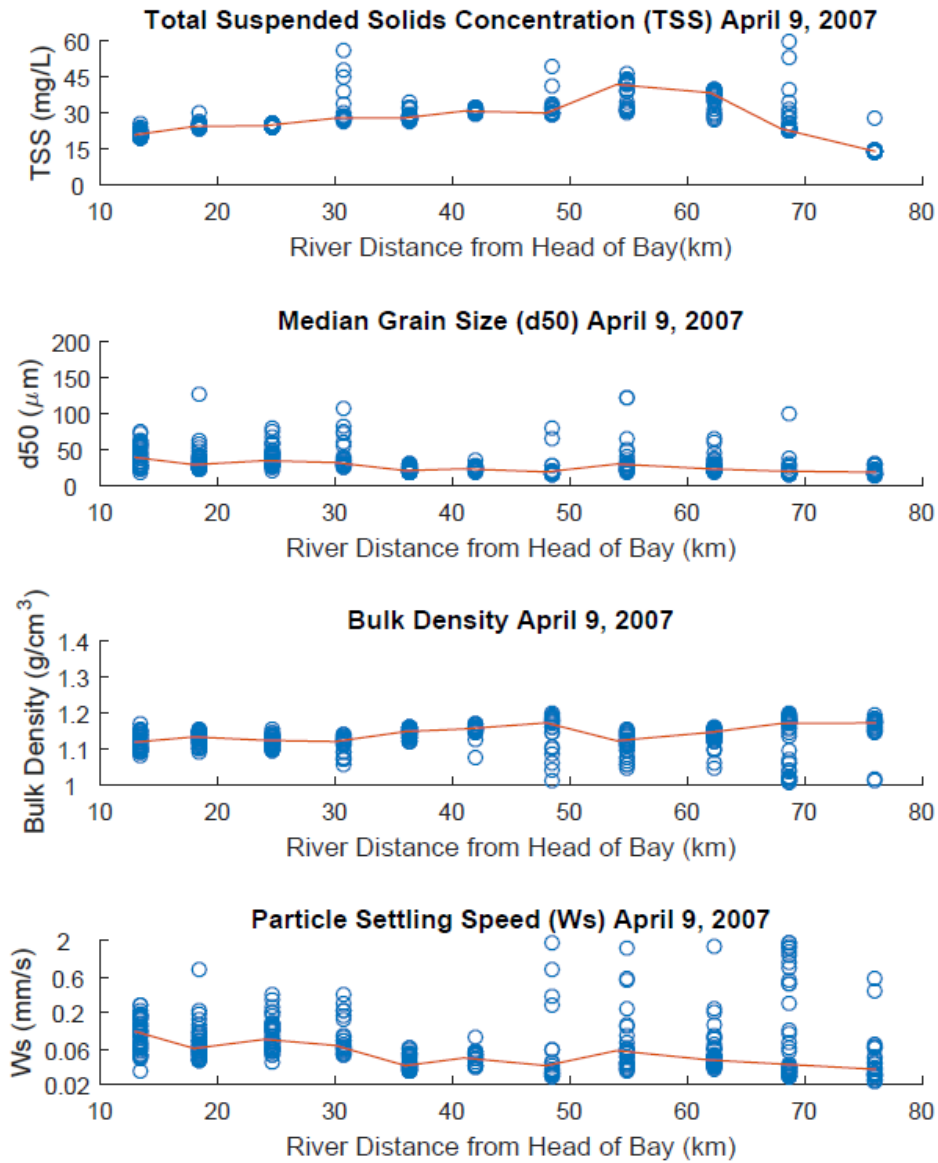


Figure A4.6. Surface layer data for key parameters (TSS, d50, bulkD,  $w_s$ ) from upper Bay axial analysis, surveyed on April 9, 2007. Blue circles represent all sample data, while red lines indicate median values.

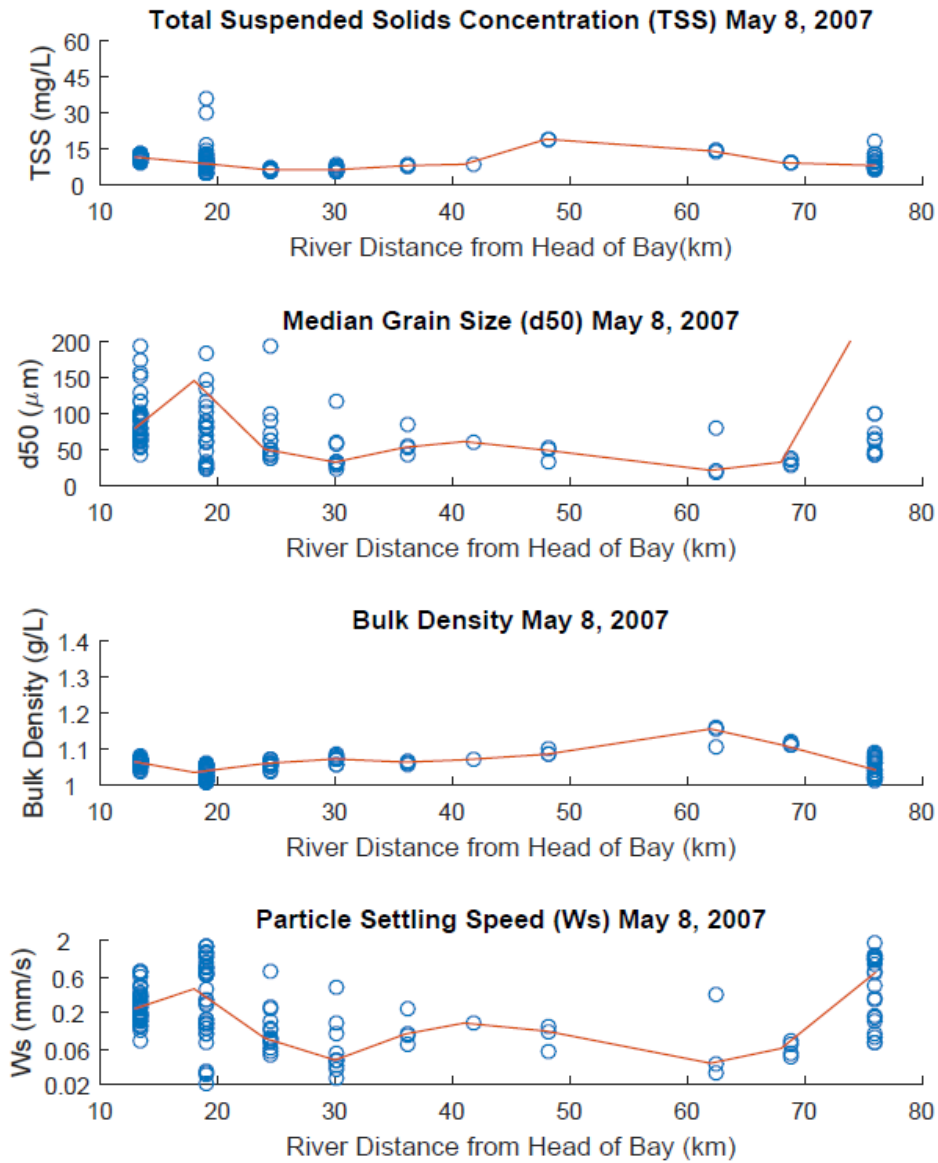


Figure A4.7. Surface layer data for key parameters (TSS, d50, bulkD,  $w_s$ ) from upper Bay axial analysis, surveyed on May 8, 2007. Blue circles represent all sample data, while red lines indicate median values.

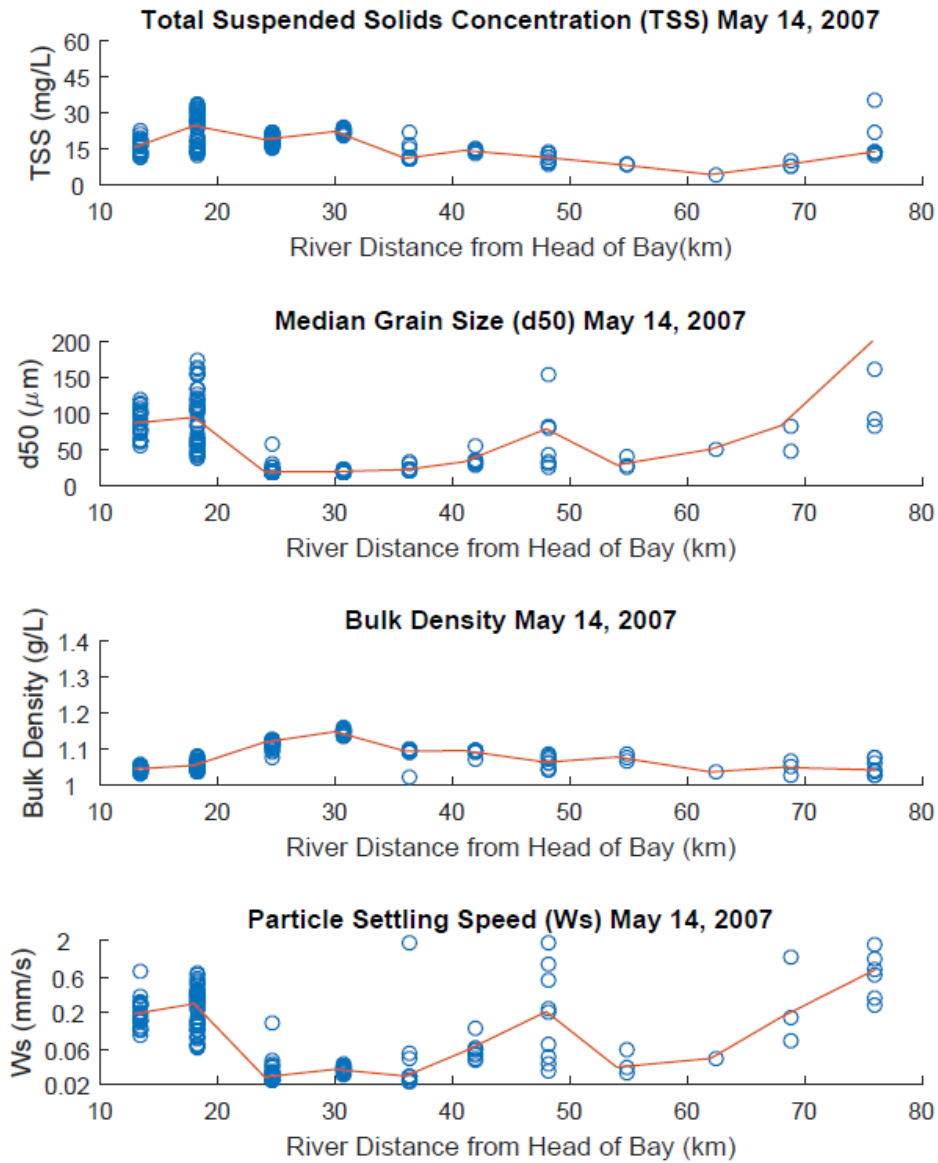
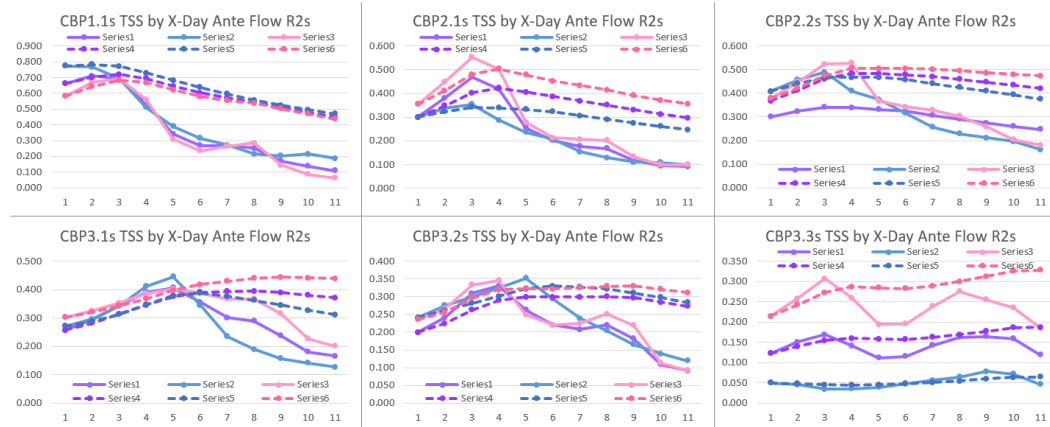


Figure A4.8. Surface layer data for key parameters (TSS, d50, bulkD,  $w_s$ ) from upper Bay axial analysis, surveyed on May 14, 2007. Blue circles represent all sample data, while red lines indicate median values.

## Appendix 5



*Figure A5.* Initial BEAD calculations'  $r^2$  values for linear correlations between Conowingo river discharge and CBP TSS values at each of the six stations for 0-10 antecedent day lags, values calculated during initial BEAD calculations.



Appendix 6

*Second iteration of BEAD calculations classified by flow class from first iteration*

	CBP Station Number					
	<u>1.1</u>	<u>2.1</u>	<u>2.2</u>	<u>3.1</u>	<u>3.2</u>	<u>3.3</u>
1st iter. BEAD	1	2	3	5	5	7
1st iter. corr.	0.798	0.576	0.387	0.268	0.216	0.284
Low BEAD	1	10	4	1	4	8
Low flow corr.	0.209	0.108	0.133	0.099	0.035	0.003
Med. flow BEAD	1	0	0	3	3	1
Med. flow corr.	0.243	0.104	0.036	0.236	0.367	0.115
High flow BEAD	1	2	1	4	10	2
High flow corr.	0.821	0.861	0.355	0.237	0.088	0.684
All flows BEAD	0	2	2	4	4	2
All flows corr.	0.801	0.576	0.439	0.368	0.264	0.298

*Note.* BEAD in this table refers to the highest correlated antecedent day for that iteration and flow condition. BEAD typically referred to throughout this thesis is represented by the first two rows, all other values are from the second iteration of BEAD testing which uses flow classifications determined by the first iteration.

Appendix 7. Station TSS versus BEAD TSS for 4 flows for stations 2.1-3.2

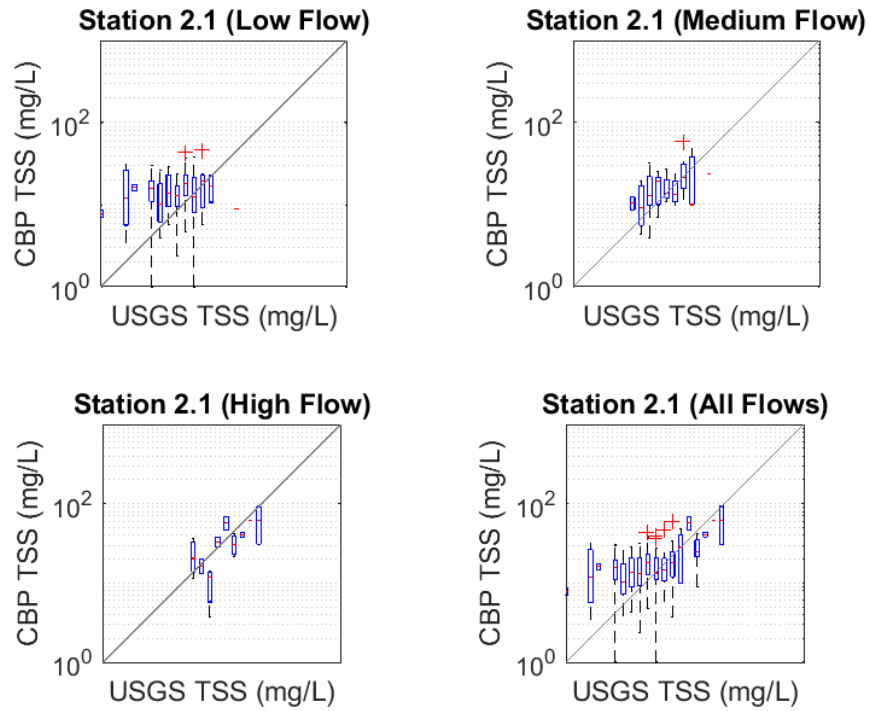


*Figure A7.1.* Comparisons of downstream CBP TSS at station 2.1 compared to upstream antecedent USGS TSS at Conowingo Dam under low (upper left), medium (upper right), high (lower left) and all (lower right) flow conditions. All plots are on a loglog scale with a diagonal black 1:1 reference line.

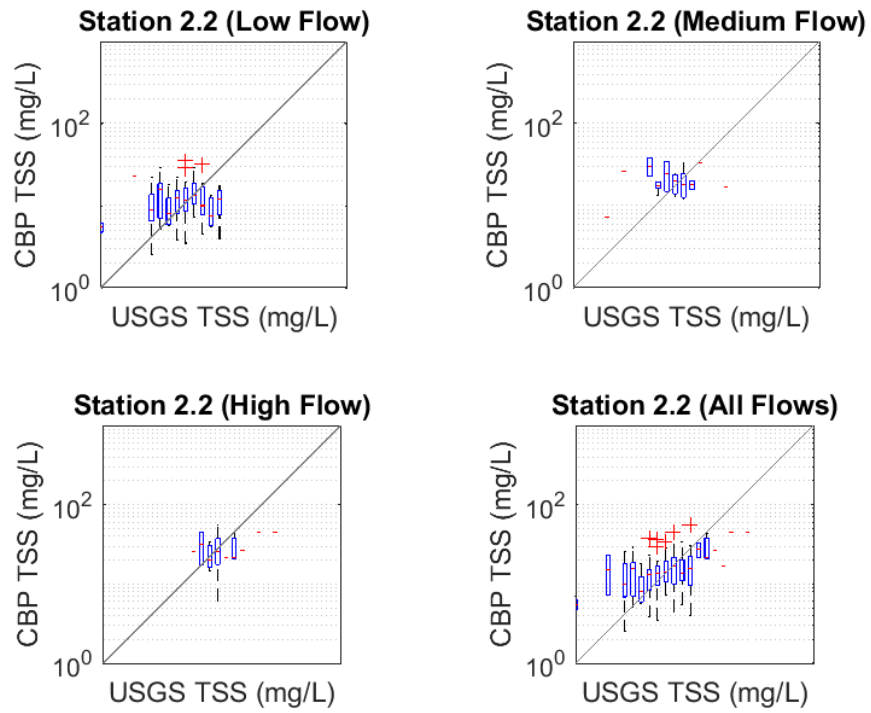


*Figure A7.2.* Comparisons of downstream CBP TSS at station 2.2 compared to upstream antecedent USGS TSS at Conowingo Dam under low (upper left), medium (upper right), high (lower left) and all (lower right) flow conditions. All plots are on a loglog scale with a diagonal black 1:1 reference line.

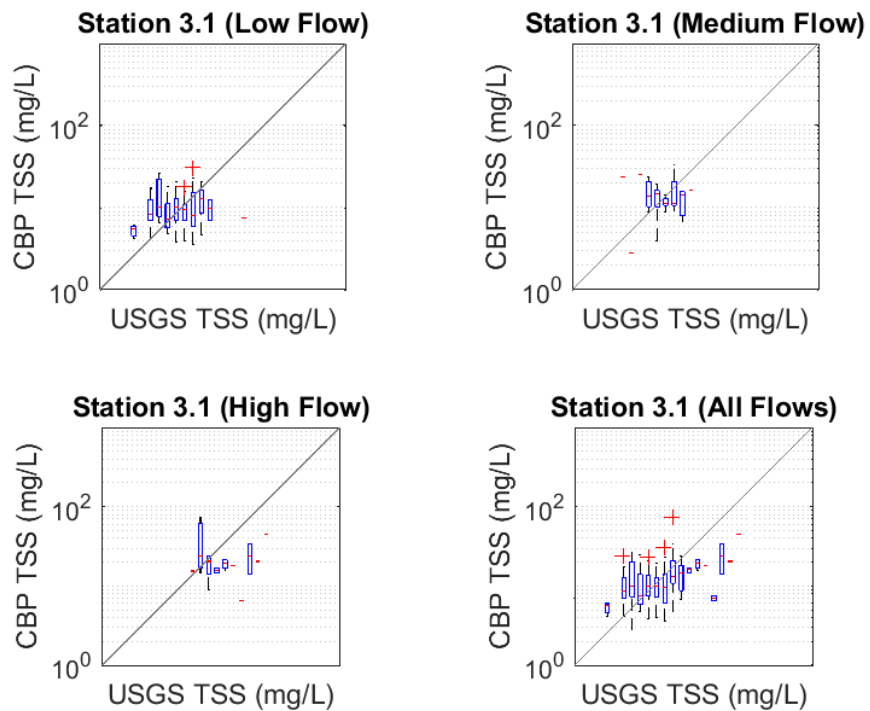


*Figure A7.3.* Comparisons of downstream CBP TSS at station 3.1 compared to upstream antecedent USGS TSS at Conowingo Dam under low (upper left), medium (upper right), high (lower left) and all (lower right) flow conditions. All plots are on a loglog scale with a diagonal black 1:1 reference line.

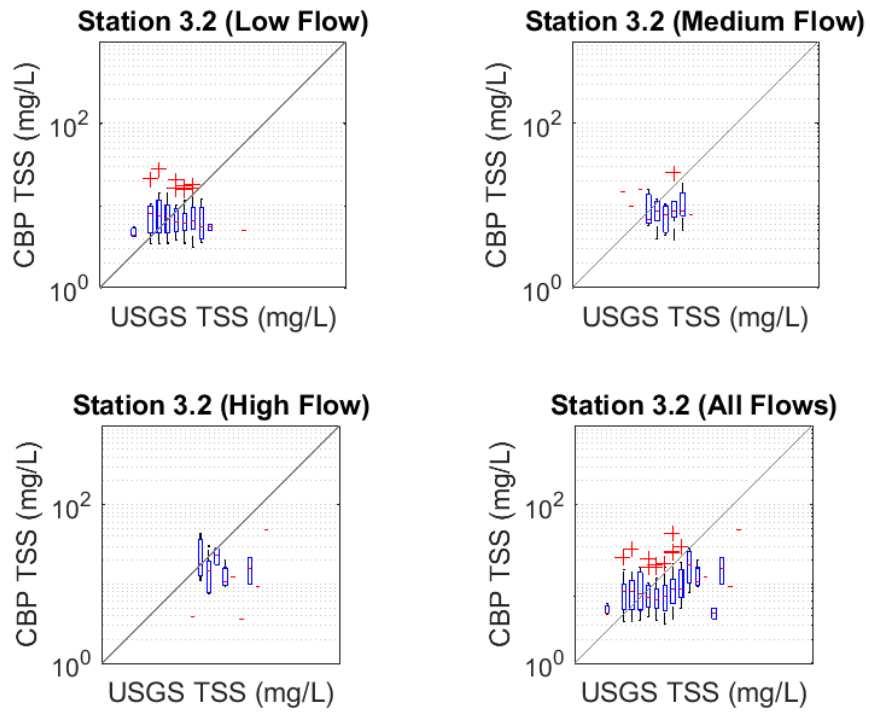


*Figure A7.4* Comparisons of downstream CBP TSS at station 3.2 compared to upstream antecedent USGS TSS at Conowingo Dam under low (upper left), medium (upper right), high (lower left) and all (lower right) flow conditions. All plots are on a loglog scale with a diagonal black 1:1 reference line.

## Appendix 8

### *Median BEAD TSS, median station TSS, and downstream averages*

<u>Flow</u>	<u>Cono</u>	<u>Station number</u>						Avg. Downstream	Avg. % Reduction
		<u>1.1</u>	<u>2.1</u>	<u>2.2</u>	<u>3.1</u>	<u>3.2</u>	<u>3.3</u>		
Low	9.0	5.4	14.6	11.0	8.8	6.2	6.6	8.8	2.7
Medium	13.3	11.5	14.4	18.6	12.7	8.6	7.0	12.1	9.1
High	31.8	33.3	33.0	26.0	18.0	12.1	12.6	22.5	29.1
All	11.0	7.6	15.5	13.6	10.6	7.4	7.0	10.3	6.6

*Note.* All values are TSS in mg/L except for the rightmost column. The average downstream TSS is calculated from stations 1.1 through 3.3.

## Bibliography

- Acker, J., Liu, Z. (2011). *Remote-sensing case study of the Chesapeake Bay region during drought (2002) and flood (2003) years* (Handbook of Satellite Remote Sensing Image Interpretation). Retrieved from International Ocean Colour Coordinating Group website:  
[https://www.ioccg.org/handbook/casestudy1\\_acker\\_liu.pdf](https://www.ioccg.org/handbook/casestudy1_acker_liu.pdf)
- Biggs, R. B. (1970). Sources and distribution of suspended sediment in Northern Chesapeake Bay. *Marine Geology*, 9(3), 187-201. doi:10.1016/0025-3227(70)90014-9
- Cartwright, G. M., Friedrichs, C. T., & Sanford, L. P. (2011). In situ characterization of estuarine suspended sediment in the presence of muddy flocs and pellets. In J. D. Rosati, P. Wang, & T. M. Roberts (Eds.), *Proceedings of coastal sediments 2011: Vol. 3* (pp. 642-655). World Scientific.
- Chesapeake Bay Program. (2020a). Bay 101. Retrieved from  
<https://www.chesapeakebay.net/discover/bay-101>
- Chesapeake Bay Program. (2020b). Watershed. Retrieved from  
<https://www.chesapeakebay.net/discover/watershed>
- Cerco, C. F., Kim, S.-C., & Noel, M. R. (2013). Management modeling of suspended solids in the Chesapeake Bay, USA. *Estuarine, Coastal and Shelf Science*, 116(0), 87-98. doi: <http://dx.doi.org/10.1016/j.ecss.2012.07.009>
- Cheng, P., Li, M., & Li, Y. (2013). Generation of an estuarine sediment plume by a tropical storm. *Journal of Geophysical Research*, 118, 1-13.
- Cronin, T. M., Sanford, L. P., Langland, M. L., Willard, D., & Saenger, C. (2003). Chapter 6: Estuarine sediment transport, deposition, and sedimentation. In T. M. Cronin, M. L. Langland, & S. Phillips (Eds.), *A summary report of sediment processes in Chesapeake Bay and watershed, water resources investigations report 03-4123* (pp. 129-160). New Cumberland, PA: U.S. Geological Survey.
- Donoghue, J. F., Bricker, O. P., & Owen, C. R. (1989). Particle-borne radionuclides as tracers for sediment in the Susquehanna River and Chesapeake Bay. *Estuarine, Coastal and Shelf Science*, 29(4), 341-360. doi:10.1016/0272-7714(89)90033-4
- Fisher, T. R., Harding, L. W., Jr., Stanley, D. W., & Ward, L. G. (1988). Phytoplankton, nutrients, and turbidity in the Chesapeake, Delaware, and

- Hudson estuaries. *Estuarine, Coastal and Shelf Science*, 27(1), 61-93.  
Retrieved from  
<http://gateway.isiknowledge.com/gateway/Gateway.cgi?GWVersion=2&SrcAuth=ResearchSoft&SrcApp=EndNote&DestLinkType=FullRecord&DestApp=WOS&KeyUT=A1988P749300005>
- Fox, J. M., Hill, P. S., Milligan, T. G., Ogston, A. S., & Boldrin, A. (2004). Floc fraction in the waters of the Po River prodelta. *Continental Shelf Research*, 24(15), 1699-1715. Retrieved from  
[http://www.sciencedirect.com/science?\\_ob=MIimg&\\_imagekey=B6VBJ-4D4D1F0-1-11&\\_cdi=5928&\\_user=961275&\\_orig=na&\\_coverDate=10%2F01%2F2004&\\_sk=999759984&view=c&wchp=dGLbVtb-zSkWA&md5=b210a3ff3df4d7cd83e71a0c344106c9&ie=/sdarticle.pdf](http://www.sciencedirect.com/science?_ob=MIimg&_imagekey=B6VBJ-4D4D1F0-1-11&_cdi=5928&_user=961275&_orig=na&_coverDate=10%2F01%2F2004&_sk=999759984&view=c&wchp=dGLbVtb-zSkWA&md5=b210a3ff3df4d7cd83e71a0c344106c9&ie=/sdarticle.pdf)
- Fugate, D. C., Friedrichs, C. T., & Sanford, L. P. (2007). Lateral dynamics and associated transport of sediment in the upper reaches of a partially mixed estuary, Chesapeake Bay, USA. *Continental Shelf Research*, 27(5), 679–698. Retrieved from  
[http://www.sciencedirect.com/science?\\_ob=MIimg&\\_imagekey=B6VBJ-4MSR8W9-1-Y&\\_cdi=5928&\\_user=961275&\\_orig=search&\\_coverDate=01%2F10%2F2007&\\_sk=999999999&view=c&wchp=dGLbVzW-zSkzS&md5=42c0304b692ddd2fb631c0994d25c0d1&ie=/sdarticle.pdf](http://www.sciencedirect.com/science?_ob=MIimg&_imagekey=B6VBJ-4MSR8W9-1-Y&_cdi=5928&_user=961275&_orig=search&_coverDate=01%2F10%2F2007&_sk=999999999&view=c&wchp=dGLbVzW-zSkzS&md5=42c0304b692ddd2fb631c0994d25c0d1&ie=/sdarticle.pdf)
- Geyer, W. R. (1993). The importance of suppression of turbulence by stratification on the estuarine turbidity maximum. *Estuaries*, 16(1), 113-125. Retrieved from  
[http://estuariesandcoasts.org/cdrom/ESTU1993\\_16\\_1\\_113\\_125.pdf](http://estuariesandcoasts.org/cdrom/ESTU1993_16_1_113_125.pdf)
- Gibbs, R. J., Mathews, M. D., & Link, D. A. (1971). The relationship between sphere size and settling velocity. *Journal of Sedimentary Petrology*, 41(1), 7-18. Retrieved from <http://jsedres.sepmonline.org.proxy-um.researchport.umd.edu/cgi/reprint/41/1/7.pdf>
- Guo, L., & He, Q. (2011). Freshwater flocculation of suspended sediments in the Yangtze River, China. *Ocean Dynamics*, 61(2-3), 371-386.  
doi:10.1007/s10236-011-0391-x
- Guo, X., & Valle-Levinson, A. (2007). Tidal effects on estuarine circulation and outflow plume in the Chesapeake Bay. *Continental Shelf Research*, 27(1), 20-42. Retrieved from <http://www.sciencedirect.com/science/article/B6VBJ-4M7VFNF-1/2/b0359c9e5093a6173e52c308b4d670e3>
- Guy, H. P. (1969). Laboratory theory and methods for sediment analysis (Techniques of Water-Resources Investigations). Retrieved from U.S. Geological Survey website: <https://pubs.usgs.gov/twri/twri5c1/html/pdf.html>



- Hainley, R. A., Reed, L. A., Flippo, H. N., & Barton, G. J. (1995). *Deposition and simulation of sediment transport in the lower Susquehanna River reservoir system* (Water-Resources Investigations Report No. 95-4122). Retrieved from U.S. Geological Survey website:  
<https://pubs.er.usgs.gov/publication/wri954122>
- Hill, P. S., Milligan, T. G., & Geyer, W. R. (2000). Controls on effective settling velocity of suspended sediment in the Eel River flood plume. *Continental Shelf Research*, 20, 2095–2111.
- Hill, P. S., & McCave, I. N. (2001). Suspended particle transport in benthic boundary layers. In B. P. J. Boudreau & Bo Barker (Eds.), *The benthic boundary layer* (pp. 78-103). New York: Oxford University Press.
- Hill, P. S., Newgard, J. P., Law, B. A., & Milligan, T. G. (2013). Flocculation on a muddy intertidal flat in Willapa Bay, Washington, Part II: Observations of suspended particle size in a secondary channel and adjacent flat. *Continental Shelf Research*, 60(2000), 2067-2093.  
doi:<http://dx.doi.org/10.1016/j.csr.2012.06.006>
- Hirsch, R. M. (2012). *Flux of nitrogen, phosphorus, and suspended sediment from the Susquehanna River basin to the Chesapeake Bay during Tropical Storm Lee, September 2011, as an indicator of the effects of reservoir sedimentation on water quality* (Scientific Investigations Report No. 2012-5185). Retrieved from U.S. Geological Survey website:  
<https://pubs.usgs.gov/sir/2012/5185/pdf/sir2012-5185-508.pdf>
- Hobbs, C. H., Halka, J. P., Kerhin, R. T., & Carron, M. J. (1992). Chesapeake Bay sediment budget. *Journal of Coastal Research*, 8(2), 292-300. Retrieved from <http://gateway.isiknowledge.com/gateway/Gateway.cgi?GWVersion=2&SrcAuth=ResearchSoft&SrcApp=EndNote&DestLinkType=FullRecord&DestApp=WOS&KeyUT=A1992KX28600004>
- Horowitz, A. J., Stephens, V. C., Elrick, K. A., & Smith, J. J. (2012) Concentrations and annual fluxes of sediment-associated chemical constituents from conterminous US coastal rivers using bed sediment data. *Hydrological Processes*, 26(7), 961-1118. Retrieved from <https://onlinelibrary.wiley.com/doi/abs/10.1002/hyp.8437>
- Jay, D. A., Orton, P. M., Chisholm, T., Wilson, D. J., & Fain, A. M. V. (2007). Particle trapping in stratified estuaries: Consequences of mass conservation. *Estuaries and Coasts*, 30(6), 1095-1105. Retrieved from [http://estuariesandcoasts.org/journal/ESTU2007/ESTU2007\\_30\\_6\\_1095\\_1105.pdf](http://estuariesandcoasts.org/journal/ESTU2007/ESTU2007_30_6_1095_1105.pdf)

- Jiang, L., & Xia, M. (2016). Dynamics of the Chesapeake Bay outflow plume: Realistic plume simulation and its seasonal and interannual variability. *Journal of Geophysical Research: Oceans*, 121(2), 22. Retrieved from <http://onlinelibrary.wiley.com.proxy-um.researchport.umd.edu/doi/10.1002/2015JC011191/pdf>
- Lang, D. J. (1982). *Water quality of the three major tributaries to the Chesapeake Bay, the Susquehanna, the Potomac, and James rivers, January 1979-April 1981* (Water-Resources Investigations Report No. 82-32). Retrieved from U.S. Geological Survey website: <https://pubs.er.usgs.gov/publication/wri8232>
- Langland, M. J. (2009). *Bathymetry and sediment-storage capacity change in three reservoirs on the lower Susquehanna River, 1996-2008* (Scientific Investigations Report No. 2009-5110). Retrieved from U.S. Geological Survey website: <http://pubs.usgs.gov/sir/2009/5110/pdf/sir2009-5110.pdf>
- Langland, M. J. (2012) *Sediment transport and capacity change in three reservoirs, lower Susquehanna River basin, Pennsylvania and Maryland, 1900–2012* (Open-File Report No. 2014–1235). Retrieved from U.S. Geological Survey website: <https://pubs.usgs.gov/of/2014/1235/pdf/ofr2014-1235.pdf>
- Langland, M. L., & Cronin, T. M. (2003). *A summary report of sediment processes in Chesapeake Bay and watershed* (Water-Resources Investigations Report No. 03-4123). Retrieved from U.S. Geological Survey website: <https://pubs.usgs.gov/wri/2003/4123/wri20034123.pdf>
- Langland, M. J., Lietman, P. L., & Hoffman, S. A. (1995). *Synthesis of nutrient and sediment data for watersheds within the Chesapeake Bay drainage basin* (Water-Resources Investigations Report No. 95-4233). Retrieved from U.S. Geological Survey website: <https://pubs.usgs.gov/wri/1995/4233/report.pdf>
- Lee, H. J., & P. L. Wiberg. (2002). Character, fate, and biological effects of contaminated, effluent-affected sediment on the Palos Verdes margin, southern California: An overview. *Continental Shelf Research*, 22, 835–840.
- Liu, X., & Wang, M. (2014). River runoff effect on the suspended sediment property in the upper Chesapeake Bay using MODIS observations and ROMS simulations. *Journal of Geophysical Research: Oceans*, 119(12), 8646-8661. doi:10.1002/2014JC010081

- Malarkey, J., Jago, C. F., Hübner, R., & Jones, S. E. (2013). A simple method to determine the settling velocity distribution from settling velocity tubes. *Continental Shelf Research*, 56, 82-89. doi:<http://dx.doi.org/10.1016/j.csr.2013.01.018>
- Malpezzi, M. A., Sanford, L. P., & Crump, B. C. (2013). Abundance and distribution of transparent exopolymer particles in the estuarine turbidity maximum of Chesapeake Bay. *Marine Ecology Progress Series*, 486, 23-35. Retrieved from <http://www.int-res.com.proxy-um.researchport.umd.edu/articles/meps2013/486/m486p023.pdf>
- Milligan, T. G., Hill, P. S., & Law, B. A. (2007). Flocculation and the loss of sediment from the Po River plume. *Continental Shelf Research*, 27(3-4), 309-321. Retrieved from [http://www.sciencedirect.com/science?\\_ob=MIimg&\\_imagekey=B6VBJ-4MSY8N1-2-3W&\\_cdi=5928&\\_user=961275&\\_orig=na&\\_coverDate=02%2F01%2F2007&\\_sk=999729996&view=c&wchp=dGLbVtz-zSkWA&md5=9b27993cf21c9d9757110f1d989ba909&ie=/sdarticle.pdf](http://www.sciencedirect.com/science?_ob=MIimg&_imagekey=B6VBJ-4MSY8N1-2-3W&_cdi=5928&_user=961275&_orig=na&_coverDate=02%2F01%2F2007&_sk=999729996&view=c&wchp=dGLbVtz-zSkWA&md5=9b27993cf21c9d9757110f1d989ba909&ie=/sdarticle.pdf)
- Mitchell, S. B., Green, M. O., MacDonald, I. T., & Pritchard, M. (2017). Field studies of estuarine turbidity under different freshwater flow conditions, Kaipara River, New Zealand. *Estuarine, Coastal and Shelf Science*, 198, Part B, 542-554. doi:<https://doi.org/10.1016/j.ecss.2016.06.009>
- Najjar, R. G., Pyke, C. R., Adams, M. B., Breitburg, D., Hershner, C., Kemp, M., . . . Wood, R. (2010). Potential climate-change impacts on the Chesapeake Bay. *Estuarine, Coastal and Shelf Science*, 86(1), 1-20. Retrieved from <http://www.sciencedirect.com/science/article/B6WDV-4XFPR43-2/2/a5f14fcb7f9a6e8517d309c3ab6d3691>
- North, E. W., Hood, R. R., Chao, S.-Y., & Sanford, L. P. (2002). *Retention of fish early-life stages and copepod prey in an estuarine nursery area: The influence of environmental variability*. Paper presented at the ICES Journal of Marine Science.
- Owen, M. W. (1976). Determination of the settling velocities of cohesive muds. Wallingford, United Kingdom: Hydraulics Research.
- Palinkas, C. M., Halka, J. P., Li, M., Sanford, L. P., & Cheng, P. (2014). Sediment deposition from tropical storms in the upper Chesapeake Bay: Field observations and model simulations. *Continental Shelf Research*, 86(0), 6-16. doi:<http://dx.doi.org/10.1016/j.csr.2013.09.012>

- Palinkas, C. M., Testa, J. M., Cornwell, J. C., Li, M., & Sanford, L. P. (2019). Influences of a river dam on delivery and fate of sediments and particulate nutrients to the adjacent estuary: Case study of Conowingo Dam and Chesapeake Bay. *Estuaries and Coasts*, 42(8), 2072-2095. doi:10.1007/s12237-019-00634-x
- Park, K., Wang, H., Kim, S.-C., & Oh, J.-H. (2008). A model study of the estuarine turbidity maximum along the main channel of the upper Chesapeake Bay. *Estuaries and Coasts*, 31(1), 115-133. doi:10.1007/s12237-007-9013-8
- Pritchard, D. W., & Vieira, M. E. C. (1984). Vertical variations in residual current response to meteorological forcing in the mid-Chesapeake Bay. In *Wind stress and residual currents* (pp. 27-64). New York, NY: Academic Press, Inc.
- Sanford, L. P. (1994). Wave-forced resuspension of upper Chesapeake Bay muds. *Estuaries*, 17(1B), 148-165. Retrieved from <http://www.springerlink.com.proxy-um.researchport.umd.edu/content/m1342p214463v777/fulltext.pdf>
- Sanford, L. P., Dickhudt, P., Rubiano-Gomez, L., Yates, M., Suttles, S., Friedrichs, C. T., . . . Romine, H. (2005). Variability of suspended particle concentrations, sizes and settling velocities in the Chesapeake Bay turbidity maximum. In I. G. Droppo, G. G. Leppard, P. Liss, & T. Milligan (Eds.), *Flocculation in natural and engineered environmental systems* (pp. 211-236). Boca Raton, Florida: CRC Press, LLC.
- Sanford, L. P., Suttles, S. E., & Halka, J. P. (2001). Reconsidering the physics of the Chesapeake Bay estuarine turbidity maximum. *Estuaries*, 24(5), 655-669. Retrieved from <http://www.springerlink.com.proxy-um.researchport.umd.edu/content/77607871t60155hk/fulltext.pdf>
- Schubel, J. R. (1968). *Suspended sediment of the northern Chesapeake Bay*. Baltimore, MD: The Chesapeake Bay Institute of the Johns Hopkins University.
- Schubel, J. R., & Biggs, R. B. (1969). Distribution of seston in upper Chesapeake Bay. *Chesapeake Science*, 10(1), 18-23. Retrieved from [http://estuaries.olemiss.edu/cdrom/CPSC1969\\_10\\_1\\_18\\_23.pdf](http://estuaries.olemiss.edu/cdrom/CPSC1969_10_1_18_23.pdf)
- Schubel, J., & Pritchard, D. (1986). Responses of upper Chesapeake Bay to variations in discharge of the Susquehanna River. *Estuaries*, 9(4A), 236-249. Retrieved from [http://estuariesandcoasts.org/cdrom/ESTU1986\\_9\\_4A\\_236\\_249.pdf](http://estuariesandcoasts.org/cdrom/ESTU1986_9_4A_236_249.pdf)

- Scientific Technical Advisory Committee. (2007, Jan. 30-31). *An introduction to sedimentsheds: Sediment and its relationship to Chesapeake Bay water clarity*. Retrieved from Chesapeake Bay Program website: <http://www.chesapeake.org/stac/Pubs/SedShedReportFINAL.pdf>
- Sequoia Scientific. (2007). LISST-100X Particle Size Analyzer, User's Manual Version 4.65. Bellevue, WA.
- United States Environmental Protection Agency. (2020). Chesapeake Bay Total Maximum Daily Load (TMDL). Retrieved from <https://www.epa.gov/chesapeake-bay-tmdl>
- United States Environmental Protection Agency, Office of Research and Development. (1979). Method No. 160.2 (with slight modification) in Methods for chemical analysis of water and wastes (Report No. EPA-600/4-79-020). Cincinnati, OH.
- Van der Lee, W. T. B. (2000). Temporal variation of floc size and settling velocity in the Dollard estuary. *Continental Shelf Research*, 22, 1495–1511, doi:10.1016/S0278-4343(00)00034-0
- Winterwerp, J. C. (2002). On the flocculation and settling velocity of estuarine mud. *Continental Shelf Research*, 22(9), 1339-1360. Retrieved from <https://www.sciencedirect.com/science/article/pii/S0278434302000109>
- Wells, R. C., Bailey, R. K., & Henderson, E. P. (1929) Salinity of the water of the Chesapeake Bay (Shorter Contributions to General Geology). Retrieved from U.S. Geological Survey website: <https://pubs.usgs.gov/pp/0154c/report.pdf>
- Woźniak, S. B., Sagan, S., Zabłocka, M., Stoń-Egiert, J., & Borzycka, K. (2018). Light scattering and backscattering by particles suspended in the Baltic Sea in relation to the mass concentration of particles and the proportions of their organic and inorganic fractions. *Journal of Marine Systems*, 182, 79-96. doi:<https://doi.org/10.1016/j.jmarsys.2017.12.005>
- Zhang, Q., & Blomquist, J. D. (2018). Watershed export of fine sediment, organic carbon, and chlorophyll-a to Chesapeake Bay: Spatial and temporal patterns in 1984–2016. *Science of the Total Environment*, 619-620, 1066-1078. doi: <https://doi.org/10.1016/j.scitotenv.2017.10.279>
- Zhang, Q., Brady, D. C., & Ball, W. P. (2013). Long-term seasonal trends of nitrogen, phosphorus, and suspended sediment load from the non-tidal Susquehanna River Basin to Chesapeake Bay. *Science of the Total Environment*, 452–453(0), 208-221. doi:<http://dx.doi.org/10.1016/j.scitotenv.2013.02.012>

Zhang, Q., Hirsch, R. M., & Ball, W. P. (2016). Long-term changes in sediment and nutrient delivery from Conowingo Dam to Chesapeake Bay: Effects of reservoir sedimentation. *Environmental Science & Technology*, 50(4), 1877-1886. doi:10.1021/acs.est.5b04073